UNIVERSITY OF FOGGIA

PhD course in

"Translational medicine and management of health systems"

(XXXV Cycle)

Coordinator: PROF. TERESA ANTONIA SANTANTONIO

PhD Thesis

"DETECTION OF PROGNOSTIC BIOMARKERS AND APPLICATION IN CLUSTERING PATIENTS WITH ORAL SQUAMOUS CELL CARCINOMA, ACCORDING TO THE RISK OF RELAPSE"

PhD candidate: Vito Carlo Alberto Caponio

Tutor: Prof. Lorenzo Lo Muzio

Academic years: 2019/2022

SUMMARY

Appendix 2: Abstracts and Conference Proceedings

Appendix 3: Oral presentations

Appendix 4: Honors and awards

ABSTRACT

Most head and neck cancers derive from the mucosal epithelium of the oral cavity, pharynx and larynx and are known collectively as head and neck squamous cell carcinoma (HNSCC), accounting for over 600,000 new cases diagnosed per year and of these, more than 300.000 new cases annually are reported to take origin from the surface of the oral mucosa. Current evidence supports that these subsites exhibit distinctive molecular and clinical behaviors, leading to an "anatomical bias" both for research and clinical decision-making. Oral squamous cell carcinoma (OSCC), in particular involving oral tongue (OTSCC) is the most common malignancy of the head and neck region, characterized by a high rate of local and regional recurrences, which strongly decreases patients' survival rates. The American Joint Committee on Cancer (AJCC) staging system is the standard tool used to classify oncological patients and predict their clinical outcomes. Despite advancements in patients' prognostic stratification, the 8th edition of AJCC fails to identify patients characterized by early relapse and poor prognosis. Currently, no prognostic biomarkers have been validated to stratify these patients and their risk of recurrence and death. This scenario calls for the investigation of biomarkers from basic research combined with bioinformatics to clinical and routine diagnostic application in a translational pathway.

This project aimed to investigate prognostic biomarkers in HNSCC, OSCC and OTSCC,

by different approaches, such as reviews and meta-analysis, histopathology, and bioinformatics. This is to highlight possible histopathologic and genetic biomarkers to be integrated in future staging systems in a precision medicine environment.

Different histopathologic features were tested, such as tumour budding, eosinophils infiltration, lymph-vascular invasion, perineural invasion, lymphocytes infiltration, and tumour-stroma ratio. This investigation led to the development of promising and easy to be assessed histopathologic biomarkers, such as immune-phenotype, thresholds, and improved staging systems. Furtherly, a new prognostic classification system was developed based on TP53 gene mutations.

In conclusion, the heterogeneous background of HNSCC, including OSCC and, OTSCC emerged, and new prognostic biomarkers were proposed to be furtherly evaluated in other cohorts for routine translational application in the aim of precision medicine.

1. INTRODUCTION

Most head and neck cancers derive from the mucosal epithelium of the oral cavity, pharynx and larynx and are known collectively as head and neck squamous cell carcinoma (HNSCC), accounting for over 600,000 new cases diagnosed per year and of these, more than 300.000 new cases annually are reported to take origin from the surface of the oral mucosa [1]. Current evidence supports that these subsites exhibit distinctive molecular and clinical behaviors, leading to an "anatomical bias" both for research and clinical decision-making [2]. Oral squamous cell carcinoma (OSCC) and, oral tongue squamous cell carcinoma (OTSCC) is the most common malignancy of the head and neck region, characterized by a high rate of local and regional recurrences, which strongly decreases patients' survival rates. The approximate 5-year survival rate of 65%, drops to an average of 40% for patients diagnosed in advanced stage; this is due to a poor response to standard

anti-cancer treatments such as chemotherapy and radiotherapy, which has remained almost unchanged over the past decade [3]. The tumor is remarkably heterogeneous, based on localization in the oral cavity, oropharynx, larynx, and hypopharynx, on the types of cells within the tumor tissue and the molecular subtypes [4, 5]. The prognosis for patients with HNSCC and OSCC is determined by the stage of the tumour at presentation, as well as the presence of lymph-node metastases and distant metastases. Unfortunately, only one-third of patients are diagnosed with early-stage disease, whilst two-thirds are diagnosed with advanced cancer with lymph node metastases [6]. Surgery combined with adjuvant radiation therapy and/or chemotherapy is the standard of care, but in these cases, patients often experience notable complications related to disease treatments, including different degrees of hoarseness or aphonia, dysphagia, dry mouth, and facial distortion after surgery [7, 8]. Indeed, it is important to obtain tumor-free resection margins in these patients, and to achieve this, surgeons usually remove the tumor with a margin of 10 mm of macroscopically normal tissue, thus creating a large surgical defect that needs free flap reconstruction in more than half of patients [9].

The American Joint Committee on Cancer (AJCC) staging system is the standard tool used to classify oncological patients and predict their clinical outcomes. Despite advancements in patients' prognostic stratification, the 8th edition of AJCC fails to identify patients characterized by early relapse and poor prognosis [10]. Currently, no prognostic biomarkers have been validated to stratify these patients and their risk of recurrence and death [11]. Moreover, immunotherapy has been approved, although is still not clear which patients may benefit from such treatment. This emphasizes the need for comprehensive predictive models that could lead to clinical-therapeutical strategies, based on individual bio-clinical characteristics [12]. Recently, researchers focused on the morphological features of tumour microenvironment (TME). In particular, the study of

tumour-infiltrating inflammatory and immune cells and their spatial organization provided substantial evidence that a higher level of immune infiltration is indicative of ongoing immune reactivity in cancers and better prognosis [13, 14]. However, cancers are characterized by a broad spectrum of biological and morphological alterations, since several genetic, epigenetic, and histological changes occur. Recent advances in computational genomics provided an avenue to explore such genetic and functional heterogeneity. In this sense, The Cancer Genome Atlas (TCGA) was one of the first projects molecularly characterizing in bulk over 20,000 (over 500 HNSCCs) primary cancer and matched normal samples spanning 33 cancer types, generating genomic, epigenomic, transcriptomic and proteomic data [15].

This scenario calls for the investigation of biomarkers from basic research combined with bioinformatics to clinical and routine diagnostic application in a translational pathway.

This project aimed to investigate new prognostic biomarkers in HNSCC, OSCC and OTSCC, by different approaches, such as reviews and meta-analysis, histopathology, and bioinformatics. This is to highlight possible histopathologic and genetic biomarkers to be integrated in future staging systems in a precision medicine environment.

2. HISTOPATHOLOGIC BIOMARKER

2.1. Background

Nowadays, the Tumor-Node-Metastasis (TNM) staging system is employed worldwide to predict tumor prognosis and to guide physicians towards the correct treatment choice, however, survival outcomes in patients classified within the same TNM stage class could be dramatically different, with discrepancies in therapy response and tumor management [16]. One of the main limitations of OSCC-related TNM system is focused on the anatomical extension of the disease. However, within each staging group, the prognosis

can be modified by tumor-related factors, such as genetics, patient age, sex, race, or comorbidities. For this reason, the need for a more "personalized" approach to the oncologic patient was underlined in the recent eighth edition of the AJCC staging system [17]. It is, therefore, necessary to investigate further prognostic factors to construct prognostic models to carry out a personalized prognosis evaluation [18].

2.2. Methods

The cohort included in this retrospective study consisted of randomly selected patients with OTSCC. Patients were treated with curative intent at the Department of Maxillofacial Surgery, 'Ospedali Riuniti' General Hospital (Ancona, Italy), between 1997 and 2018. The clinical and pathological data were collected from the archives of the Institute of Pathology, Marche Polytechnic University, Italy. The inclusion criteria were as follows: (a) surgical samples of primary OTSCC; (b) age above 18 years; (c) absence of preoperative chemo- or radiation therapy; (d) no human papilloma virus (HPV) infection (assessed by using HPV 16-specific fluorescence in situ hybridization and p16Ink4a-specific immunohistochemistry); (e) follow-up data of at least 3 years for alive patients. Exclusion criteria were as follows: (a) OTSCC cases involving other anatomical sites, and when the exact site from which the tumor originated could not be identified; (b) relapsed or secondary primary OTSCC; (c) OTSCC patients with immediate postoperative death. The staging classification was revised according to the 8th edition of the AJCC Cancer Staging Manual [19]. Follow-up data were updated by a single researcher blinded to clinical and pathological data and group allocation. The clinical endpoints examined were disease-specific survival (DSS), overall survival (OS), and disease-free survival (DFS). The follow-up time was defined as the time from the date of surgical operation to the date of recurrence (for DFS), to the date of death due to cancer

(for DSS) or death from any cause (OS), or to the date of the last clinic visit. Informed consent was obtained from all included patients, and the study was conducted in accordance with the 'Ethical Principles for Medical Research Involving Human Subjects' statement of the Helsinki Declaration [20]. The study received ethical approval from the institutional review board of Marche Polytechnic University, Italy (CERM 2019-308). The study was conducted according to the REMARK checklist [21].

Histopathology evaluation was performed for tumour-stroma ratio (TSR), immune-phenotype, perineural invasion (PNI), eosinophils invasion (TATE) and tumour budding (TB). In general, for each patient, investigators also retrieved other clinic-pathological characteristics, such as lymph-vascular invasion (LVI), margin status, tumor thickness, grading, worst-pattern of invasion (WPOI), extra-nodal extension (ENE), and depth of invasion (DOI). Margin status was assessed by performing multiple serial cuts into the margins at 5-mm intervals, perpendicular to the resection plane. The distance between resection margin and carcinoma (margin clearance) was measured, and patients were grouped into two groups ("positive" and "negative") based on a cutoff of 5 mm. Tumor thickness was measured as the perpendicular distance between the highest point of the tumor surface to the deepest point of the infiltrative front of the tumor, considering both the exophytic and the infiltrative component of the tumor [19]. Tumor grade was assessed according to the 4th edition of the World Health Organization classification of head and neck tumors. WPOI was defined as the worst manner of infiltration present at the tumor/host interface [22].

2.2.1. Tumour-Stroma Ratio

Hematoxylin and eosin (H&E)-stained sections (4 µm) were obtained from formalin-fixed paraffin-embedded blocks of the primary tumour specimens. Two experienced pathologists independently performed the histological evaluation, blinded to the clinical

and pathological data. The TSR was visually assessed as previously reported [23]. Slides were selected from the most invasive part of the OTSCC (i.e. the same slides routinely used to assess the T status). Then, the invasive area appearing to have the highest percentage of desmoplastic stroma was jointly identified by the two pathologists by the use of conventional light microscopy at low magnification. Subsequently, each pathologist independently evaluated the same area at high magnification (×200), and a single high-power field was selected and scored for each case. Only those areas where tumour cell nests were present at all borders of the selected image field were evaluated (Figure 1). The percentage of stroma tissue was manually estimated per 10-fold, from 0% to 100%, per image field. The mean value of the percentages provided by both pathologists was used as the final score. For statistical analysis, patients were subsequently dichotomized into a stroma-rich group, defined by the presence of a high proportion of stroma and a low proportion of tumour cells (TSR < 50%), and a stroma-poor group, defined by the presence of a low proportion of stroma and a high proportion of tumour cells (TSR ≥ 50%).

Specific areas, such as skeletal muscle tissue, salivary gland tissue, large nerve bundles, large blood vessels, and necrotic tissue, were left out of the microscopic scoring field whenever possible. If this was not possible, these areas were ignored for scoring.

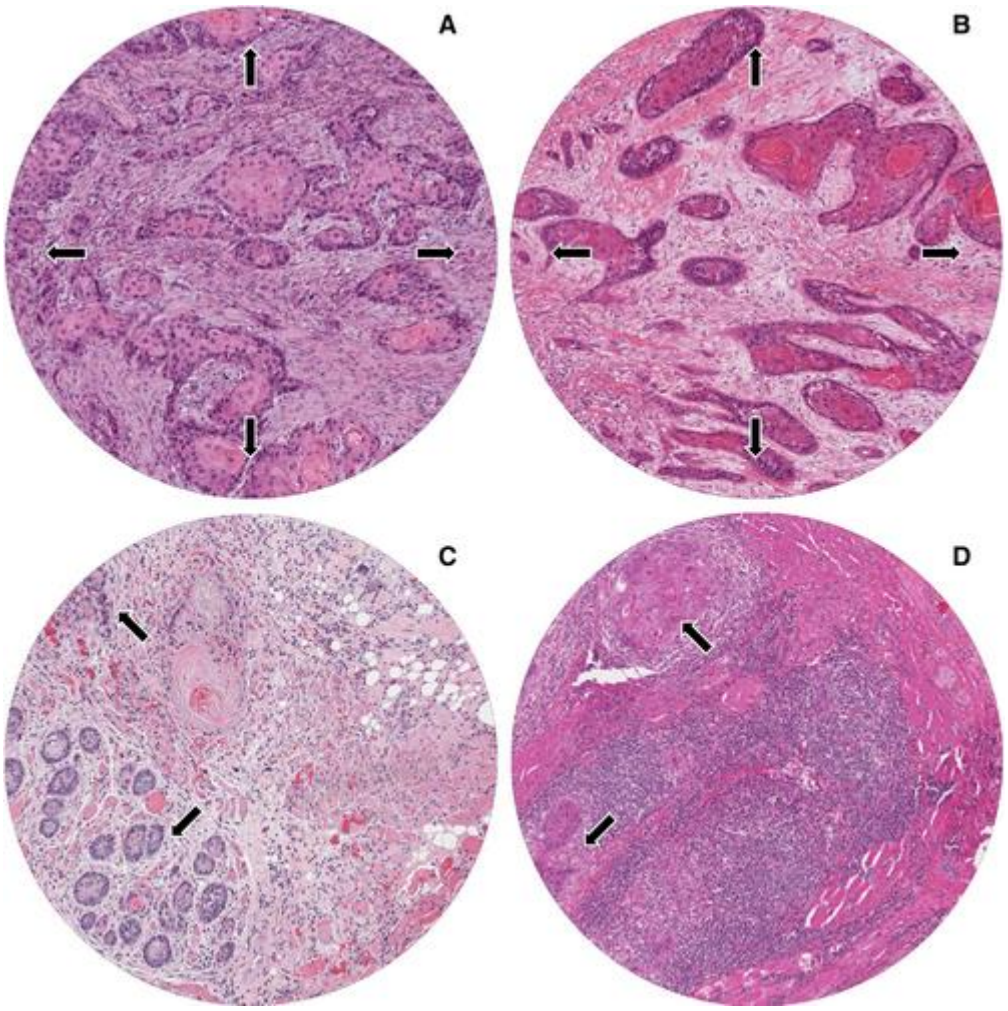

Figure 1: Examples of the tumour–stroma ratio in hematoxylin and eosin-stained sections of oral tongue squamous cell carcinoma. **A,B,** Correct field of vision: tumour cells are present on all four sides (black arrows). **C,D,** Wrong field of vision: tumour cells are present only on two sides (black arrows).

2.2.2. Immune Phenotype

Routine 4-µm hematoxylin-eosin (H&E) stained sections, obtained from formalin-fixed, paraffin-embedded blocks of the primary tumor specimens, were carried out from the most invasive part of the primary tumor (i.e., the same slides routinely used to assess the T status). The density and localization of lymphocytes were determined, based on the recommendation of the International TILs Working Group [24].

Briefly, for each patient, one H&E-stained section was considered. A full assessment of the tumor area was initially conducted by light microscopy at low magnification.

Subsequently, five high-power fields with a magnification of ×200 (ocular ×10, with an objective of ×20) were randomly selected. The presence of TILs was evaluated in the stromal compartment within the borders of invasive tumor, by considering all the mononuclear cells. In particular, the percentage of TILs was estimated based on the percentage of the area occupied by mononuclear cells over the stromal area both around the tumor border and inside the tumor mass in proximity to the tumor cells. Necrotic areas have been left out of the microscopic scoring field whenever possible, if this was not possible, these areas have been ignored for scoring. The area percentage was estimated per 10-fold, from 0% to 100%, per image-field. For each patient, the mean value of scored percentages was considered.

Based on the results, patients were divided into the following groups: (a) Group 1 ("immune-inflamed phenotype" group) if the mean percentage of lymphocytes detected inside the tumor mass in proximity to the tumor cells was ≥10%, regardless the presence of lymphocytes in the stromal area around the tumor border (Figure 2); (b) Group 2 ("immune-excluded" group) if the mean percentage of lymphocytes detected in the stromal area around the tumor border was ≥10%, but there was a negligible amount of lymphocytes inside the tumor mass (<10%) (Figure 3); and (c) Group 3 ("immune-desert phenotype" group) if the mean percentage of lymphocytes detected both in the tumor mass and in the stromal area was negligible (<10%) (Figure 4). Histological analysis of immune-phenotype was performed by two pathologists independently, each author gave a judgment on the belonging of each specimen to a single class of immune-phenotype. Such independent scores were used to assess the degree of agreement between the observers by calculating a Cohen's Kappa. Subsequently a joint session with a third researcher was scheduled in order to give a final judgment on the allocation of the specimen to a single class of immune phenotype in cases of disagreement between the

two pathologists; such final “score” was then used to perform all the other statistical analysis. Each specimen was analyzed three times. In order to perform an external analysis about the predictive capability of the immune phenotype in OTSCC, the Cancer Slide Digital Archie (CDSA) was accessed and analyzed. CDSA is a web-based platform, which collects digital pathological data from The Cancer Genome Atlas (TCGA) database. Codes were input on https://cancer.digitalslidearchive.org/ and pathological slides were analyzed and classified according to the abovementioned parameters. Clinic-pathological data were downloaded from Genomic Data Commons Data Portal (https://portal.gdc.cancer.gov/), and patients who underwent neoadjuvant therapy were excluded from the analysis.

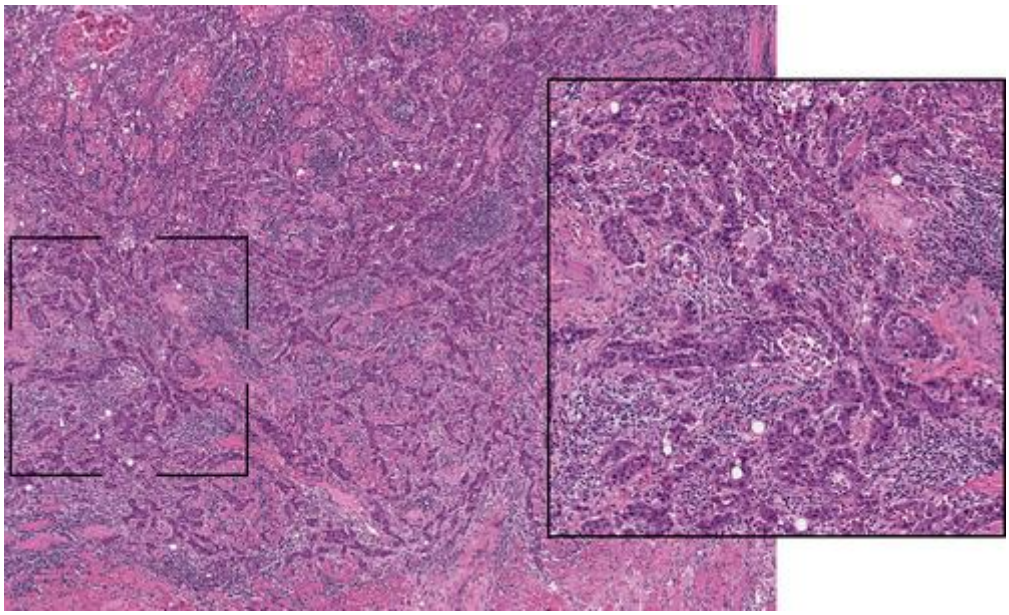

Figure 2: Representative pictures of immune-inflamed phenotype in oral tongue squamous cells carcinoma (hematoxylin-eosin staining, ×20 magnification). The inset area of greater magnification showed the presence of a dense T cell infiltrate both in the tumor mass and in the stromal area.

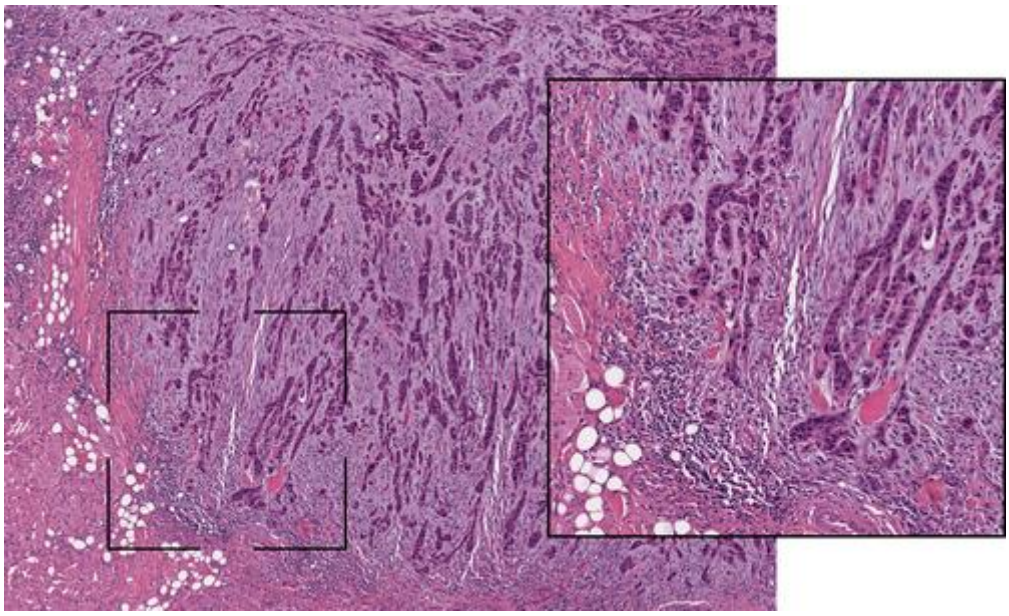

Figure 3: Representative pictures of immune-excluded phenotype in oral tongue squamous cells carcinoma (hematoxylin-eosin staining, ×20 magnification). The inset area of greater magnification showed the presence of a T cell infiltrate only in the stromal area around the tumor border.

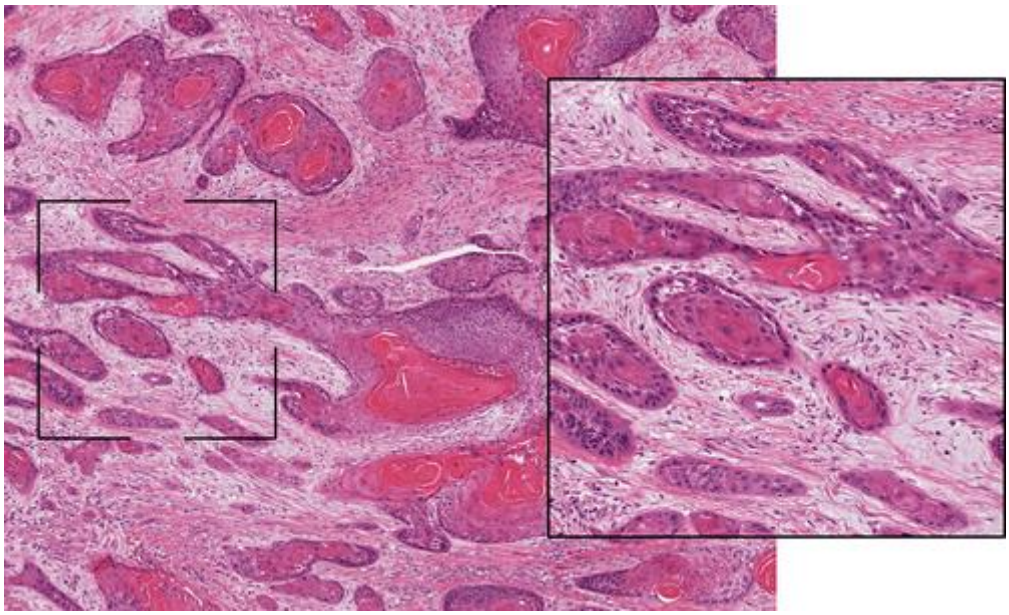

Figure 4: Representative pictures of immune-desert phenotype in oral tongue squamous cells carcinoma (hematoxylin-eosin staining, ×20 magnification). The inset area of greater magnification showed the presence of a negligible number of lymphocytes both in the tumor mass and in the stromal area.

2.2.3. Perineural Invasion

Hematoxylin and eosin (HE)-stained sections obtained from formalin-fixed, paraffin-embedded blocks of the primary tumor specimens, were considered in this study. For each case, we detected the block carried out from the most invasive part of the primary tumor. From each selected block, 5 HE-stained slides (4 μm) were examined (i.e., the same slides routinely used to assess the depth of invasion status). The slide with the highest number of discrete sites of PNI was selected for each case. Negative cases were defined if no PNI foci were found in the tumor sections. In this study, a senior head and neck cancer pathologist and an associated trained head and neck pathologist with 6 years of experience, independently performed the histological evaluation, blinded to the clinical and pathological data. The independent scores were used to assess the degree of agreement between the observers according to Cohen's kappa.

Perineural invasion was visually assessed as previously reported by Liebig et al. [25]. Briefly, the presence of PNI was reported when cancer cells were identified in any of the 3 layers of the nerve sheath (endoneurium, perineurium, and epineurium) and/or tumor was near the nerve, involving at least one-third its circumference. The total number of PNI foci in the entire sampled specimen was counted. Unifocal PNI was defined as involvement of a single nerve twig, while multifocal PNI was defined as involvement of ≥2 nerve twigs in any part of the specimen. Multifocal PNI also included the involvement of multiple nerve twigs in the same area that cannot be explained by the tortuous course of the nerve or tangential sectioning alone (Figure 5). Patients were classified in a dichotomous manner as PNI-positive or PNI-negative [26]. Furtherly, in order to investigate PNI characteristics, patients were also classified according to the PNI localization as being intratumoral and/or peritumoral and according to the involved number of foci, for such feature patients are usually classified as unifocal (1 focus) or multifocal (>1 foci) [27, 28]. In addition, we also classified samples according to Wei et

al. [29] and Chinn et al. [30], since such authors proposed an additional subclassification according to the number of foci. At last, patients were stratified according to the PNI status and T-status as already reported by Subramaniam et al., [31].

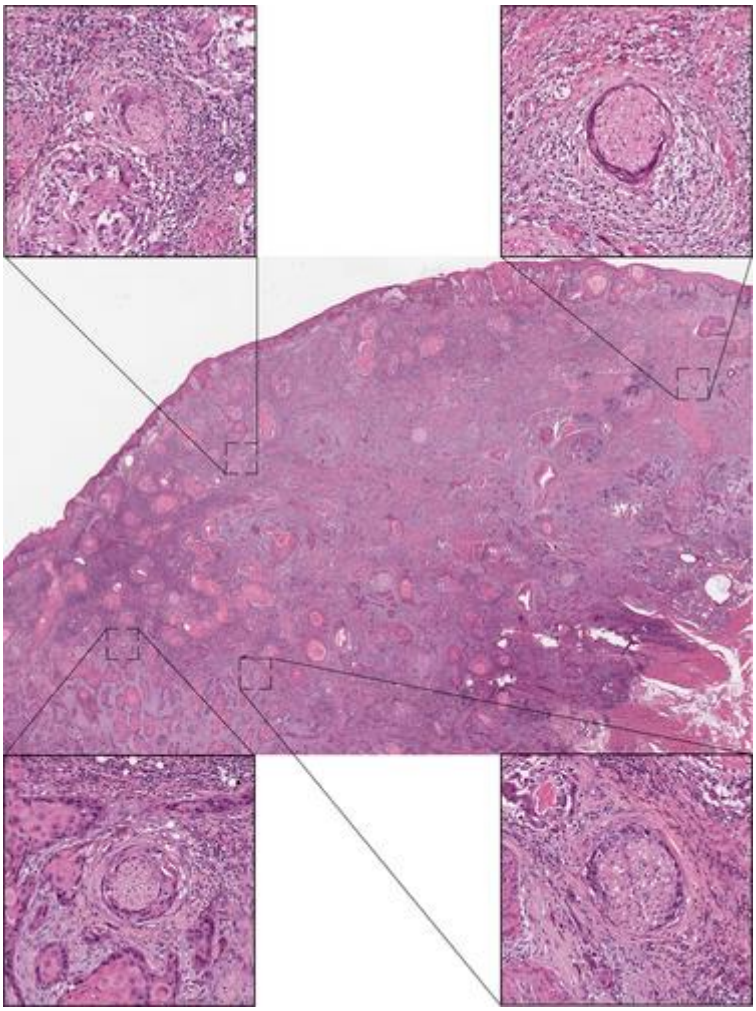

Figure 5: Evaluation of Perineural Invasion in OTSCC: representative pictures of squamous cell carcinoma encircling the nerve trunk (HE-staining, ×20 magnification)

2.2.4. Tumour Budding

Hematoxylin and eosin (HE)-stained sections obtained from formalin-fixed, paraffin-embedded blocks of the primary tumour specimens were considered in the study. Two pathologists independently performed the histological evaluation, blinded to the clinical and pathological data. The block included the most invasive part of the primary tumour

was selected for each case. From each selected block, a 4-µm-HE slide was carried out (i.e., the same routinely used to assess the depth of invasion status).

TB was visually assessed as previously reported [32]. Briefly, the slide was initially scanned at ×40 magnification (×4 objective lens and ×10 ocular) using an Olympus BM50 light microscope (Olympus), to select the area with the greatest number of budding foci. Subsequently, the number of budding foci was counted in one field along the tumoral infiltrative front at ×200 magnification (Figure 6). Patients were subsequently divided into two or three groups, according to the most used cutoff values reported in the literature. In particular, we used (TB1) a two-tier system with a single cutoff of 5 buds/field (low TB < 5/field, high TB ≥ 5/field) [33]; (TB2) a two-tier system with a single cutoff of 3 buds/field (low TB < 3/field, high TB ≥ 3/field) [32]; and (TB3) a three-tier system with two cutoffs of 5 and 10 buds/field (low TB < 4/field, intermediate TB = 5–9/field, high TB ≥ 10/field) [34]. Furthermore, two other combined models were investigated: (d) the BD model, using TB and DOI values (BD0: DOI < 4 mm and TB < 5 buds, BD1: DOI ≥ 4 mm and TB < 5 buds/field or DOI < 4 mm and TB ≥ 5 buds/field, BD2: DOI ≥ 4 mm and TB ≥ 5 buds/field) [35]; and (e) the revised-Grading (RG) system, using TB and pathological grading (RG1: G1 tumor without TB, RG2: G2 tumor with TB < 5 buds/field, RG3: G3 tumor with TB ≥ 5 buds/field) [36]. Therefore, in addition to considering TB as a continuous variable, 5 different methods to count TB were evaluated. The independent scores were used to assess the degree of agreement between the observers according to Cohen's kappa. Subsequently, for each case, the mean value of TB provided by the pathologists was used.

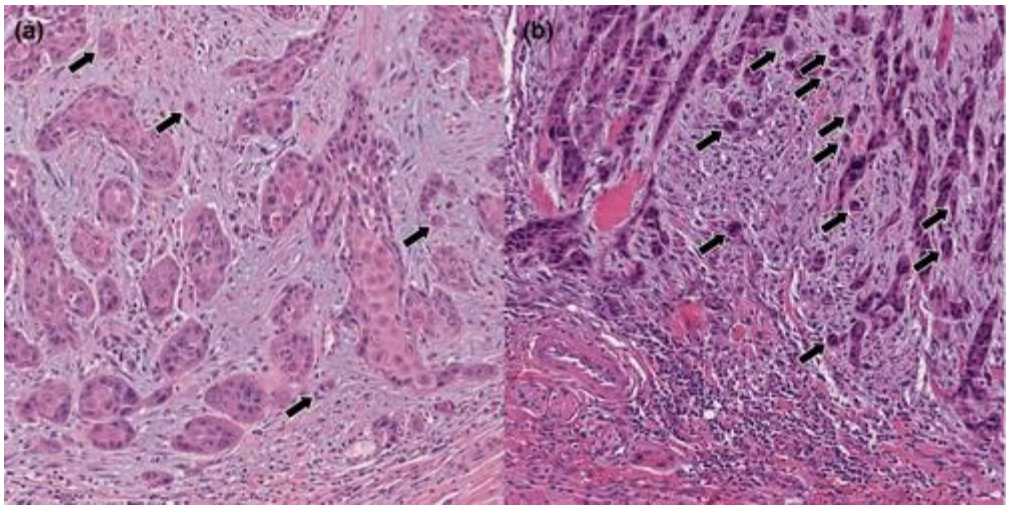

Figure 6: Evaluation of tumour budding in hematoxylin and eosin-stained sections of oral tongue squamous cell carcinoma with **(a)** low number of tumour buds (×200 magnification); **(b)** high number of tumour buds (×200 magnification). The arrows indicate the tumor budding foci.

2.2.5. Tumor-Associated Tissue Eosinophilia

Routine 4 μm hematoxylin and eosin (H&E)-stained sections were obtained from formalin-fixed, paraffin-embedded blocks of the primary tumor specimens. Histological slides were selected from the most invasive part of the OTSCC, used to assess the T status. For each patient, one H&E-stained section was considered. Two pathologists independently performed the evaluation of tumour-associated tissue eosinophilia (TATE), blinded to the clinic-pathological data. Only mononuclear cells with eosinophilic cytoplasmic granules were considered. Eosinophils located within extensive necrotic areas and blood vessels were excluded from the analysis. At the invasive front, the number of eosinophils around the tumor border and inside the tumor mass in proximity to the tumor cells was manually estimated for each case. Eosinophils were counted under a high-power objective (×400 magnification) using an Olympus BM50

light microscope (Olympus), which is equivalent to 0.237 mm^2 in a 22 mm field of view. The number of eosinophils per square millimeter was evaluated by using two methods, according to the literature [37-39]. In the density method, called TATE-1, a single high-power fields (HPF) area containing the highest eosinophil numbers that could be found in the tumor was counted; while in the classical method, called TATE-2, 10 randomly HPF areas were analyzed for each case (Figure 7). For each of the 2 methods tested, patients were subsequently divided into two or three groups, according to the most used cutoff values reported in literature [38, 39]. In particular, we used: (A) a single cutoff of 67 eosinophils/mm^2 (low TATE = 0–67/mm^2, high TATE>67/mm^2); (B) a single cutoff of 100 eosinophils/mm^2 (low TATE = 0–100/mm^2, high TATE>100/mm^2); (C) two cutoffs of 10 and 100 eosinophils/mm^2 (low TATE = 0–10/mm^2, medium TATE = 11–100/mm^2, high TATE>100/mm^2); and (D) two cutoffs of 50 and 120 eosinophils/mm^2 (low TATE = 0–50/mm^2, medium TATE = 51–120/mm^2, high TATE>120/mm^2). Therefore, 8 different methods to count TATE were considered, namely TATE-1a, TATE-1b, TATE-1c, TATE-1d, TATE-2a, TATE-2b, TATE-2c, and TATE-2d.

Interobserver agreement was calculated using Cohen's Kappa statistics. Subsequently, for each case the mean value of TATE provided by both pathologists was used as the final score.

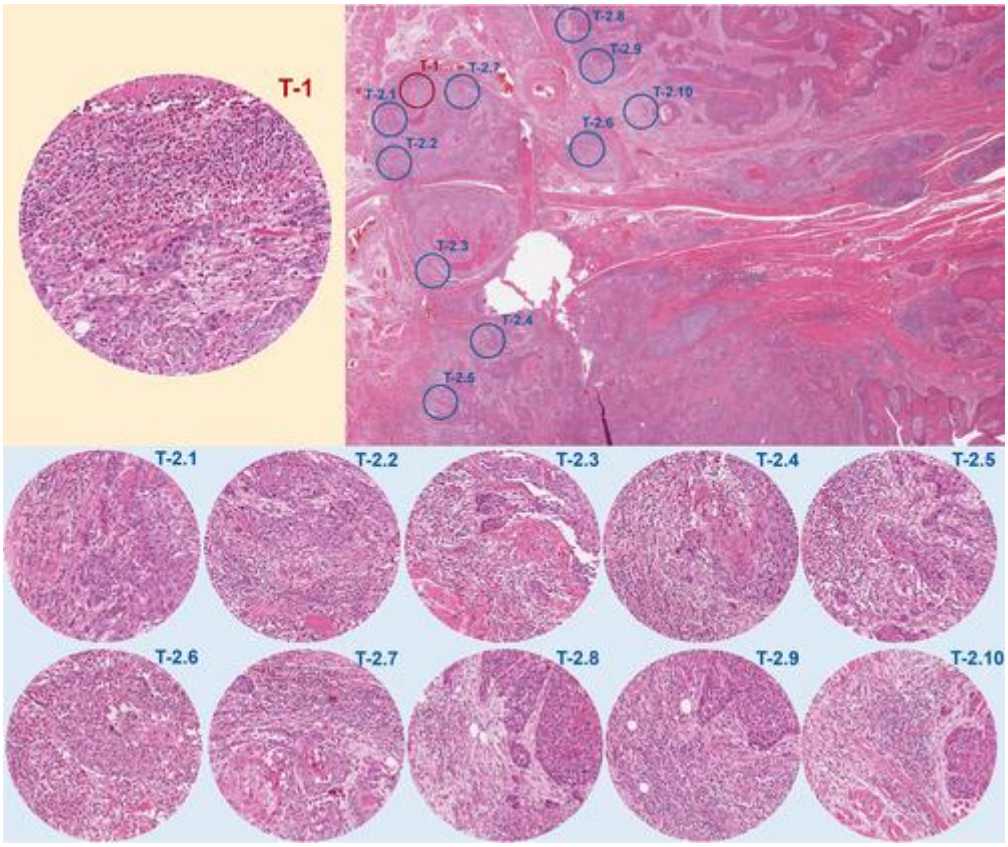

Figure 7: Description of the two main methods for TATE counting in OTSCC: a representative image of H&E-stained section of OTSCC, focused on low magnification (top right panel). The red circle area is the area containing the highest eosinophil numbers at the invasive front for the evaluation of eosinophils according to TATE-1, or density, method (top left panel, ×400 magnification). The blue circled areas represent the 10 HPF randomly selected at the invasive front for the evaluation of eosinophils according to TATE-2, or classical, method (bottom panel, ×400 magnification).

2.2.6. Statistical analysis

All the statistical analyses were performed by using the following tools: SPSS 21.0 (IBM Corporation) and Stata 16.0 (StataCorp LLC). Variables were tested for normal distribution by Shapiro–Wilk test. Aiming to analyze correlations among clinic-pathologic variables, Chi-square test was used for dichotomous variables, while for linear variables, Mann–Whitney, Kruskal–Wallis, or ANOVA test was applied. Post hoc Bonferroni–Holm false discovery rate was applied to correct for multiple comparisons,

when applicable. Univariate Cox Regression analysis was used to estimate the association among variables. In addition, a multivariate Cox proportional hazard model was built to assess the prognostic capability of predictive variables. In detail, the statistically significant variables in univariate survival analysis were used to build a multivariate Cox regression model; the proportional hazard assumption was checked with the test of nonzero slope in a generalized linear regression of the scaled Schoenfeld residuals on time (estat command on Stata 16.0). In addition, aiming to investigate the best predictive model for categorization, measurements of prognostic performance (Harrell's c-index) and model fit (Akaike Information Criterion and Bayesian Information Criterion) were calculated for the different thresholds on both univariate and multivariate survival models. At last, stepwise backward binary regression investigated the relation among these variables and certain outcomes. A modified approach of Sahoo et al. was appled, by putting in the stepwise backward multivariate method only the clinic-pathological variables that resulted statistically significant at univariate analysis, while α value for p-value in the stepwise backward model was set to 0.157 as suggested by Heinze et al. [40, 41].

2.3. Results

2.3.1. Tumour-Stroma Ratio

A total of 211 samples from OTSCC patients admitted to and treated at the Department of Maxillofacial Surgery, 'Ospedali Riuniti' General Hospital, Ancona, Italy, in the period between 1997 and 2014, were included in this study. All these patients had been staged according to the 7th edition AJCC staging system. In addition, 139 OTSCC patients were 'restaged' according to the 8th edition AJCC staging system, based on the information available about DOI and ENE. The retrospective analysis revealed a mean

follow-up time of 50.4 ± 36.8 months (range, 3–120 months). Furthermore, 44.5% (94/211) of patients died from OTSCC, 6.2% (13/211) died from cancer-unrelated reasons, and 49.3% (104/211) were alive at the last follow-up date. The results showed that 32.7% (69/211) of patients had locoregional recurrence, defined as disease recurrence in the local site or regional lymph node but not a secondary primary tumour, with a mean follow-up time of 52.6 ± 37.5 months (range, 8–120 months). Good interobserver agreement (Cohen $\kappa = 0.807$) was obtained by independent evaluation of the TSR by two authors, suggesting good reproducibility in the scoring of this histological variable. More details on the clinicopathological data of patients included in the cohort are shown in Table 1 of respective published paper [42]. No significant relationships were found between the TSR (both as a continuous variable and as a categorical variable) and other clinicopathological variables (WHO grade, PNI, sex, pT stage, and pN stage). PNI significantly correlated with pN in the 7th edition AJCC staging system ($\rho = 0.319$, $P = 0.003$) and pT in the 7th edition AJCC staging system ($\rho = 0.256$, $P < 0.001$); in addition, a correlation between pN and pT in the 7th edition AJCC staging system was found ($\rho = 0.186$, $P = 0.008$). Survival analysis was first performed for the whole group of 211 OTSCC patients according to the 7th edition AJCC staging system, and then repeated for the subgroup of 139 restaged OTSCC patients according to the 8th edition AJCC staging system. Stage, WHO grade, the TSR, PNI and male sex were significantly correlated with worse DSS and OS and were included in the multivariate analysis. The results of the Cox proportional hazard model showed that patients with stroma-rich (low TSR) OTSCC had significantly decreased DSS, with a hazard ratio (HR) of 1.598 and a 95% confidence interval (CI) of 1.034–2.745 ($P = 0.036$), and poor OS (HR = 1.685, 95% CI 0.998–2.560; $P = 0.051$), as compared with patients with stroma-poor (high TSR) tumours (Figure 8).

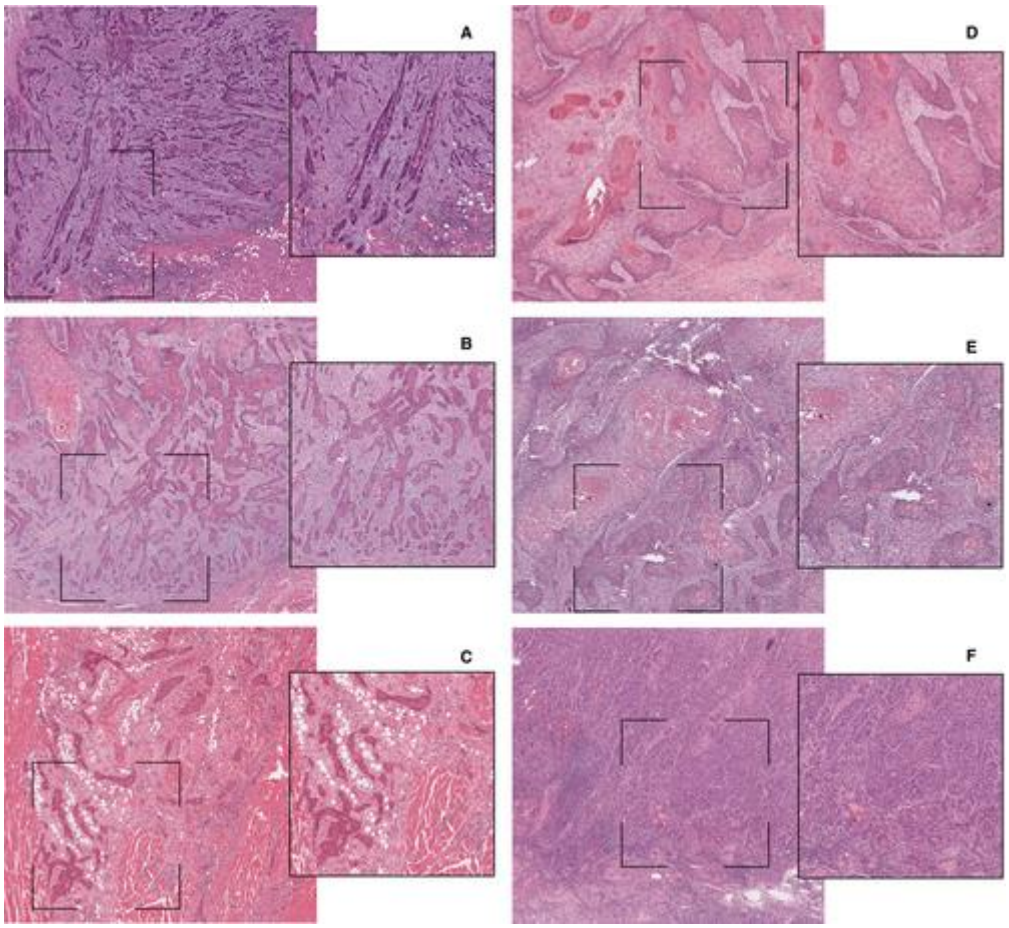

Figure 8: Evaluation of the tumour–stroma ratio (TSR) in hematoxylin and eosin-stained sections of oral tongue squamous cell carcinoma. **A–C**, Three examples of stroma-rich tumours. The inset areas of greater magnification showed a TSR of <50%. **D–F**, Three examples of stroma-poor tumours. The inset areas of greater magnification showed a TSR of ≥50%.

Among the predictors included in the multivariate analysis stage, PNI, male sex and advanced age showed significant associations with survival outcomes, whereas WHO grade was not significantly correlated with DSS or OS. Age was entered as a continuous variable, and an association was found between a progressive increase in patient age and a worse survival outcome. The same multivariate model was built with DFS as the outcome; however, none of the predictors was significant. On the basis of these results, we performed multivariate survival analysis for the subgroup of 139 patients restaged according to the 8th edition AJCC staging system. As WHO grade did not correlate with survival in the multivariate models, we decided to exclude it from the subsequent

analyses. Thus, Cox proportional hazard models were built for DSS, OS, and DFS, including stage (8th edition AJCC staging system), sex, age, PNI, and the TSR. Also, for this group of patients, for whom results were adjusted according to the 8th edition AJCC staging system, the TSR correlated with both DSS (HR = 1.883, 95% CI 1.033–3.432; P = 0.039) and OS (HR = 1.747, 95% CI 0.967–3.154; P = 0.044).

2.3.2. Immune Phenotype

A total of 211 OTSCC patients' samples admitted and treated at the Department of Maxillofacial Surgery, “Ospedali Riuniti” General Hospital, Ancona, Italy, in the period between 1997 and 2014 were included in this study. All these patients had been staged according to the 7th AJCC staging system. In addition, for 139 OTSCC patients' information about DOI and ENE were available, and patients were “restaged” according to the 8th AJCC staging system. In the total cohort of 211 patients, (137/211) 64.9% were males and (74/211) 35.1% were females; the average age of the cohort was 64.15 ± 14.1 years. The histological analysis revealed as most of OTSCC tumors had an immune-excluded phenotype (109/211, 51.7%), inflamed tumors represented the second most common groups (77/211, 36.5%), while immune-desert OTSCC were the less represented group (25/211, 11.8%). Details on other clinic-pathological characteristics of the studied cohort are available in the original manuscript [43]. No significant correlation was detected between immune-phenotype and patients' clinic-pathological variables, such as stage, grading, sex, and perineural invasion.

Results of univariate survival analysis performed on the whole cohort of 211 patients showed that OTSCC patients with an immune-desert phenotype had lower likelihood of survival compared to the other groups: DSS (HR = 2.309; [CI: 95% 1.335-3.995]; P = .003), OS (HR = 2.308; [CI: 95% 1.352-3.939]; P = .002), and DFS (HR = 2.241; [CI: 95% 1.139-4.411]; P = .020). Univariate Kaplan-Meier curves for DSS, OS, and DFS in

our cohort and curves for OS and DFS for TCGA cohort are shown in Figure 9.

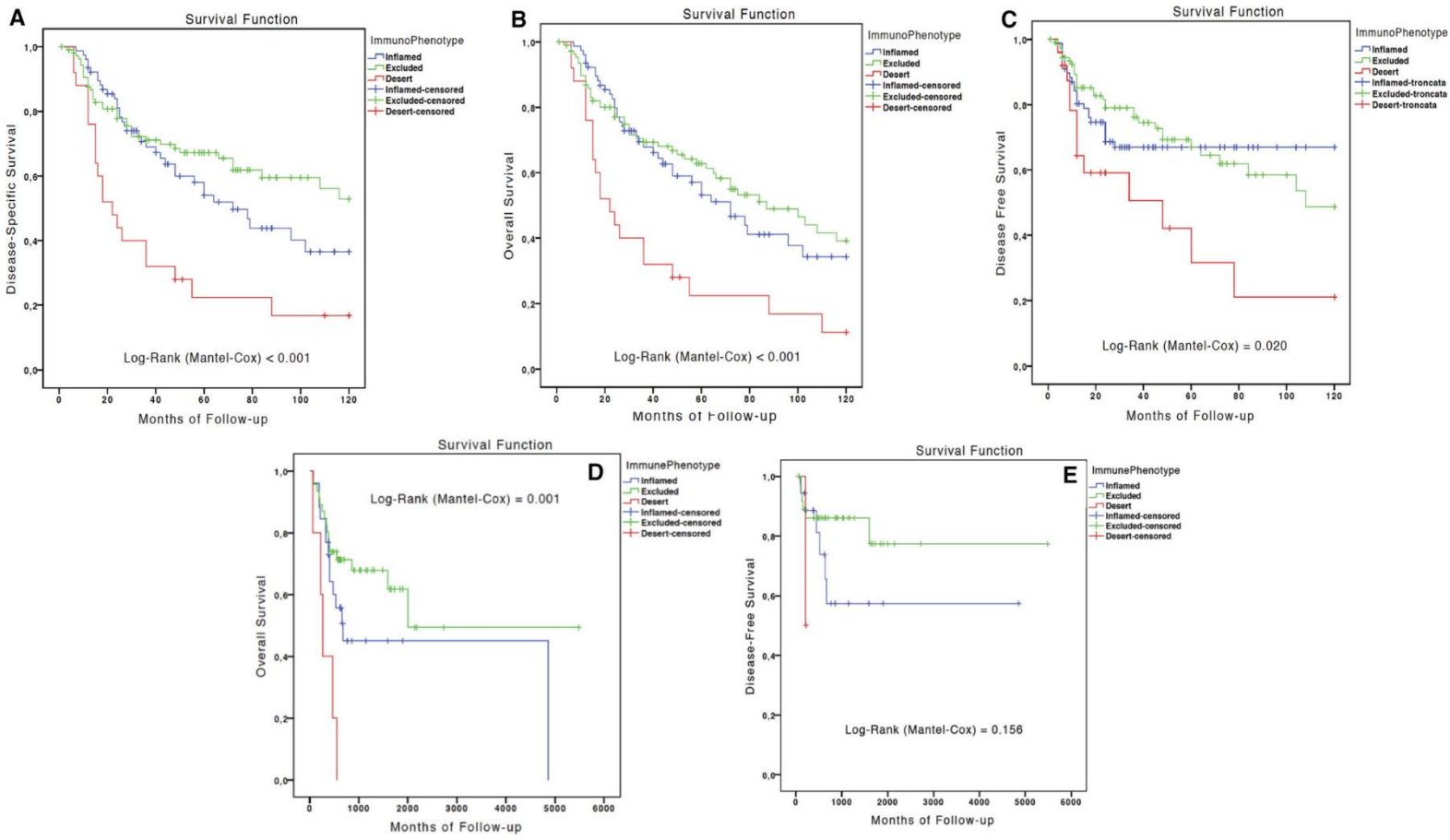

Figure 9: Kaplan-Meier curves for disease-specific survival **(A)**, overall survival (OS) **(B)**, and disease-free survival (DFS) **(C)** in the Italian cohort; and OS **(D)** and DFS **(E)** in the The Cancer Genome Atlas cohort.

Other variables that significantly influence OS and DFS at univariate analysis were: 7th AJCC stage, grade, perineural invasion, age, and gender. Based on these results, a multivariate Cox proportional hazard model was built including the significant variables (immune-phenotype, 7th AJCC stage, grade, perineural invasion, and gender). Results of such multivariate analysis confirmed the significant association between immune-desert phenotype and both DSS (HR = 2.673; [CI: 95% 1.497-4.773]; P = .001) and OS (HR = 2.591; [CI: 95% 1.468-4.572]; P = .001). In addition, applying the same multivariate model, the immune-desert phenotype resulted to be an independent prognostic factor for

DFS (HR = 2.313; [CI: 95% 1.118-4.786]; P = .024). It is worth noting that tumor grade lost its statistical significance in the multivariate model, while 7th AJCC Stage, perineural invasion, and gender all resulted to correlate with a worse DSS.

Next, a new model which excluded tumor grade from analysis was built for the subgroup of 139 patients "restaged" according to the 8th AJCC staging system; similarly, results of this analysis revealed a significant worse DSS (HR = 2.280; [CI: 95% 1.107-4.696]; P = .025) and OS (HR = 2.299; [CI: 95% 1.115-4.742]; P = .024) for immune-desert patients. Regarding DFS, results for the immune-desert phenotype were close to the threshold of statistical significance (HR = 2.146; [CI: 95% 0.941-4.893]; P = .070), while none of the other clinic-pathological variables correlated with a worse DFS. To analyze the results obtained on our internal cohort, digital pathological slides and clinical data from the TCGA database were evaluated from the same researchers who performed the analysis on authors' cohort. A total of 76 patients' code from Head and neck TCGA database fulfilled the inclusion criteria and were included in the analysis. In this cohort of patients, immune-desert OTSCCs showed a worse prognosis at univariate analysis: OS (HR = 3.354; [CI: 95% 1.187-9.479]; P = .022). However, due to the limited number of immune-desert phenotype obtained from the TCGA database, these results were not significant at the multivariate analysis OS (HR = 2.634; [CI: 95% 0.615-11.272]; P = .192). Indeed, all the five immune-desert patients were classified in Stage 4; therefore, multivariate analysis was unable to determine whether the poor prognosis was due to the advanced stage or the immune-desert phenotype. Taken together, these results demonstrate that the immune-phenotype, particularly immune-desert tumors, is an independent prognostic factor in OTSCC patients.

2.3.3. Perineural Invasion

Histopathological slides were available for 200 patients with diagnosis of OTSCC. All patients were tested for HPV infection and none of them resulted positive. Mean age of included patients was 64.6 ± 14.0 (range 23–93 years). Of the total number, 126 were male (63%) versus 74 (37%) female patients. According to the AJCC 8th staging system, 38 patients were Stage 1, and 59 were Stage 2, while 56 and 47 patients belonged respectively to Stage 3 and 4. According to PNI, 119 patients were negative; meanwhile, 40, 19, and 22 patients had intratumoral, peritumoral, and both intra/peritumoral PNI, respectively. By using a dichotomous score (PNI-positive and PNI-negative), we obtained excellent interobserver agreement (Cohen $\kappa = 0.885$). Of these PNI-positive patients, in 25 there was focal PNI, while 56 patients reported multifocal PNI (>1 foci), obtaining a good interobserver agreement (Cohen $\kappa = 0.745$). Patients with multifocal PNI reported a mean of 3.09 ± 1.16 foci with a minimum of 2 and a maximum of 6 foci. Clinic-pathological variables are summarized in the original published manuscript [44].

Linear clinic-pathological variables were firstly explored by Spearman rank correlation analysis. Number of PNI foci positively correlated with tumor thickness ($\rho = 0.342$; p-value < 0.001), T Staging system status ($\rho = 0.277$; p-value < 0.001), Grading ($\rho = 0.220$; p-value = 0.002), WPOI ($\rho = 0.197$; p-value = 0.005), N Staging system status ($\rho = 0.180$; p-value = 0.011), and Staging 8th AJCC system ($\rho = 0.297$, p-value < 0.001).

Chi-square test was used to further explore differences among groups. Firstly, PNI was considered as a dichotomous variable, as present or absent. Chi-square test showed a statistically significant difference among various tumor grades and number of PNI-positive/negative tumors (Chi-square test, p-value = 0.013). When adjusting p-value for multiple comparisons, higher number of PNI-positive tumors was observed in patients with grade 3 tumors (p-value = 0.0035). Number of positive/negative PNI tumors statistically differed among T-status (Chi-square test, p-value < 0.001). When adjusting

p-value for multiple comparisons, a higher number of positive PNI tumors was observed in T3 tumors (p-value = 0.0001) and T4 tumors (p-value > 0.05); while considering DOI, positive PNI tumors showed also higher DOI (Chi-square test, p-value = 0.001; 23/35 positive PNI with DOI >10 mm; 52/72 negative PNI with DOI ≤5 mm).

Of interest, LVI was more observed in PNI-positive tumors (Chi-square test, p-value < 0.001), in particular higher number of LVIs were reported together with intratumoral PNI when adjusting p-values for multiple comparison (p-value = 0.00002–14 intratumoral PNI over 28 positive LVI tumors).

Higher number of positive PNI tumors were noticed in patients with N-positive lymph–node metastasis (Chi-square test, p-value = 0.017). When furtherly exploring this variable according to the topographical classification of PNI, Chi-square test p-value resulted 0.009 counting 24 intratumoral PNI-positive tumors over 74 patients with N-positive status (adjusted p-value for multiple comparison = 0.00076).

At last, a distinct number of PNI-positive tumors came out among patients with particular Staging system status (Chi-square test, p-value < 0.001). Adjusted p-value for multiple comparison showed a higher number of negative PNI tumors in Stage 1 patients (p-value = 0.0066—30 negative PNI tumors over 38 Stage 1 patients) and a higher number of positive PNI tumors in Stage 4 patients (p-value = 0.00681—27 positive PNI tumors over 47 Stage 4 patients; α p-value for this multiple comparison = 0.00625).

Number of foci seemed to be associated to LVI; in particular, Mann–Whitney analysis showed a statistically significant difference between patients with positive (2.11 ± 0.28) and negative (0.81 ± 0.11) LVI patients (p-value < 0.001). Patients with positive N-status lymph–node metastasis reported a higher number of PNI foci (positive N-status, 1.27 ± 0.19 versus negative N-status, 0.83 ± 0.12; Mann–Whitney test, p-value = 0.027). When considering N-status lymph–node metastasis in grades, Kruskal–Wallis test reported a p-

value of 0.020 with an increasing number of foci from N0 to N2 (respectively mean value of 0.82 ± 0.13; 0.91 ± 0.25; 1.61 ± 0.23). Since only 1 patient reported N3 status, Bonferroni post hoc comparison was not applicable. Kruskal–Wallis test also showed a higher number of PNI foci in patients with higher grades of tumor grading system (G1 mean value of 0.76 ± 0.24 versus G2 mean value of 0.79 ± 0.12 versus G3 mean value of 1.66 ± 0.25, Kruskal–Wallis test p-value = 0.003) (Bonferroni post hoc correction G1 versus G2 p-value = 1.0, G1 versus G3 p-value = 0.017, G2 versus G3 p-value = 0.001). Similar results turned up when evaluating WPOI (Kruskal–Wallis test, p-value = 0.05). Concerning 8th AJCC Staging system, greater number of PNI foci were found in higher stages (Kruskal–Wallis test, p-value < 0.001). Stage 4 reported highest mean value of 1.51; against Stage 1 mean value of 0.47; (p-value = 0.007) and Stage 2 mean value of 0.63; (p-value = 0.011). Stage 3 reported a mean value of 1.30; (p-value = 1.0).

Follow-up period was available for all the 200 patients included in the study. Minimum follow-up period reported was 6 months against a maximum of 120 months. Mean follow-up period was 51.81 ± 36.40 months and a median of 41 months.

Statistically significant variables at Univariate analysis were included in the Multivariate Cox Regression analysis. Sex, LVI, treatment modalities, and staging significantly influenced DSS at univariate analysis, while age resulted close to significant level. In multivariate analysis, these variables were included to evaluate the prognostic value of PNI. Tumours with positive PNI reported a worse DSS (Hazard Ratio (HR) = 1.996, 95% C.I. 1.241–3.211, p-value = 0.004). When considering patients according to PNI localization, patients reporting both intra- and peritumoral PNI had poorest DSS (HR = 2.713, 95% C.I. 1.372–5.367, p-value = 0.004). Effects of number PNI foci were investigated in a dichotomous approach [26] and according to Wei et al. [29] and Chinn et al. [30] classifications. Although the promising results coming from multivariate

analysis, only 3 patients reported a number of foci greater of 5 (Wei et al. DSS, HR = 6.530, 95% C.I. 1.403–30.403, p-value = 0.017 – Chinn et al. DSS, HR = 6.508, 95% C.I. 1.392–30.422, p-value = 0.017). When applying dichotomous categorization (focal versus multifocal), patients with multifocal PNI reported statistically significant poor DSS (HR = 2.001, 95% C.I. 1.183–3.384, p-value = 0.010). Patients with tumours with focal PNI reported also worse DSS compared to patients without PNI (HR = 1.987, 95% C.I. 1.047–3.772, p-value = 0.036). A higher number of foci correlated with unfortunate events when the number of PNI foci was entered as a continuous variable (HR = 1.434, 95% C.I. 1.225–1.678, p-value < 0.001). In addition, we grouped patients according to both location and number of PNI foci. In the multivariate analysis for DSS, patients with both intra- and peritumoral PNI and a number of foci greater than one reported a statistically significant worse survival (HR = 2.700, 95% CI 1.362–5.352, p-value = 0.004). Based on these results, patients with multifocal and contemporary presence of intra- and peritumoral PNI were considered at high risk of death and were reclassified upstaging the 8th AJCC edition in three different ways: all patients belonging to any stage, but showing multifocal with both intra- and peritumoral PNI, were upstaged by one, two classes or to stage 4 from any stage. We obtained three new staging systems. AJCC 8th staging system edition reported the following values of Harrell's C-statistic 0.6787, AIC 846.9044, and BIC 866.6943. All the three new staging systems reported better values of stratification performance (data not shown). In particular, when upstaging patients with multifocal and intra- and peritumoral PNI from any stage to Stage 4, this model outperformed the others, marking a Harrell's C-statistic value of 0.7022, AIC of 838 and BIC of 858, showing an overall improvement of the prognostication [45, 46]. Results from multivariate Cox Regression survival analysis for DSS of AJCC 8th Staging system versus the new developed system, including PNI, are shown in Figure 10. When

evaluating Harrell's C-statistic, AIC, and BIC in univariate analysis, same improvement was confirmed (AJCC 8th edition Harrell's C-statistic = 0.6317, AIC = 857 and BIC = 867; new staging system Harrell's C-statistic = 0.6679, AIC = 847 and BIC = 857).

Figure 10: Regression survival analysis for DSS according to the 8th Edition of the AJCC staging system **(A)** and the new system with PNI **(B)**.

Subramaniam et al. [31] classification was also applied to our cohort of patients for which different T-status was associated to PNI-positive/negative status. Similar results were obtained, showing positive PNI tumors related to a poorer DSS. When looking at single comparisons, patients with negative PNI in any T-status contrast (T2vsT1–T3vsT1–T4vsT1–T3vsT2–T4vsT2–T4vsT3) did not suffer of statistically significant worse DSS.

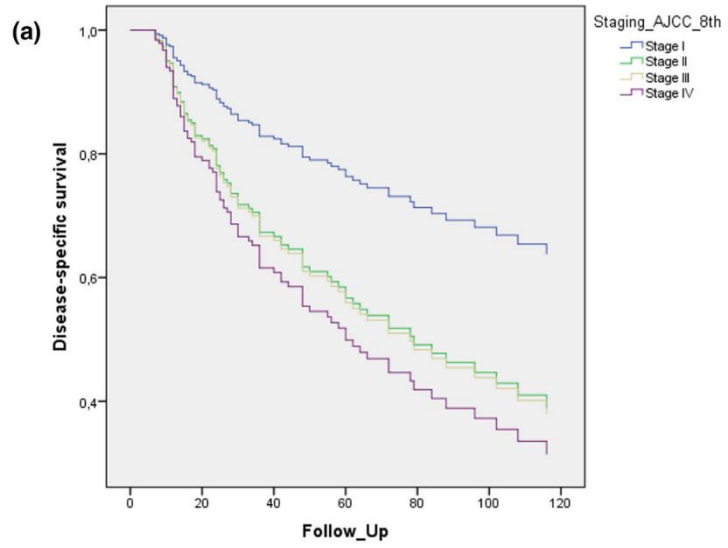

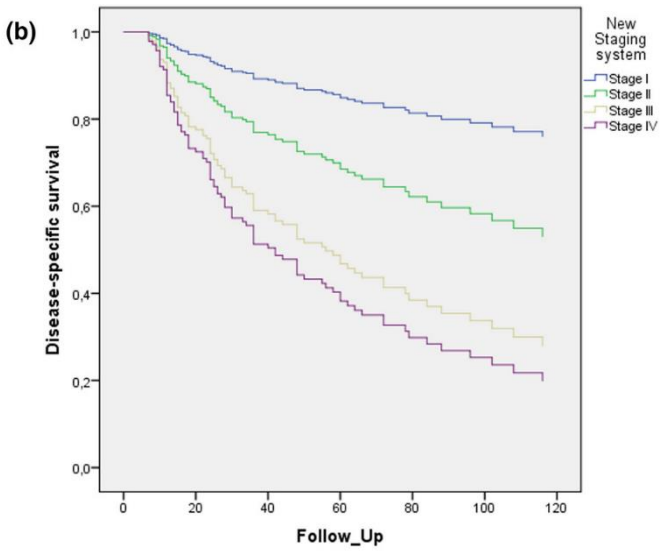

(a)	Sig.	Hazard Ratio	IC 95,0% Lower	IC 95,0% Upper
Age	,009	1,023	1,006	1,041
Sex	,084	,647	,394	1,060
Staging_AJCC_8th	,279			
Stage II vs Stage I	,073	2,101	,934	4,725
Stage III vs Stage I	,158	2,151	,744	6,219
Stave IV vs Stage I	,125	2,574	,769	8,611
LVI	,013	2,005	1,162	3,461
Treatment	,325			
Surgery + radiotherapy vs surgery alone	,424	1,460	,577	3,694
Surgery + radio-chemotherapy vs surgery alone	,145	2,622	,717	9,590

(b)	Sig.	Hazard Ratio	IC 95,0% Lower	IC 95,0% Upper
Age	,015	1,022	1,004	1,039
Sex	,113	,670	,408	1,100
New Stage system	,008			
Stage II vs Stage I	,077	2,307	,914	5,820
Stage III vs Stage I	,003	4,638	1,692	12,718
Stage IV vs Stage I	,001	5,870	2,087	16,511
LVI	,014	2,001	1,153	3,474
Treatment	,400			
Surgery + radiotherapy vs surgery alone	,635	,851	,437	1,657
Surgery + radio-chemotherapy vs surgery alone	,419	1,538	,542	4,364

Similarly, no significant differences were obtained in patients with positive PNI in any T-status contrast (T2vsT1–T3vsT1–T4vsT1–T3vsT2–T4vsT2–T4vsT3). Of interest, when comparing patients with same T-status tumors but negative versus positive PNI, only patients with T1 and T2 status showed statistically significant poor DSS (T1_PNIpositive versus T1_PNInegative p-value=0.032 – T2_PNIpositive versus T2_PNInegative p-value = 0.019). Of 200 patients, 66 relapsed (33%) in an average period of 23.6 months; of these, 51, 8, and 6 patients reported local recurrence, regional recurrence, or both, respectively, while only one patient had distant recurrence. In Univariate Kaplan–Meier analysis, none of clinic-pathological data shown statistically significant difference. Focusing on PNI, no differences emerged between negative and positive PNI tumors (p-value = 0.791). Same results were retrieved when considering PNI localization (intratumoral, peritumoral, or both – p-value = 0.858). Looking at number of foci, according to the different classification systems, none of them resulted to be significant (Wei et al. p-value = 0.788; Chinn et al. p-value = 0.822; dichotomous approach, p-value = 0.745); also, when considering number of foci as a linear variable, no difference in RFS was found (p-value = 0.592).

Logistic regression analysis was performed to ascertain the effects of age, sex, grading, margin status, LVI, T-status, and WPOI on the likelihood that participants have positive lymph–node metastasis at diagnosis. At the univariate analysis, Grading, WPOI, and PNI significantly influenced N-status (p-value < 0.05). Linear number of PNI foci and different categorizations (Wei et al.; Chinn et al; and dichotomous approach) and positive/negative PNI status were excluded in the multivariate binomial logistic regression with backward selection, since were not statistically significant associated to N-status. When PNI was considered as intratumoral, peritumoral, or both intra-peritumoral, the logistic regression model was completed in one step. The analysis found

that patients with G2 and G3 tumors were at higher risk of lymph–node metastasis (Odds Ratio (OR) G2 versus G1 = 2.301, 95% CI 0.891–5.941, p-value = 0.085; G3 versus G1 = 3.577, 95% C.I. 1.255–10.196, p-value = 0.017). In this model, PNI localization contributed to an increase of likelihood of exhibiting lymph–node metastasis, in particular patients with intratumoral PNI (OR = 2.996, 95% C.I. 1.354–6.630, p-value = 0.007), while both peritumoral or contemporary presence of intra-peritumoral PNI was not significantly associated to an increased risk (peritumoral PNI, OR = 1.043, 95% C.I. 0.355–3.063, p-value = 0.939 – intra-peritumoral PNI, OR = 0.751, 95% CI 0.264–2.135, p-value = 0.591). Moreover, high-grade WPOI tumors were more prone to determine lymph–node metastasis (OR = 2.611, 95% CI 1.369–4.982, p-value = 0.004). Slightly better results were achieved when considering patients according to both focal/multifocal and intratumoral/peritumoral or both intra-peritumoral PNI. In fact, patients with G2 and G3 tumors were at higher risk of lymph–node metastasis (G2 versus G1 OR = 2.273, 95% CI 0.878–5.888, p-value = 0.091; G3 versus G1 = 3.575, 95% CI 1.257–10.172, p-value = 0.017). High-grade WPOI tumors were more prone to determine lymph–node metastasis (OR = 2.633, 95% CI 1.377–5.033, p-value = 0.003). In this model, both focal and multifocal intratumoral PNI contributed to an increase of likelihood of exhibiting lymph–node metastasis, in particular for patients with focal intratumoral PNI (OR = 3.386, 95% C.I. 1.090–10.519, p-value = 0.035) and multifocal intratumoral PNI (OR = 2.740, 95% CI 1.027–7.316, p-value = 0.044). Intratumoral PNI, regardless of number of foci, together with grading and WPOI could be useful to predict patients at high risk of being diagnosed with lymph–node metastasis.

2.3.4. Tumour Budding

The study included 211 OTSCC surgical samples (detailed description, please refer to

published article [47], consisting of 135 males (64%) and 76 females (36%). The mean age at diagnosis was 64.7 ± 13.8 years (range: 23–93 years) and the mean tumoral diameter was equal to 2.5 ± 1.3 cm (range: 0.3–7 cm). All patients were tested for HPV infection and none of them resulted positive. According to the 8th Edition of AJCC staging system, 40 patients (19.0%) were Stage I, 60 (28.4%) were Stage II, while 51 (24.2%) and 60 (28.4%) patients belonged to Stage III and IV, respectively. According to 4th Edition of WHO Grading, 37 cases (17.5%) resulted well-differentiated tumors (G1), 115 cases (54.5%) were moderately differentiated (G2) and 59 cases (28%) showed a poor grade of differentiation (G3). Finally, perineural invasion (PNI), lymph-vascular invasion (LVI), and worst pattern of invasion (WPOI-5) were observed in 39.3%, 14.2%, and 4.7% of OTSCCs, respectively.

The mean count of TB was equal to 4.5 ± 5.0 (range: 0–26), and 38 patients (18%) did not exhibited TB. According to the two-tier system proposed by Seki et al. [34], a low and high TB were observed in 96 (45.5%) and 115 (54.5%) cases, respectively. In agreement with Wang et al. [33], 141 (66.8%) and 70 (33.2%) OTSCCs were scored as low and high TB, respectively. Using the three-tier system of Lugli et al. [32, 48], 141 cases (66.8%) were classified as low TB, 42 (19.9%) as intermediate TB, and 28 (13.3%) as high TB. According to BD model, 48 (22.9%), 103 (48.8%), and 60 (28.4%) patients were scored as BD0, BD1, and BD2, respectively. Regarding the RG system, 11 (5.2%), 92 (43.6%), and 108 (51.2%) cases were classified as RG1, RG2, and RG3, respectively. Locoregional recurrences occurred in 31.3% of cases after 24.0 ± 25.0 months from the initial surgical treatment (range: 3–108 months), while the 45.0% of patients died due to OTSCC whit a DSS equal to 31.8 ± 25.9 months (range: 3–116 months).

The Shapiro–Wilk test showed a non-normal distribution of TB ($p < 0.001$). A raw number of buds correlated with tumoral size, higher grade, advanced stage, and DOI. The

mean number of buds did not differ between male and female (Mann–Whitney p = 0.338), positive or negative LVI (Mann–Whitney p = 0.104), node positive or negative patients (Mann–Whitney p = 0.090) and the presence or absence of extra-nodal extension (ENE) (Mann–Whitney p = 0.105). Higher number of buds was found in higher G grading cases (Kruskal–Wallis p = 0.033; mean value G3 = 5.86 ± 5.76 vs G1 = 3.59 ± 4.64). Noteworthy, multifocal PNI tumors reported highest mean number of buds compared with patients without PNI (Kruskal–Wallis p < 0.001; mean value multifocal PNI = 7.07 ± 5.52 vs negative PNI = 3.41 ± 4.50). Finally, advanced Stage tumors showed higher mean number of buds (Kruskal–Wallis p < 0.001; mean value Stage IV = 5.25 ± 4.98 vs Stage I = 2.65 ± 4.52).

As a continuous variable, a significant association between TB and DSS was found (HR = 1.07, 95% CI: 1.04–1.11, p < 0.001). Similar results were obtained when TB was included in a multivariate model cohort (HR = 1.07, 95% CI: 1.03–1.11, p < 0.001) with other significant factors (Stage, Age, Sex, PNI, and LVI). Significant results were obtained also for the risk groups categorized according to Wang et al. both at univariate (HR = 2.38, 95% CI: 1.57–3.55, p < 0.001) and multivariate (HR = 2.21, 95% CI: 1.41–3.45, p < 0.001) analysis. Conversely, the model by Seki et al. was not able to predict DSS both at univariate (HR = 1.38, 95% CI: 0.91–2.07, p = 0.124) and multivariate (HR = 1.03, 95% CI: 0.66–1.60, p = 0.888) analyses. The model by Lugli et al. significantly predicted poor survival in OTSCC both at univariate and multivariate analysis. At univariate analysis, only BD2 group of BD model was associated with poor DSS compared with the BD0 patients, while no significant differences were detected between BD0 and BD1 groups. Focusing on the RG system, no significant differences were detected between the risk groups. Regarding the DFS, only the two-tier system proposed by Wang et al., correlated with poor DFS (p = 0.021) at the univariate analysis. Results

from Kaplan–Meier analysis of DSS regarding the TB scores and models are represented in Figure 11.

Figure 11: Kaplan–Meier analysis for disease-specific survival in oral tongue squamous cell carcinoma based on the different tumor budding scores and models. TB, tumor budding; RG, revised-grading.

To assess the prognostic stratification of models and to detect at baseline a future aggressive behavior of the disease, the prognostic performance of the included models was analyzed by Harrell's c-index. Results of the univariate analysis showed the model by Lugli et al. had the better prognostic stratification capability (c-index = 0.616), followed by the RG system (0.615) and the inclusion of the normal TB evaluation as a continuous variable (0.614). All the other models showed a lower prognostic

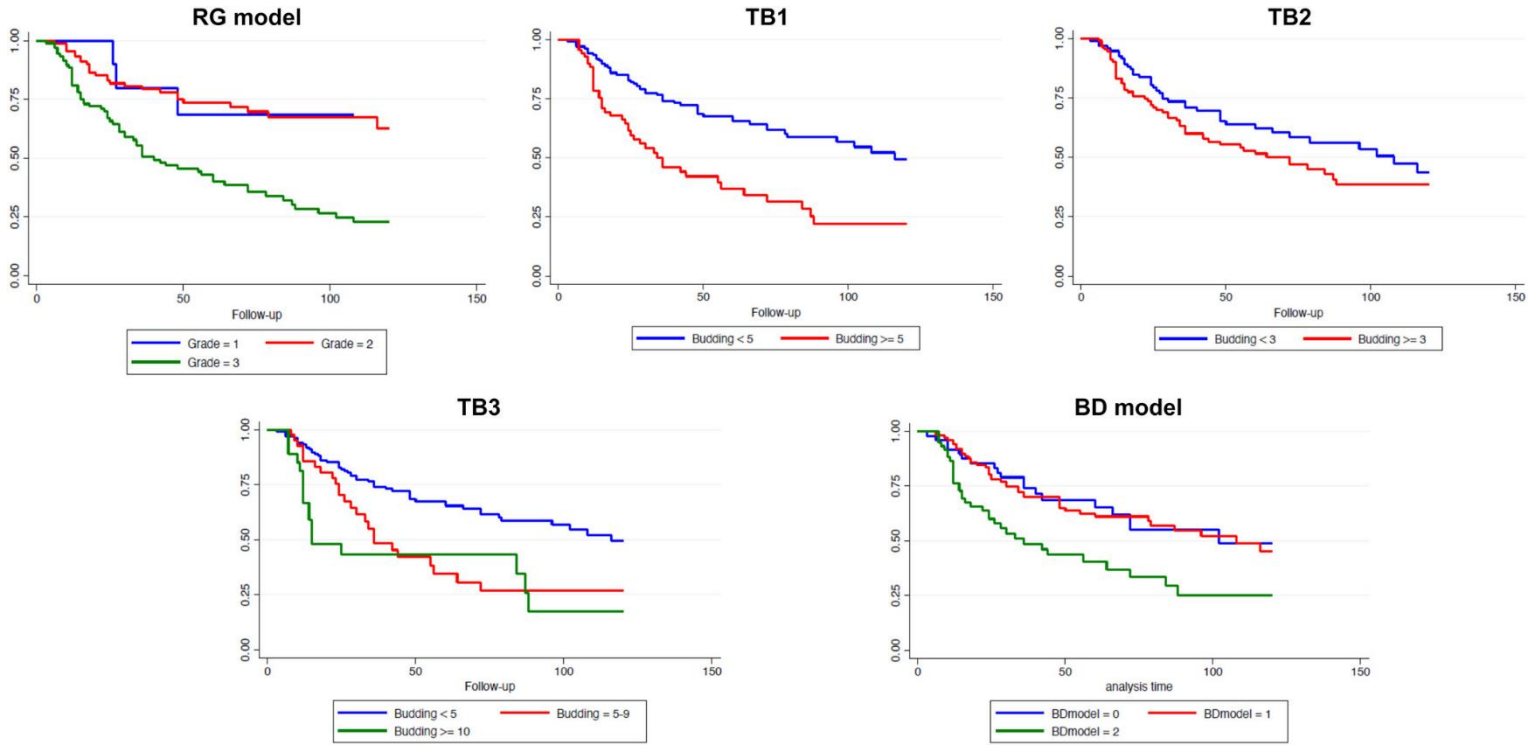

performance. In addition, the prognostic performance was also assessed in multivariate models with other known predictive variables resulting from a stepwise process.

Likewise, the model by Lugli et al. showed a better prognostic stratification capability (c-index = 0.739) compared with the others.

2.3.5. Tumour-Associated Tissue Eosinophilia

In the present study, 204 histological samples from OTSCC patients were analyzed. Overall, 204 cases 130 (63.7%) were males and 74 (36.3%) females, with a mean age of 64.6 ± 13.9 years (range 26–93). Regarding Stage groups according to 8th AJCC cancer staging system, 90 patients were staged as early OTSCC (Stage I-II) and 113 as advanced OTSCC (Stage III-IV). The histological analysis showed the presence of Perineural Invasion (PNI) and Lymph-vascular Invasion (LVI) in 80 (39.4%) and 29 (14.3%) patients, respectively. The retrospective analysis revealed a mean follow-up time of 51.5 ± 36.5 months (range 6–120). Results showed that 93 patients (45.6%) died from OTSCC, whereas 111 patients (54.4%) were alive at the last follow-up date or were dead for reasons other than OTSCC. Moreover, 66 patients (32.3%) demonstrated locoregional recurrence, defined as disease recurrence in the local site or regional lymph node but not secondary primary tumor, showing a mean follow-up time of 41.8 ± 35.3 months (range 3–120) for DFS. The morphometric analysis revealed a mean value of 182 and 76 eosinophils per mm2 for TATE-1 and TATE-2 methods, respectively, ranging from a minimum of 0/mm2 to a maximum of 1097/mm2 (TATE-1) and 539/mm2 (TATE-2).

As reported in the original manuscript [49], OTSCC patients were stratified based on TATE levels in the invasive front of tumors, according to different methods of eosinophil quantification and cutoff values. Moreover, good interobserver agreement was obtained by the independent evaluation of TATE by two pathologists, suggesting a good reproducibility in the scoring of this variable.

Spearman's rank correlation showed no statistically significant correlations between both

TATE-1 and TATE-2 with age. The raw number of TATE-1 and TATE-2 resulted statistically significant different between patients with LVI, while only a statistically significant lower number of eosinophils was found in stroma-rich tumors, according to TATE-2.

Concerning survival analysis, stage, PNI, treatment modalities, males, TATE-2a, TATE-1c, and TATE-1d were significantly correlated with a worse DSS, whereas only stage was associated with a worse DFS. Based on these results, a multivariate Cox proportional hazard model was built including the significant variables (Stage, PNI, sex, and treatment modalities). The results of the multivariate Cox proportional hazard model showed that, almost regardless of the method of eosinophil quantification or the cutoff values used, patients with high TATE had a significantly better DSS (Figure 12).

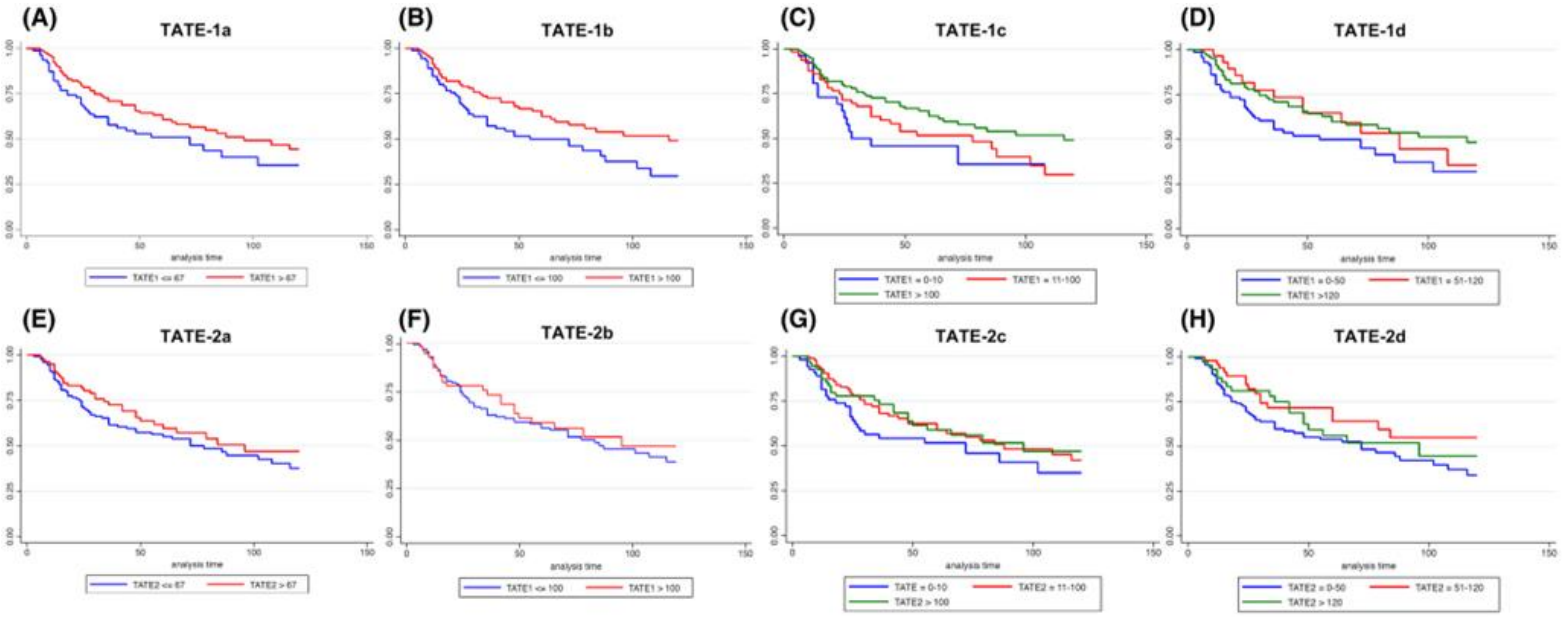

Figure 12: Kaplan-Meier curves according to TATE-1 (A-D) and TATE-2 (E-H) methods which were statistically significant for univariate DSS

In particular, High TATE showed the following values of hazard ratio (HR) and 95% confidence interval (CI): TATE-1a (HR = 0.58, 95% CI 0.37–0.90; p = 0.017); TATE-2a

(HR = 0.60, 95% CI 0.37–0.95; p = 0.030); TATE-1b (HR = 0.56, 95% CI 0.36–0.86; p = 0.009); TATE-1c (HR = 0.39, 95% CI 0.21–0.74; p = 0.004—Bonferroni adjusted p = 0.012); TATE-2c (HR = 0.44, 95% CI 0.24–0.81; p = 0.009–Bonferroni adjusted p = 0.027); TATE-1d (HR = 0.47, 95% CI 0.29–0.76; p = 0.002—Bonferroni adjusted p = 0.006); and TATE-2d (HR = 0.49, 95% CI 0.28–0.88; p = 0.018—Bonferroni adjusted p = 0.053). Harrell's C-statistic, Akaike information criterion (AIC), and Bayesian information criterion (BIC) were then used to compare the predictive performance of the different TATE evaluation methods and cutoff points. The worst predicting ability was referred to the TATE-2 method, in particular when considering the cutoff values of TATE-2b (Harrell's C-statistic = 0.718; AIC = 798; BIC = 828). The method described as TATE-1 reported in general better predictive performance, in particular when applying the cutoff points of TATE-1a model (Harrell's C-statistic = 0.728; AIC = 798; BIC = 828), with similar improvements with the TATE-1d (Harrell's C-statistic = 0.727; AIC = 796; BIC = 829) and TATE-1b cutoff values (Harrell's C-statistic = 0.725; AIC = 797; BIC = 826). Subsequently, applying the same multivariate model, none of the TATE classifications resulted to be an independent prognostic factor for DFS.

3. GENETIC BIOMARKER

3.1. Background

HNSCC frequently presents in individuals with a history of tobacco and alcohol consumption [50, 51]. Both tobacco and alcohol cause DNA damage with an increased likelihood of generating mutations in cancer-related genes [52]. Consistently, several studies have shown that such carcinogens contribute to the mutational profile of TP53 [53-56]. TP53 encodes p53, a protein that regulates the expression of a vast array of target genes. In early studies, p53 was considered an oncogene because of the lower expression

level in normal cells compared with the cancerous one. In 1989, Levine et al. showed that wild-type p53 works as an oncosuppressor. Because of its important role in cancer biology, p53 has been defined “the guardian of the genome”. The protein is involved in different cellular functions, such as apoptosis, differentiation, and cell-cycle control. In addition, it plays a central role in the control of cell proliferation and death in response to various urges like DNA damage, hypoxia, oxidative stress, DNA mutations and nutrient deprivation [57, 58]. Not surprisingly, TP53 gene alterations are frequent in a large proportion of human cancers, and occur in a tissue-specific manner. For example, TP53 mutation rates vary from 2.2% in renal cell carcinoma to 89% and 94.9% in endometrial carcinoma and serous ovarian cancers, respectively [59]. Inherited TP53 mutations lead to a wide spectrum of early-onset cancers [60]. In contrast to other tumour-suppressor genes that are mainly altered by truncating mutations, the majority of TP53 mutations are missense substitutions (75%). Other alterations include frameshift insertions and deletions (9%), nonsense mutations (7%), silent mutations (5%) and other infrequent alterations [61]. However, whether different types of TP53 mutations bear distinct clinical and pathophysiological significance in HNSCC has not been elucidated so far.

Structurally, p53 is a multifunctional 393-residue protein; it is encoded by a gene localised on chromosome 17p13.1 and is composed of 25,772 bases. The protein is constituted by three subunits: N-terminal, Core domain and C-terminal. The N-terminal subunit is composed of a transactivation domain (residues 1–42) and a proline-rich domain (residues 63–97). The central core domain (residues 98–292) is composed of a single unit that contains sequence-specific DNA-binding activity of p53 (DNA-binding domain). The C-terminal domain is characterized of a flexible linker region (residues 293–323), a tetramerisation domain (residues 324–355) and C-terminal regulatory domain (residues 363–393) that undergoes a number of post-translational modifications

such as acetylation and phosphorylation [62, 63]. A growing body of evidence now suggests that differential mutational profiles of TP53 gene can influence disease prognosis in several types of tumours; for example, distinct TP53 mutations are independent predictors of survival in CD20+ lymphomas [64]. The same results have also been reported for ALK+ NSCLC [65], hepatocellular carcinoma, HNSCC, acute myeloid leukaemia, clear-cell renal cell carcinoma (RCC), papillary RCC, uterine endometrial carcinoma and thymoma [66]. Whether mutations in p53 subdomains differentially affect disease prognosis, however, has not been elucidated so far.

The aim of this study was to investigate the mutational landscape of TP53, and to correlate these molecular features with clinical variables. To do so, we used a bioinformatics approach by analysing data from The Cancer Genome Atlas (TCGA) database [15]. The results from this analysis revealed that a wide landscape of TP53 mutations exists in HNSCC and, for the first time, demonstrated that these mutations are associated with distinct clinical behaviour in a site-specific manner.

3.2. Methods

This study has been performed according to the Recommended Guidelines for Validation, Quality Control and Reporting of TP53 Variants Clinical Practice [67]. TCGA data have been accessed and downloaded through UCSC Xena Browser (https://xena.ucsc.edu/). Data for mRNA expression profile of TP53 gene (ENSG00000141510) were downloaded as RNAseq data HTSeq-Fragments Per Kilobase Million (FPKM)-dataset ID TCGA- HNSC/Xena_Matrices/TCGA-HNSC.htseq_fpkm.tsv, and the mutational profile with the variant-allele frequency (VAF), such as the type of mutation (MuTect2 Variant Aggregationand Masking-dataset ID TCGA-HNSC/Xena_Matrices/TCGA-HNSC.mutect2_snv.tsv). The mutation dataset was also download from the cBioPortal for cancer genomics website. This

website was also useful for downloading the RPPA-Z-score expression of p53 protein (http://www.cbioportal.org) [68]. In this analysis, only patients with a single mutation of theTP53 gene were included. Patients with double mutations on the same gene or mismatchingmutation type in the two datasets were excluded. At the end of the inclusion process, 415 patients' profiles were eligible for statistical analysis. Genomic Data Commons (GDC) Data Portal (https://portal.gdc.cancer.gov/) was used to download clinical and follow-up information. Data were pasted and organized in SPSS 21.0 to perform the statistical analysis for the evaluation of clinical and prognostic correlations. The amino-acid sequencechanges were assessed and used to classify mutation profiles according to the secondary structure of p53 protein. In the Research Collaboratory for Structural Bioinformatics ProteinData Bank (RCSB-PDB), it was possible to retrieve the Secondary Structure data for the TP53 protein (https://www.rcsb.org/pdb/explore/remediatedSequence.do?params.showJmol=false&structureId=3Q01). Data grouping Of 415 patients with HNSCC included in the study (for clinc-pathologic details, please refer to original manuscript [69]), 129 patients had no mutations in the TP53 gene and were defined as "wild type" (WT); meanwhile, 286 patients had one single mutation in the gene sequence (MUT) (of these, 51 patients had a frameshift mutation, 8 an inframe mutation, 152 a missense mutation, 26 a splice-site mutation and 49 patients had a stop mutation). The p53 mRNA expression for 411 patients (log2 (fpkm + 1)) in the TCGA Database ranged between 0.71 and 6.47 with a mean of 3.740184 (S.D. 1.2168926) and a median of 3.88. The p53 RPPA-Z-score protein was available for only 173 patients and ranged from −4.3211 to 3.0036 with a mean of −0.001732 (S.D. 0.91044) and a median of −0.0933. Both for mRNA expression and RPPA- Z score, patients were classified as high and low expression using the median as threshold. It is important to note that RPPA-Z-score protein was available

for only 173 patients, and it is not representative of the whole cohort. Patients were also divided according to VAF, intended as the proportion of DNA molecules bringing the variant. From 40 to 64% VAF, patients were classified as being heterozygous loci; meanwhile, 65–100% VAF patients were grouped as homozygous loci [70]. VAF was reported for 271 patients and ranged from 5 to 97% with a mean of 46.73% (S.D. 19.33%). To further evaluate the relation of the location and the type of mutation with the clinicopathological characteristics, patients were divided according to:

1. The position of the mutated base on the DNA sequence of the gene, such as in the N- terminal transactivation domain (residues 1–97), in the DNA-binding domain (residues 98–292) and in the C-terminal domain (residues 293–393) [62]. In total, 19 patients had a mutation in the N-terminal domain, 37 patients in the C-terminal domain and 230 patients inthe DNA-binding domain. In total, 152 of 230 mutations in the DNA-binding domain were missense.

2. The secondary structure extracted from the RCSB-PDB, such as mutation affecting the helix region (3/10 helix, alpha-helix structure), a strand region (beta bridge, beta strand), a turn region (turn, bend) [71] and an unknown region, for which no secondary structure is assigned.

3. Well-known hotspot mutations, such as the ones occurring in the residues 175, 245, 248,273 and 282 [72]. In particular, residue R175 was affected in 5 patients, G245 in 7 patients,R248 in 11 patients, R273 in 14 patients and R282 in 6 patients (43 hotspot mutations/286 total mutations). In addition to these frequent spots, we decided to include new residues, which were also frequently mutated; only residues involved in at least six patients includedin the cohort were also included as new hotspots mutations; such sites were H179 (seven patients), H193 (six patients), R196 (eight patients) and R213 (seven patients).

4. The residues involved in the zinc ion ligand, such as C176, H179, C238 and C242, whichwere involved in 17 on 286 patients.

5. Mutations were classified according to the type of single amino-acid substitution, such astransition and transversion.

In order to investigate random deamination or tobacco smoke- related mechanisms of mutations, transitions of C–T in CpG islands and transversions of G:C–T:A were also highlighted. In addition, mutations involving CpG sites, reported in http://p53.iarc.fr/p53Sequence.aspx, were also investigated.

6. Mutations in conserved residues were compared with their non-conserved sites, accordingto a previously reported analysis by Martin et al. [73]. Conserved residues were retrieved from their online platform at http://bioinf.org.uk/p53/analysis/index.html#conserved, such as pro98, phe113, lys120, ser121, val122, thr125, ser127, leu130, lys132, leu137, lys139, pro142, pro151, pro152, arg158, ala159, lys164, val172, val173, arg175, pro177, his178, his179, arg196, glu198, gly199, tyr205, asp208, ser215, val216, val218, pro219, tyr220, glu221, pro223, thr230, asn239, ser240, ser241, cys242, met243, gly244, gly245, asn247, arg249, ile251, thr253, leu257, gly262, leu265, gly266, arg267, phe270, glu271, val272, cys275, ala276, cys277, pro278, gly279, arg280, asp281 and arg282.

7. Martin et al. also characterized amino-acid substitutions according to their ability to donate

or accept hydrogen bonds. The amino acids K, R and W are only able to donate H+;

meanwhile, E and D are only able to accept hydrogen bonds. The amino acids H, N, Q, S, Tand Y are both able to accept and donate as reported by Baker et al. [74]. Patients were classified as missense-disruptive mutation with substitution of K, R

and W with E and D andvice versa, or in the case of forming H+ bond amino acids, substituted by nonforming H+ bonds.

8. We also categorized two further amino-acid substitutions, such as (1) mutations resulting in a substitution by proline, and (2) mutations from native glycine in residues at codons 117,154, 187, 244, 245 and 262. These kinds of mutations, because of their sidechain features, are more restricted in the allowed conformations [73].

All these analyses were performed in the TCGA database of patients with squamous cell carcinoma of the head and neck (HNSCC). Patients were further categorized into four main subgroups [75]:

1. Oral cavity (OC), such as alveolar ridge, buccal mucosa, floor of the mouth, hard palate, oral tongue, general oral cavity and lips
2. Oropharynx (OP), such as base of the tongue, oropharynx and tonsils
3. Hypopharynx (HP)
4. Larynx (L)

Data were also download for oesophagus and lung squamous cell carcinoma, in order to investigate and compare the TP53 mutational landscape among these groups of cancers. UCLA, TCGA and ICGC oesophagus databases from cBioPortal and TCGA (PanCancer Atlas) lung squamous cell carcinoma, were downloaded following the previous descripted criteria, including only patients with histologically confirmed squamous cell carcinoma. Interactome–genome–transcriptome network analysis based on co-alteration data. In order to highlight co-differential gene network between WT and MUT groups, we combined interactome–transcriptome analysis and interactome–genome analysis to construct dynamic, tumour-specific networks based on predicted

changes of p53 interactors resulting from genetic (mutations, CNA) or transcriptional (mRNA expression) modifications occurring in the same HNSCC cohorts. Specifically, patients were compared according to WT/MUT and subsite (OC, OP, HP and L) to evaluate if different genes/pathways were modified in relation to the distinct mutational profile of TP53 at different subsites. cBioPortal gene network tool highlights alterations per each gene, such as mutations, CNA or mRNA dysregulation. Moreover, cBioPortal gene network tool was used to build the interactome by filtering the interactions according to "controls state change of", "controls transport of", "controls of phosphorylation of", "control expression of", "in complex with" and "neighbour of". This analysis was also performed between HPV-positive and HPV- negative OP tumours. When more than 50 neighbour genes existed in the network, these were ranked by genomic alteration frequency within the selected group of patients. To provide an effective visualisation of networks that highlighted the most relevant genes to the query, we adopted an alteration frequency of 16.9% as cut-off [68]. For HP subgroup, a 33.3% cut-off was applied because of the low number of patients included. Gene ontology (GO) analysis to evaluate the main pathway alterations in each subgroup analysis was performed by using http://geneontology.org/ tool and retrieving the results from PANTHER. Gene, percentage and type of both alteration and cell function are summarised in Supplemental material (please, refer to the original manuscript [69]), by including only the results with a fold enrichment over ten.

Because of the non-normal distribution of variables, nonparametric tests were used (normaldistribution of variables was explored through Shapiro–Wilk normality test). Spearman rank correlation analysis was performed to investigate the relation between the expression profile of p53, the mutational profile and the clinicopathological characteristics. For dichotomous variables, chi-square test was used. The difference

in expression between groups was further investigated through the non-parametric test of Mann–Whitney or by Kruskal–Wallis one-way or two-way ANOVA test. Bonferroni–Holm false-discovery rate was applied to correct for multiple comparisons. Kaplan–Meier analysis with log-rank test was applied to explore differences in the overall and disease-free survival by univariate analysis. In order to estimate the effect of clinicopathological variables, a multivariate Cox regression model was built, including the following parameters as covariates: age, gender, staging and grading. All tests were performed by using SPSS 21.0 and STATA 16.0; only $P< 0.05$ results were considered statistically significant.

We generated an algorithm based on modifications of the algorithm previously reported by Poeta et al. [76]. In Poeta's algorithm, patients are grouped as bringing a TP53-disruptive mutation versus conservative mutation. Stop, frameshift, inframe and splice mutations are classified as disruptive, together with missense mutations in L2–L3 segment of the protein (codons 163–195 and 236–251) with changes in charge or polarity of the substituted amino acid. Any missense mutation outside L2–L3 segment or in L2–L3 segment without changes in charge or polarity, are considered conservative. First, we applied this algorithm to TCGA head and neck cancer, and then we implemented this model in order to highlight patients at high risk of death, according to deleterious missense substitutions in the secondary structure of the protein. Mutations were reclassified as disruptive if:

- in homozygous loci, such as DNA–VAF from 65 to 100%;[195]
- in zinc ligand involved;
- changing from K, R and W to E and D and vice versa, or in the case of forming H+ bondamino acids, substituted by nonforming H+ bonds;

- affecting an amino acid in a non-assigned secondary structure (unknown, as reported inRCSB-PDB http://www.rcsb.org/pdb/explore/remediatedSequence.do?structureId=1TUP).

Mutations were reclassified as conservative if assigned to any other secondary structure, when maintaining their ability to donate or accept hydrogen bonds. Harrell's C-statistic, AIC (Akaike information criterion) and BIC (Bayesian information criterion) were used to assess possible improvements of the prediction model.

3.3. Results

Survival analysis of TP53 mutational landscape reveals novel prognostic signatures. We aimed to investigate whether the presence of mutations in the TP53 gene correlated with the prognosis of HNSCC. By comparing wild-type (WT) HNSCCs with the ones with mutated TP53, univariate survival analysis showed a worse overall survival for patients carrying one mutation in TP53 gene. Multivariate Cox regression analysis confirmed that TP53 mutation was an independent prognostic factor in HNSCC patients (multivariate analysis: HR = 1.613; 95% CI: 1.119–2.325; P = 0.010) (Figure 13). Interestingly, in the OP subgroup, the mutated profile was an independent prognostic factor of overall survival (multivariate analysis: HR = 11.657; 95% CI: 2.668–50.929; P = 0.001); meanwhile, it was close to the threshold of statistical significance for disease-free survival (multivariate analysis: HR = 5.773; 95% CI: 0.896–37.174; P = 0.065). Next, we investigated whether there was an association between specific characteristics of the mutation and patients' survival, as follows. When analysing TP53 mutations according to the predicted p53 domains affected (N-terminal, C-terminal or DNA-binding domain), no differences in survival emerged in subgroups, except larynx, where at the univariate analysis, patients with mutations in the DNA-binding domain

had a worse overall survival than those with mutations in the N-terminal segment of the gene (multivariate analysis: HR = 0.223; 95% CI: 0.050–0.998; P = 0.050).

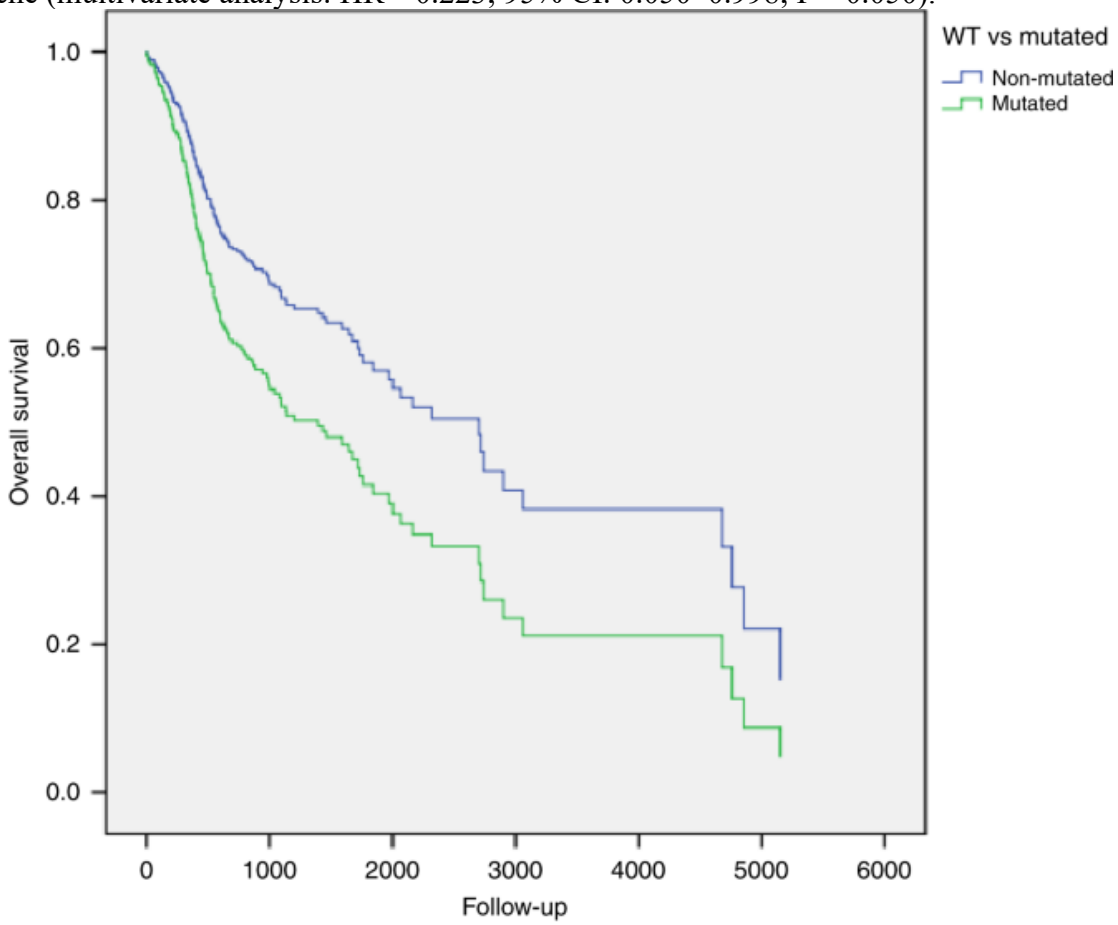

Clinic-pathological covariates	Sig.	Hazard ratio	95% CI	
			Lower limit	Upper limit
Age	0.020	1.018	1.003	1.034
Stage	0.464	1.065	0.900	1.260
Grading	0.157	1.191	0.935	1.518
Gender	0.204	1.247	0.887	1.753
WT vs MUT	0.010	1.613	1.119	2.325

Figure 13: Multivariate survival analysis revealed that patients with mutations (MUT) in TP53 gene sequence (green line) showed a worse survival compared to patients with wild-type (WT) TP53 (blue line).

TP53 mutations were then analysed according to their occurrence in the predicted

secondary structure of the protein. No differences in survival emerged between WT patients and those with mutations in the helix or in turn region of the protein. Patients with mutations in a strand region had a worse overall survival, both in HNSCC (multivariate analysis: HR = 1.559; 95% CI: 1.007–2.413; P = 0.046) (Figure 14) and larynx (multivariate analysis: HR 0.071; 95% CI: 0.005–0.935; P = 0.044) subgroups, compared with WT. Poor overall survival was also detected for patients with mutations in unknown regions. In particular, patients in HNSCC (multivariate analysis: HR = 2.476; 95% CI: 1.525–4.019; P < 0.001), OP (multivariate analysis: HR = 0.072; 95% CI: 0.011–0.490; P = 0.007) and L (univariate analysis: HR = 0.133; 95% CI: 0.03–0.598; P = 0.008) subgroups had a worse overall survival compared with the WT group.

Survival analysis was also performed to investigate whether particular hotspot mutations could influence patients' prognosis. Specifically, the comparison was performed between hotspot mutations and non-hotspot residues. Mutations affecting the residue R175 were associated with a worse overall survival in HNSCC (multivariate analysis: HR = 6.855; 95% CI: 1.635–28.75; P = 0.008) compared with the non-hotspot group. The same result emerged from the analysis of the residue H193 (multivariate analysis: HR = 3.578; 95% CI: 1.380–9.277; P = 0.009). Finally, R213 was linked to poor overall survival in HNSCC (univariate analysis: P = 0.024). Although the results from this analysis could be clinically relevant, it should be noted that the small sample size available for this cohort bears high risk of bias; therefore, the results should be further validated in larger sample size. Differences in mutation type (frameshift, missense, inframe, splice site and stop) showed variable prognostic capabilities. In particular, missense (multivariate analysis: HR = 1.688; 95% CI: 1.129–2.526; P = 0.011) and stop (multivariate analysis: HR = 2.016; 95% CI: 1.220–3.332; P = 0.006) mutations were predictive of worse overall survival compared with WT patients in HNSCC.

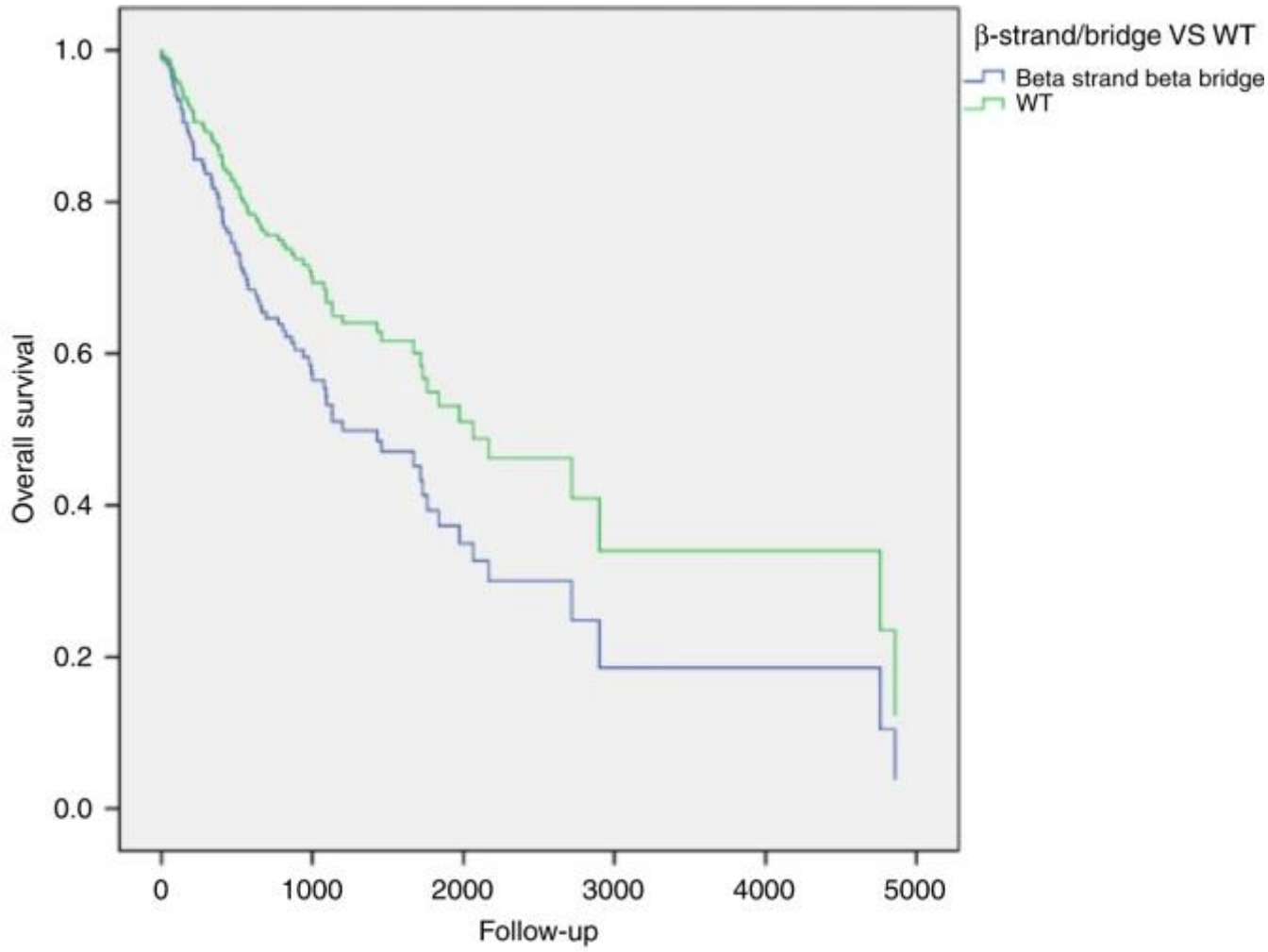

Clinic-pathological covariates	Sig.	Hazard ratio	95% C.I.	
			Lower limit	Upper limit
Age	0.215	1.014	0.992	1.036
Stage	0.730	1.043	0.822	1.323
Grading	0.723	1.061	0.765	1.471
Gender	0.481	1.189	0.735	1.923
β-strand/bridge VS WT	0.046	1.559	1.007	2.413

Figure 14: Multivariate survival analysis in head and neck squamous cell carcinoma, showing that patients with mutations in β-strand/bridge of p53 secondary structure (blue line) have a worse survival

compared to patients with wild-type (WT) TP53 gene (green line).

In the last analysis, HNSCC patients with higher VAF, such as those carrying the mutation in homozygous loci, reported a worse overall survival (multivariate analysis: HR = 1.747; 95% CI: 1.055–2.891; P = 0.030) and higher risk of relapse (multivariate analysis: HR = 2.421; 95% CI: 1.168–5.020; P = 0.017) compared with patients with lower VAF (i.e. mutations in heterozygous loci) (Fig. 4). Differential mRNA expression did not influence the overall survival in HNSCC and its subgroups.

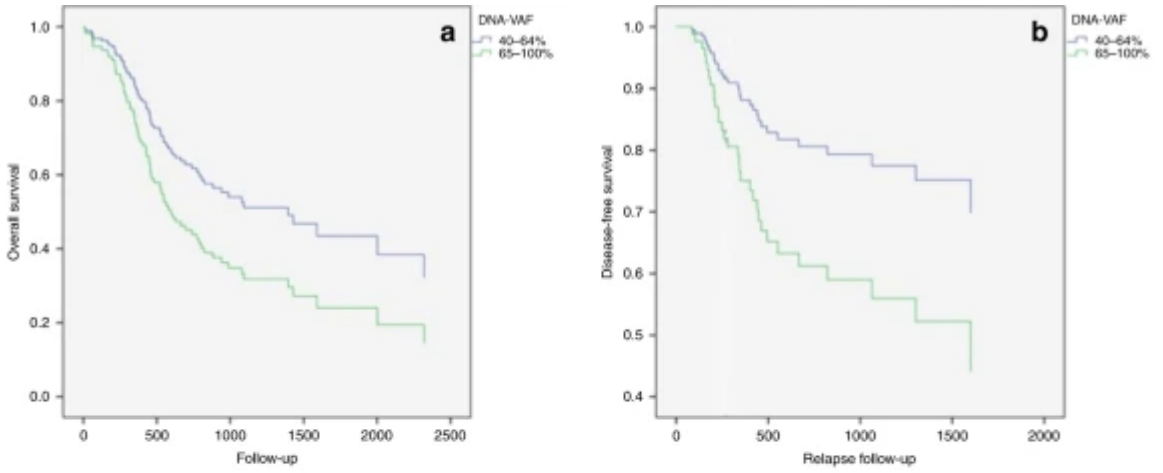

	Sig.	Hazard ratio	95% CI a	
			Lower limit	Upper limit
Stage	0.498	1.098	0.837	1.441
Age	0.020	1.030	1.005	1.057
Grading	0.623	0.890	0.561	1.414
Gender	0.171	1.444	0.853	2.443
dnaVAFEtero_Omo	0.030	1.747	1.055	2.891

	Sig.	Hazard ratio	95% CI b	
			Lower limit	Upper limit
Stage	0.101	1.505	0.924	2.454
Age	0.024	1.048	1.006	1.091
Grading	0.842	1.071	0.544	2.111
Gender	0.695	1.183	0.512	2.734
dnaVAFEtero_Omo	0.017	2.421	1.168	5.020

Figure 15: Multivariate survival analysis for patients with head and neck squamous cell carcinoma, showing that subjects with homozygous mutations in TP53 gene sequence (green line) showed a worse overall **(a)** and relapse-free **(b)** -survival, compared to patients with heterozygous mutations (blue line).

Finally, because cancers arising in lung and oesophagus share common histopathological characteristics with HNSCC, we compared available datasets for these groups of carcinomas. Surprisingly, the results failed to show an association between p53 mutations and prognosis. In particular, in lung squamous cell cancer, patients with wild-type TP53 had worse overall survival compared with patients with mutated p53 (multivariate analysis: HR = 0.636; 95% CI: 0.437–0.926; P = 0.018).

Taken together, these data demonstrate that TP53 mutations are not only predictors of patient survival but, also, that different types of mutations have distinct prognostic significance in HNSCC.

TP53 genotype correlates with expression profile and clinicopathological variables. Indeed, the expression of p53 mRNA differed between WT and MUT patients (Mann–Whitney $P < 0.001$) in HNSCC. In the WT cohort, the expression (log2 (fpkm + 1)) ranged from 0.71 to 6.47 with a mean of 4.2825 and a median of 4.39. In the MUT cohort, mRNA expression varied from 0.76 to 5.85 with a mean of 3.492 and a median of 3.665. This differential expression was also reported in the OP subgroup (Mann–Whitney $P < 0.001$) where in the WT cohort, the expression ranged from 2.23 to 6.47 with a mean of 5.1579 and a median of 5.21; meanwhile, for the MUT cohort, the expression reported was from 1.82 to 5.62 with a mean of 3.6789 and a median of 3.90. mRNA expression was also variable in HPV+ and HPV− tumours, in particular in OP subgroup (Mann–Whitney P = 0.006). In HPV− tumours, the expression ranged with a mean of 3.86 and a median of 3.73; meanwhile, HPV+ tumours reported a mean of 5.2373 and a median of 5.1754. A two-way ANOVA was conducted that examined the effect of the anatomical subsite and mutational status on TP53 mRNA expression. There was a statistically significant interaction between the anatomical subsite and mutational status on mRNA

expression, two-way ANOVA $P = 0.003$. Simple main effect analysis showed that mutational status significantly affected mRNA expression ($P < 0.001$), but there were no differences between anatomical subsites ($P = 0.684$). Bonferroni–Holm post hoc test showed a differential mRNA expression between OP and the other subsites (O, L and HP; $P < 0.001$) and a higher mRNA expression in WT, missense and inframe MUT, compared with frameshift, splice and stop MUT ($P < 0.001$). mRNA expression poorly correlated with its protein expression (Spearman rank-correlation test $\rho = 0.382$, $P < 0.001$). Of interest, TP53 mRNA expression differed among tumour grades (Bonferroni–Holm post hoc test G1 vs G2 $P = 0.045$; G1 vs G3 $P < 0.001$; G2 vs G3 $P = 0.031$) with the following expression means in G1 of 3.2434, in G2 of 3.6753 and in G3 of 4.0424.

Chi-square test showed a differential ratio between WT/MUT patients and tumour subgroup (OC, OP, HP and L) and HPV positive/negative ($P < 0.001$). In total, 176/246 MUT in OC (Bonferroni post hoc test $P = 0.08239$), 19/62 in OP (Bonferroni post hoc test $P < 0.000001$), 5/9 in HP (Bonferroni post hoc test $P = 0.40597$) and 78/90 in L (Bonferroni post hoc test $P = 0.00002$); for the HPV status, 3/30 HPV-positive patients were mutated in TP53 gene; meanwhile, 52/64 were mutated in HPV-negative tumours. In addition, perineural invasion was more frequent in MUT ($P = 0.031$); 28/78 WT reported perineural invasion against 101/201 MUT. This event was also notable in the OC subgroup where 21/50 WT reported perineural invasion against 82/140 MUT ($P = 0.044$). Interestingly, 110/143 smoking patients were mutated against 176/272 non-smokers ($P = 0.011$). Spearman analysis showed a correlation between DNA–VAF and grading in HNSCC ($\rho = 0.131$, $P = 0.035$), in particular higher DNA–VAF was present in patients with higher tumour grade (Kruskal–Wallis $P = 0.041$—Bonferroni–Holm post hoc test G1 vs G2 $P = 0.134$; G1 vs G3 $P = 0.059$; G2 vs G3 $P = 1.00$). Different characteristics were also found between male and female patients. Chi-square test showed

a higher RPPA-Z-score protein expression in males, compared with females, 65/119 males and 17/51 females (P = 0.011). In addition, the occurrence of hotspot mutations taken into consideration, differed between genders. Mutations in H193 occurred only in males; meanwhile, of 8 patients mutated in R196, 6/8 were female patients (chi-square test P = 0.003). R196 resulted mutated only in the OC subgroup. In the last analysis, R273 mutations were characterised by a missense mutation by a substitution of the R (arginine) amino acid to C (cysteine) or H (histidine). Changes in C involved one male over five patients; meanwhile, H involved seven male patients over nine (chi-square test P = 0.036). R273 missense mutations were also linked to alcohol consumption; in particular, of five patients with a change from R to C, four reported alcohol consumption in the anamnesis; meanwhile, 8/9 patients with H change did not report alcohol history (chi-square test P = 0.01); the same result was also detected for the OC subgroup (chi-square test P = 0.044). Cigarette consumption was also considered as a clinical variable in HNSCC. Transitions of C–T in CpG islands are reported to be a common consequence of random deamination; meanwhile, transversions of G:C–T:A are tobacco smoke-related mechanisms of mutations. Chi-square test (P = 0.018) showed a lower number of transversion events in never-smoker patients (6/16) (Bonferroni post hoc test P = 0.00237). A higher number of transversion of G:C–T:A events occurred in current smokers (24/31) (Bonferroni post hoc test P = 0.1815) and in ex-smokers less than 15 years (20/25) (Bonferroni post hoc test P = 0.1423). Indeed, a higher number of smoked cigarettes emerged in patients with transversions, compared with patients with transitions of C–T in CpG islands (Mann–Whitney P = 0.032). Patients with mutations in Alpha secondary structure showed lower number of smoked packs of cigarettes, against Turn and Bend (Mann–Whitney P = 0.005), unknown (Mann–Whitney P = 0.03) and β-strand/bridge patients (P = 0.021). Although Bonferroni–Holm post hoc test failed to find

significant difference (P = 0.190; P = 0.288; P = 0.096, respectively), chi-square test showed a significant difference between the smoking history and the secondary structure involved. In particular, only 8/124 current smokers reported a mutation in Alpha secondary structure (P = 0.019). Collectively, our data show distinct correlations between TP53 genotype, p53 expression profile and clinicopathological features of HNSCC.

Interactome–genome–transcriptome analysis was undertaken to build a dynamic network that highlighted the TP53 interactors that underwent genomic (mutations, CNA) or translational (mRNA expression) modifications in HNSCC. TP53 networks differed substantially in WT- and p53-mutated HNSCC subgroups (please, refer to the original manuscript supplemental material [69]). n cancer arising from the oral cavity, there were several molecules differentially involved in TP53 network. Both WT and MUT TP53 groups shared common alterations of CDKN2A, TP63 and DROSHA. In WT, the main modification involved the cellular response to DNA-damage stimulus, with changes affecting PMS2, CDK9, DDB2 and EPHA2. In MUT, changes in NDRG1, GSK3B, SNAI2, BCL6, CCNK, PRKDC and RRM2B affected mainly the intrinsic apoptotic process and the transition of the G1/S cell-cycle phase. In HNSCC of the oropharynx, both WT and MUT were associated with alterations in BCL6, TP63, GSK3B, CDKN2A, CCNK and DROSHA. Surprisingly, CDKN2A in WT resulted altered only in 18.2% of cases (13.6% reported mRNA upregulation, 2.3% homozygous deletion and 2.3% mutation), whereas in MUT, CDKN2A was affected in 78.9% of cases (57.9% reported homozygous deletion and 21.1% mutation). In particular, WT group resulted affected by deficiencies in both intrinsic and extrinsic apoptotic signals, cell-cycle growth checkpoint at G1/S phase, mismatch repair, positive histone deacetylation, negative regulation of cell–matrix adhesion, fatty acid biosynthetic process, cellular response to starvation, negative regulation of intracellular oestrogen receptor signalling pathway, morphogenesis

of embryonic epithelium and negative regulation of phosphatidylinositol 3-kinase signalling. These mechanisms are regulated in particular by PCNA, BCL6, FAS, GSK3B, TP63, TSC2, BRCA1, MDM2, PTEN, TP73, DYRK1A, MSH2, PRKAB1, PRKDC, CDK1, MDM4, RRM2B and E2F2. DGR8, AGO4 and DROSHA regulated primary miRNA processing, involved in gene silencing in the WT OP subgroup. CX3CL1 and MYB showed common alteration in both WT TP53 OP and HPV+ OP subgroups, with positive regulation of transforming growth factor beta production. BCL2, TRIM28 and CCNK emerged to be involved in the regulation of viral genome replication, sharing common alterations in both WT TP53 OP and HPV+ OP group. In MUT, there were different molecules involved in the TP53 network. Noncoding RNA (ncRNA) transcription was linked to alterations in CCNK and CDK9, and in particular, HIF1A and YY1 resulted in a positive regulation of pri-miRNA transcription by RNA polymerase II. CCNK and CDK9 were found also in the HPV– OP subgroup. In terms of pathways, the main alterations involved the apoptotic process, due to alterations in CDKN2A, NDRG1, TP63, BCL6, PRKAB2, PPP2CB, PRMT5, HIF1A, KAT5 and TTC5. Notably, alterations resulted in positive regulation of glycolytic process, beta-catenin-TCF complex assembly, regulation of cellular respiration and positive regulation of epithelial cell proliferation, led by TP63, MYC, KAT5 and HIF1A. The main alterations involved autophagy mechanisms, due to changes in PRKAB2, HIF1A, KAT5 and GSK3B. At last, changes in SERPINE1, GSK3B and TP63 resulted in modifications in epithelial differentiation. In HNSCC of the larynx, CDKN2A, BCL6, TP63, GSK3B and NDRG1 were altered in both WT and MUT; CSNK2A1 and CREBBP were downregulated in WT, whereas the same resulted upregulated in MUT. In terms of pathways, the main alteration in WT affected the signal transduction by p53-class mediators and downstream stress-activated MAPK cascade, due to modifications affecting MAPK13, UBB, TRAF6,

MAPKAPK2 and DYRK1A. In MUT, a defect emerged in the crosstalk between regulation of cell growth and cellular response to hypoxia and gamma radiation, as suggested by the alteration of PRKDC, MYC, COP1, CREBBP, NDRG1 and WRN. Alterations in the hypopharynx subgroups differed between wild-type and mutated TP53 groups. CDKN2A showed common alterations in both groups. In the WT group, PLK3, BCL2L1, CX3CL1, BAX and NGFR all resulted in upregulation in their mRNA expression, with some cases of amplification or mutation. These were mainly involved in the negative regulation of apoptotic process, and in the regulation of cell-cycle G1/S-phase transition. Interestingly, CX3CL1 resulted participating in positive regulation of calcium-independent cell-to-cell adhesion, regulation of stem cell proliferation and regulation of cell–matrix adhesion. NGFR seems to be related to the positive regulation of pri-miRNA transcription by RNA polymerase II and together with CDKN2A, in RAS protein signal transduction. MUT group showed a higher number of alterations, and CDKN2A was mainly affected. DDIT4 resulted in mRNA upregulation in 60% of cases, affecting the intrinsic apoptotic signaling pathway in response to DNA damage by p53-class mediator and negative regulation of ATP metabolic process. Alterations in metabolic pathways could be of interest in this group of patients because of changes in fatty acid biosynthetic process, vasoconstriction, ATP metabolic process and rhythmic process involving EDN2, PRKAG1, HTT, CSNK2A1, HGF, HIF1A, PRKAB2 and SNAI2. Of interest in this group are also changes in chromatin assembly and silencing because of mRNA upregulation in 40% of cases of HIST1H1D and downregulation of HIRA. In addition, differences in the TP53 network between HPV− and HPV+ HNSCCs were compared. OP HPV− tumours showed common alterations with HPV+ tumours of the same subsite. In particular, TP63, BCL6, GSK3B, DROSHA and CCNK showed similar modifications. CDKN2A mRNA resulted in upregulation in 22.2% of HPV+

tumours, whereas HPV− tumours showed homozygous deletion and mutations in 50% and 33.3%, respectively. In HPV−, a wide number of molecules were involved in a negative regulation of cell–matrix adhesion, stem cell differentiation, negative regulation of epithelial cell differentiation and regulation of intracellular oestrogen receptor signaling pathway. Of interest, an alteration in lipid metabolism emerged in alterations in PRKAB2 and PRKAA2, with consequences in lipophagy, carnitine shuttle and fatty acid transmembrane transport. HPV+ showed modifications of both intrinsic and extrinsic apoptotic processes, due to alterations in histone phosphorylation, peptidyl–threonine phosphorylation, peptidyl–serine phosphorylation and protein autophosphorylation processes, which lead to changes in ubiquitination. Notably, in this cohort, there was an upregulation of PCNA mRNA in 48.1% of samples. Taken together, these data show that distinct TP53 molecular networks are associated with HNSCC in a site- and mutation-specific manner. Notwithstanding these differences in molecular pathways, all HNSCC tumours share a common alteration landscape in the crosstalk between cellular stress response, cell-cycle progression and apoptotic process.

Survival prediction algorithm results

By applying the Poeta algorithm (PA) on the TCGA database, we found that disruptive mutations had independent prognostic significance in HNSCC, although with small difference between disruptive and conservative mutations (disruptive vs conservative mutations, multivariate analysis: HR = 1.077; 95% CI: 0.753–1.541; P = 0.684); (disruptive vs wild-type, multivariate analysis: HR = 1.663; 95% CI: 1.122–2.466; P = 0.011); (conservative vs wild-type, multivariate analysis: HR = 1.545; 95% CI: 1.013–2.357; P = 0.043) (Fig. 16a). In addition, we integrated the biochemical information from PA to the ones from Martin et al.30 with the addition of our findings according to the predicted secondary structure and the number of mutated alleles. Patients

were classified as carriers of high-risk death mutations, carriers of low-risk death mutations and wild type. Our model successfully identified patients at higher risk of death according to the mutational status, depending on the biochemical alterations, characteristics and predicted secondary structure. High risk of death mutations resulted to be an independent prognostic factor in TCGA head and neck database, with greater difference towards low risk of death mutations (high-risk vs low-risk mutations, multivariate analysis: HR = 1.818; 95% CI: 1.153–2.869; P = 0.010); (high-risk vs wild-type, multivariate analysis: HR = 1.857; 95% CI: 1.277–2.702; P = 0.001); (low-risk vs wild-type, multivariate analysis: HR = 1.005; 95% CI: 0.596–1.695; P = 0.986) (Fig. 16b).

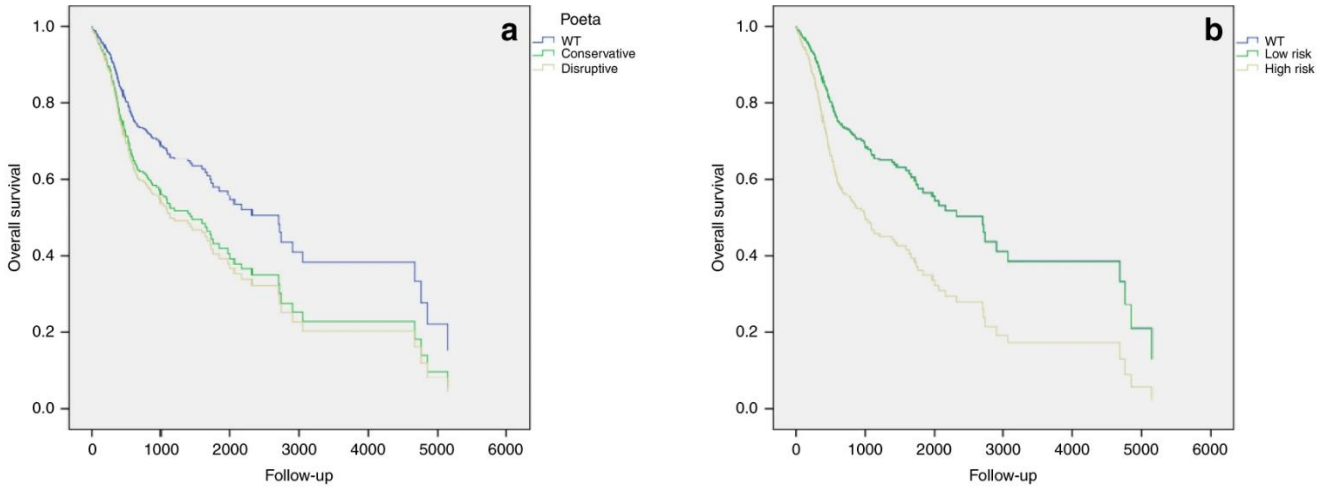

Clinic-pathological covariates	Sig.	Hazard ratio	95% CI a	
			Lower limit	Upper limit
Age	0.019	1.018	1.003	1.034
Stage	0.469	1.064	0.900	1.258
Grading	0.151	1.195	0.937	1.522
Gender	0.202	1.248	0.888	1.755
Disruptive vs wild-type	0.011	1.663	1.122	2.466
Conservative vs wild-type	0.043	1.545	1.013	2.357
Disruptive vs Conservative	0.684	1.077	0.753	1.541

Clinic-pathological covariates	Sig.	Hazard ratio	95% CI b	
			Lower limit	Upper limit
Age	0.027	1.017	0.892	1.242
Stage	0.544	1.053	0.892	1.242
Grading	0.133	1.206	0.944	1.539
Gender	0.284	1.205	0.857	1.694
High-risk vs wild-type	0.001	1.857	1.277	2.702
Low-risk vs wild-type	0.986	1.005	0.596	1.695
High-risk vs low-risk	0.010	1.818	1.153	2.869

Figure 16: Multivariate survival analysis of patients with head and neck squamous cell carcinoma,

showing differences among patients with disruptive (yellow line) and conservative (green line) mutations in TP53 gene according to Poeta's classification **(a)**; and patients with high risk (yellow line) and low risk (green line) death mutations, according to our new classification system **(b)**. Blue lines are, in both of cases, representative of wild-type (WT) patients.

Harrell's C-statistic, Akaike information criterion (AIC) and Bayesian information criterion (BIC) were then used to compare the predictive performance of our model with the PA algorithm. C-statistic, AIC and BIC resulted to be 0.5400, 1829.253 and 1837.29, respectively, using the PA. The results for our model reported a Harrell's C-statistic of 0.5700, AIC of 1819.828 and BIC of 1823.847. These results showed that our model performed better than the one published by Poeta (Very strong improvement ΔBIC = 13.443). The newly developed algorithm was applied to each subsite, namely OC, OP and L, as well as lung and oesophagus (HP was excluded because of the small number of samples available). As mentioned above, the dichotomous classification of mutational status was an independent prognostic factor only in OP. PA and our algorithm also performed well in this subgroup (PA: wild-type vs disruptive, multivariate analysis: HR = 0.082; 95% CI: 0.017–0.385; P = 0.002; our algorithm: wild-type vs high-risk, multivariate analysis: HR = 0.082; 95% CI: 0.017–0.402; P = 0.002). In OSCC, PA failed to find any significant prognostic class (wild-type vs disruptive, multivariate analysis: HR = 0.771; 95% CI: 0.483–1.232; P = 0.277 and conservative vs disruptive mutations, multivariate analysis: HR = 0.815; 95% CI: 0.520–1.277; P = 0.372); meanwhile, our algorithm found a class of mutation with a better overall survival (wild-type vs high-risk, multivariate analysis: HR = 0.714; 95% CI: 0.458–1.113; P = 0.137); (low-risk vs high-risk, multivariate analysis: HR = 0.499; 95% CI: 0.283–0.878; P = 0.016).

In L and oesophagus, both algorithms failed to find any significant results, while lung tumours showed a unique behaviour. Specifically, wild-type p53 was associated with a

worse overall survival compared with the whole group of patients carrying mutations (multivariate analysis: HR = 1.572; 95% CI: 1.080–2.287; P = 0.018). When the PA was applied, it emerged that patients with disruptive mutations had a better overall survival, compared both with wild-type (multivariate analysis: HR = 1.791; 95% CI: 1.186–2.707; P = 0.006) and nondisruptive mutated patients (multivariate analysis: HR = 1.296; 95% CI: 0.939–1.790; P = 0.115). Our algorithm, meanwhile, was able to distinguish a group of high-risk mutations (multivariate analysis: HR = 0.803; 95% CI: 0.537–1.201; P = 0.286), although wild-type patients still reported the worst overall survival compared with low risk of death mutations (multivariate analysis: HR = 1.496; 95% CI: 1.019–2.197; P = 0.040). Further material, in particular summarizing tables are reported in the original manuscript [69].

4. DISCUSSION

The recent implementation of clinicopathological parameters of the 8th edition AJCC staging system allows for better stratification of patients with OTSCC [11]. Nevertheless, the prognostic prediction for OTSCC patients is still unsatisfactory, making the search for new prognostic markers necessary. Although immunohistochemistry and other molecular techniques are well-established methods for identifying new prognostic markers, the variable results and the high cost hinder their usefulness in daily clinical practice [77]. For these reasons, the study of morphological features of tumour tissue could be a valuable source of prognostic information.

Several studies have shown that the stromal component of tumours seems to have a high prognostic value for several types of solid malignancy [78]. In particular, measurement of the TSR seems to be a reliable, accurate and economical method with which to characterise the role of tumour stroma in tumour progression. Since its first report in

colorectal cancer patients in 2007, measurement of the TSR on H&E-stained slides has demonstrated its robustness and high reproducibility in other solid epithelial tumours [79-81]. In particular, almost all of the studies have shown that a low TSR (i.e. the presence of a high proportion of stroma in tumour tissue) is significantly related to poor prognosis in patients with different types of solid tumour [78, 82, 83]. Until now, the role of the TSR in head and neck tumours has been little investigated. The first study was conducted in 2014 in a small cohort of patients with nasopharyngeal cancers to investigate the prognostic role of the TSR, and found significantly worse 5-year OS and DFS in patients with stroma-rich tumours [84]. Recently, Karpathiou et al. explored the possible prognostic role of the TSR in laryngeal and pharyngeal cancers [85]. Using two different cut-off points (50% and 30%) to classify the stroma-rich tumours, they found that a low TSR was significantly associated with advanced T-stage and poor survival. Regarding the oral cavity, in 2018 a multicentre study was conducted with the aim of evaluating the prognostic value of the TSR in early-stage (T1-2N0M0) OTSCC [86]. The results were interesting, showing that a low TSR is an independent risk factor for recurrence and cancer-related mortality in patients with early-stage OTSCC. Similarly, another pilot study on a small cohort of OSCC patients showed that patients with stroma-rich tumours had a worse prognosis than those with stroma-poor tumours. In particular, a low TSR was related to significantly worse 3-year DFS (44%) than a high TSR (69.04%).

The present study is the first to investigate the TSR in OSCC, particularly in OTSCC, using the 8th edition AJCC staging system. Our results are consistent with the orientation of the previously discussed literature. As the 8th edition AJCC staging system has been recently released, we decided to update our database in accordance with it, considering the parameters introduced by the new classification. Information on ENE could not be retrieved for 72 cases; therefore, complete reclassification was possible only for 139

samples. Indeed, ENE is now a mandatory parameter for staging OSCC patients with lymph node metastases. Nevertheless, we performed a correlation analysis on this subgroup, confirming that what was already present in the 7th edition AJCC staging system, namely that the TSR directly correlated with both DSS (HR = 1.883, 95% CI 1.033–3.432; P = 0.039) and OS (HR = 1.747, 95% CI 0.967–3.154; P = 0.044), was also true when cases were staged according to the 8th edition AJCC staging system. The possibility of implementing the TSR in daily practice is supported by other advantages, such as the low interobserver variation, especially if a cut-off-point of 50% is used. Another advantage is the small amount of extra time required to evaluate the TSR. Indeed, as reported by some authors and confirmed in this study, determination of the TSR is a feasible method to perform in daily practice, and takes a maximum of 2 min [23]. In this study, the TSR was analysed by entering this parameter either as a continuous variable or a categorical variable, and the same results were obtained. Therefore, by using a dichotomous score (TSR < 50% and TSR ≥ 50%), we obtained good interobserver agreement (Cohen κ = 0.807), suggesting that assessment of the TSR seems to be reproducible among different observers. Indeed, the use of a dichotomous score significantly reduced the confounding effect of tumour heterogeneity of the invasive front. However, in those cases in which the value of the TSR ranges between 40% and 60%, the presence of a heterogeneous tumour front might affect the categorisation, resulting in a risk of misinterpreting a stroma-poor tumour for a stroma-rich one. It is of note that in previous studies it has been advised to select stroma-rich areas as being decisive for scoring of the TSR in such heterogeneous tumours. There are several issues that must be considered when the TSR is measured. Some of these have been previously mentioned, such as the presence of skeletal muscle tissue, salivary gland tissue, large nerve bundles, large blood vessels, or necrotic tissue. These areas must be left out of the

microscopic field or ignored for scoring. However, the tongue is a muscular organ, and the areas of muscle invasion could make it particularly difficult to estimate the percentage of stroma tissue in advanced OTSCCs. In some cases, in particular T3 and T4 cancers, the skeletal muscle invasion could be the main invasion pattern of OTSCC. Although the TSR is evaluated only in the invasive area with the highest percentage of tumour stroma, a possible limitation is that, in some tumours, this parameter could be difficult to apply. Furthermore, the presence of heavy inflammation could make it particularly difficult to estimate the percentage of stroma tissue. In these cases, measurement of the TSR may take longer. Indeed, the presence of heavy inflammatory infiltration in the tumour stroma could make estimation of the TSR difficult, but the inflammatory cell component should not be excluded as such. According to some authors, evaluation of the TSR should be used with caution in patients who have been pretreated with chemoradiotherapy, because of the altered stromal formation in the tumour microenvironment [23]. However, the recent advances in head and neck imaging could be used in the near future to accurately estimate the TSR through the analysis of intratumoral heterogeneity [87]. Finally, the reliability of the TSR as prognostic parameter in incisional biopsies of OSCC has not yet been studied.

Concerning immune phenotype, In the present study, we show for the first time that the immune phenotype of OTSCC predicts early relapse and poor prognosis. Specifically, univariate and multivariate survival analysis showed that OTSCC patients with an immune-desert phenotype had lower likelihood of survival compared to the other groups. Our findings were based on the results of a single, large cohort of 211 OTSCC patients treated by means of primary surgery with or without adjuvant therapies.

Solid tumours, including OTSCC, consist of a complex cellular ecosystem with a spatial organization, where a continuous interplay between cancer cells and tumour

microenvironment takes place. Within the latter, research conducted in recent years has convincingly demonstrated that tumour immune microenvironment, in particular the TILs, play a critical role in cancer progression [13, 88]. As the name suggests, TILs consist of lymphocytes that have invaded tumour tissues and are implicated in killing tumour cells. Despite the numerous studies that have been conducted to investigate the prognostic and predictive role of several immune-related markers in OSCC, none of these has proven to be useful for adequate patient stratification [89, 90]. With regard to TILs, accumulating evidence suggests that the assessment of these cells in histopathological specimens of solid tumours is a reliable and reproducible method, both by H&E stain and immunohistochemistry [24, 91]. Nevertheless, extensive methodological research is still needed to validate TILs markers for routine clinical use [92].

Regarding the prognostic role of TILs in OSCC, several immunohistochemical studies have revealed that increased levels of TILs are associated with favorable prognosis. In particular, the presence of high levels of CD3+ TILs at invasive tumour margin was associated with increased survival in OSCC patients [89]. Low density of stromal CD4+ FOXP3+ TILs was identified as an independent prognostic marker for poor outcomes [93]. Also, the presence of high levels of CD8+ TILs correlate with longer OS [13]. Among other TILs subpopulations, a high Th17/Treg ratio was found to be associated with better outcomes in OSCC [94]. Taken together, these results suggest that high densities of CD3+ (pan T cell marker), CD4+ (T helper cell marker), and CD8+ (T cytotoxic cell marker) TILs are independent factors for favorable prognosis. However, the mere quantification of TILs seems not to be an effective prognostic marker in most cancers including OSCC. Indeed, other studies have failed to show prognostic significance of specific TIL subpopulations in OSCC, limiting the reliability of the results reported in literature [95]. A growing interest has emerged in the recent years regarding

the potential importance of the spatial organization of TIL infiltrate in relation to cancer cells [96]. The new paradigm for the classification of solid tumours, based on the distribution of immune cells, has recently emerged with the aim of improving the prognostic accuracy of TIL infiltrates. Hence, the present study aimed to investigate the prognostic role of immune phenotypes in OTSCC, staged according to both 7th and 8th editions of the AJCC Cancer Staging Manual. In our study, a three-type model for the immune phenotype [97] was applied to split up the tumour specimens of our cohort, based on the distribution of immune cells. Some authors have highlighted how the number of immune phenotypes can vary from two to four and more, based on criteria used for the classification of tumour topography [96, 98]. Nevertheless, regardless of the classification system used, the immune-desert phenotype is uniquely defined as the absence of immune cells in both the tumour parenchyma and the tumour stroma; therefore, the prognostic role of immune-desert phenotype described in the present study is not influenced by the classification system being used. Furthermore, this subgroup shows distinctive molecular features that were identified by a molecular clustering analysis on a wider cohort of squamous cell carcinoma[99, 100], thus setting this immune-desert phenotype aside of other immune phenotypes. The current paradigm in cancer immunology predicts that the adaptive immune system represents an important defence mechanism against cancer [97]. In this context, the paucity or lack of tumour T cell infiltration could be due to several reasons, such as the defective recruitment of antigens-presenting cells, the lack of T cell activation or migration in tumour tissues, or altered cytokines' production. Regardless of the cause, several lines of evidence seem to suggest that solid tumour showing an immune-desert phenotype (also called “cold tumours”) have a poor prognosis [101]. Our results confirmed this hypothesis, suggesting that OTSCC patients showing immune-desert phenotype lack of effective antitumor immune response, which is important for

limiting the tumor growth and reducing the risk of recurrences.

Several authors have pointed out that the distinction between the immune-inflamed and the immune-excluded phenotypes is not clear-cut, as a continuum of values related to the degree of immune cell infiltrate can be observed in the same specimen [97, 102]. Our results confirm this observation, as the T cell density inside and outside the tumour hinders in many cases a clear classification of the specimen and the prognostic stratification of patients. This observation is due to the temporal ordering of the immune infiltration into the tumour tissue, due to the continuous evolution of the crosstalk between cancer and immune cells [88]. Indeed, there is continuous and reciprocal communication between the tumour itself and microenvironment through cytokines, chemokines and cell-cell interactions and the histologically based tumour-immune phenotypes represent only a static description of this complex phenomenon [97].

Another relevant aspect of our study is that the immune-desert phenotype is the least common profile of OTSCC, representing 11.8% of the total. This is consistent with the data reported in solid tumours, in which the immune-desert profile is also associated with a significantly worse prognosis [88, 100]. Furthermore, results from the survival analysis were consistent with the orientation of the recent literature. When applying the 7th edition of AJCC staging system to classify the OTSCC samples, we found that the immune-desert phenotype was significantly correlated with a worse prognosis. In particular, results from multivariate analysis revealed a worse DSS (HR = 2.673; [CI: 95% 1.497-4.773]; P = .001) and OS (HR = 2.591; [CI: 95% 1.468-4.572]; P = .001). Since the 8th edition of AJCC staging system has been recently released, we decided to update our database accordingly and evaluated the parameters introduced by the new classification. Based on the data available in our database, a complete reclassification was possible for 139

samples. Survival analyses were then performed on this "restaged" subgroup, for which immune-desert phenotype resulted again to be an independent prognostic factor for both DSS (HR = 2.280; [CI: 95% 1.107-4.696]; P = .025) and OS (HR = 2.299; [CI: 95% 1.115-4.742]; P = .024).

Based on the results obtained in this present work, a specific subgroup of patients with a different prognosis was identified. Additionally, our hypothesis was subjected to external validation using independent cohort of OTSCC patients from the TCGA database. The results were encouraging, confirming the rarity of the immune-desert phenotype (5/76; 6.6%). Moreover, the limited number of cases prevented us from validating the study with a multivariate model, although the univariate analysis confirmed the prognostic implication of the immune-desert phenotype. Our results regarding the prognostic role of TILs are in agreement with those recently reported by Heikkinen et al in a multicentre cohort of OTSCC patients [103]. In particular, using a cut-off point for TIL infiltration of 20%, it was found a subgroup of OTSCC patients (16.6%) characterized by a poor prognosis. Interestingly, the authors found a moderate interobserver agreement for the detection of tumours with low TILs (Cohen $\kappa = 0.64$). This data, although acceptable, might not be optimal and highlights the presence of a certain degree of uncertainty and variability in this method. In contrast, by applying the three-type model for the immune phenotype, we found a smaller subgroup of OTSCC (11.8%), characterized by the absence of TILs in both the tumor parenchyma and stroma, that is, the immune-desert phenotype. Using this definition, we obtained an almost perfect interobserver agreement (Cohen $\kappa = 0.886$), suggesting that the use of the immune phenotype model seems to be a reliable and accurate method to feature the role of TILs in tumor progression.

There are wide clinical and translational implications of our results. The implementation of the use of the immune-desert phenotype as a prognostic factor in the daily practice of

oral pathology services is likely to be facilitated by the practical advantages of this technique, such as the use of standard H&E staining, the low inter-observer variation, and the little extra time required. Furthermore, our results will inform further investigations of the molecular milieu responsible for the suppression of T-cell immunity. Interestingly, recent studies have highlighted the contrasting role of the immune cells within the tumour microenvironment in OSCC [13, 89, 104]. Therefore, the study of the tumour-immune phenotype in OSCC will require a better understanding of the molecular network governing the immunological response both in the tumour stroma and in the tumour nests [105].

An important issue that must be considered when evaluating immune-phenotype is the presence of extensive ulcerations and necrotic areas. Indeed, it is well known that a certain number of OSCCs present with ulcerated areas and, consequently, secondary inflammation. As previously stated, the areas of immune cell infiltrate associated with necrosis must be left out of the microscopic field or ignored for scoring the immune-phenotype. Nevertheless, this aspect could make the evaluation of immune-phenotype difficult. The main limitations of the present study are the relatively low sample size of OTSCC patients with immune-desert phenotype and its retrospective nature. Beside this, the results obtained provide important insights into the prognostic significance of the tumor-immune profiles. In conclusion, evaluation of the immune-desert phenotype is simple, inexpensive and can be used in daily practice with the aim of improving risk stratification of OTSCC patients, however further OTSCC cohorts should be evaluated to confirm such promising findings.

In this project, further histopathologic biomarkers emerged. PNI in OTSCC has an important clinical relevance. Results from this study show that distinctive PNI characteristics can be related to different clinic-pathological features with consequences

on DSS and lymph–node metastasis. Moreover, introduction of PNI in 8th AJCC Staging system improved the survival prognostic stratification of these patients. The most accredited and cited PNI definition was introduced by Liebig et al, as “tumour in close proximity to nerve and involving at least 33% of its circumference or tumour cells within any of the 3 layers of the nerve sheath or tumour is identified in close proximity to the nerve and involves more than one-third of its circumference” [25]. While this annotation is useful to distinguish tumours with or without PNI, aiming to improve the use of PNI as prognostic biomarker in squamous cell carcinoma, in the last decades new classification systems were introduced [28, 29, 106, 107].

Several studies assessed the prognostic role of PNI in OSCC and OTSCC with promising results [30, 108-110], although controversial findings were obtained when adopting dissimilar classifications and when investigating the various quantitative and qualitative PNI characteristics [27, 106, 111] The present study provides an extensive analysis of 200 patients with OTSCC, aiming to determine whether the evaluation of these parameters may improve the predictive stratification of such patients. Most of published studies focus on prognostic significance of PNI, such as DSS, the number of local failures, or RFS, while only few consider the correlation to the other clinic-pathological features [110, 112, 113]. The most investigated is the association with pathological N-status, for which PNI resulted to be a significant predictor [29, 113-116]. In OSCC, Chang et al. [117] did not find any significant association between PNI and other pathological features, although higher classes of either T-status or Stage were more likely to exhibit PNI-positive tumors. In a cohort of 381 patients with OTSCC, Cracchiolo et al. proved a correlation between PNI and T- and N-status, without considering other clinic-pathological features or different characteristics of PNI [28]. Similar results are presented also in Shen et al. [118] study, where, in addition, PNI correlated with both Staging and

Grading. To our knowledge, only Hasmat et al. [26] evaluated differences among focal and multifocal PNI and other histological features. Multifocal PNI correlated to advanced T-status, N-status, and LVI, while no significant associations were found with focal PNI. Our results show that PNI marked tumours with an increased aggressive behavior; indeed, higher number of PNI-positive tumours and greater number of foci were associated to a more advanced T-status (p-value < 0.001), high grade (p-value = 0.003), and presence of LVI (p-value < 0.001). Moreover, tumours with intratumoral PNI were more likely to exhibit LVI (p-value < 0.001) and positive N-status (p-value < 0.001). In particular, from our study emerged that intratumoral PNI, regardless of number of foci, together with grading and WPOI could be useful to predict patients at high risk of being diagnosed with lymph–node metastasis. Previous studies suggest the need for elective neck dissection in patients with PNI-positive tumours and node-negative on clinical palpation [106, 119, 120]. Our study gives new hints how both focal and multifocal PNI are associated to high grading and WPOI can classify high-risk patients of N-positive status at diagnosis.

It is worth noting that PNI influences DSS and RFS [106]. Several studies proved that PNI was an independent predictor for DSS in OSCC and OTSCC [114, 117, 121, 122]. This study does not only confirm previous results, but it marks how patients with multifocal and both intra-peritumoral PNI-positive OTSCCs suffer of poorest DSS (HR = 2.700, 95% CI 1.362–5.352, p-value = 0.004). Of interest, we reported similar survival results in T1/T2 tumours when considering PNI according to Subramaniam et al., reported worse survival for T1/T2-positive PNI tumors when compared to the same T-status but negative for PNI [31]. Also, Tai et al. reported poor DSS for patients with T1-T2 OTSCC and positive PNI, suggesting a predictive role and the need of new treatment protocols [123]. Hence, the inclusion of PNI in the AJCC staging system might contribute in improving survival prediction of patients and their adverse risk stratification. In support

to this statement, Hasmat et al. demonstrated a better prognostication of multifocal PNI than depth of invasions in OSCC [26]. We included PNI characteristics in the 8th AJCC Staging system, by upstaging by two classes patients with multifocal and both intra-peritumoral PNI. The new staging model thus obtained outperformed the 8th AJCC Staging system [17]. However, there are several methodological inconsistencies in literature, such as the absence of a standardized definition of PNI and the lack of a clear method for PNI detection. Differences in slide preparation and in the number of histological sections examined for each case could compromise the reliability of the results [108]. A limitation of the present study was the evaluation of PNI in a single HE-stained section from the most invasive part of the primary tumour, compromising the accuracy of PNI evaluation in OTSCC due to errors of underreporting.

In conclusion, PNI emerged to be fingerprint of aggressive behaviour in OTSCCs. In particular, in patients with early T-status tumours, the evidence of PNI may represent a factor leading to a worse DSS. Moreover, patients with tumours characterized by intratumoral PNI, together with high-class of grading and WPOI systems, were more likely to exhibit positive lymph–node metastasis. PNI might serve as an additional prognostic factor in OTSCC and by integrating PNI in the current staging system, further improvements in prognostication might be reached.

Prognostic role has emerged in this project for the tumour budding. TB represents a single tumour cell or a small cluster of less than five neoplastic cells at the infiltrative tumour front [32]. TB resulted an independent prognostic factor in many solid tumours, included OSCC and OTSCC. Several Authors demonstrated a significantly correlation between high TB and LNM, either in OSCC and in OTSCC. In OSCC, TB resulted an independent prognostic factor of OS and DFS, regardless the pathological stage and oral subsite [47, 124]. Furthermore, TB showed an association with younger patients, ENE, tongue, and

mouth floor subsite, and positive surgical margins. The correlation with younger patients could be attribute to their higher immune response, which facilitate the EMT and tumor bud formation. TB is promoted even from the dense muscle bundles and from the lymphovascular network of the tongue and the mouth floor. Moreover, TB was associated with other adverse risk factors of oral cancer, such as DOI, POI, LVI, and PNI [34, 35, 77]. A possible explanation for the formation of tumour buds is that hypoxia could influence the behavior of cancer cells by triggering the neoplastic cell migration and invasion [77]. In early OSCC, TB resulted an independent prognostic factor of local recurrences [125], occulted LNM [34, 77], worst OS and DFS [34, 126]. In early OTSCC, occulted LNM was found in all cases with ≥3 buds/field. In particular, the combination of TB with a DOI ≥ 3 mm better predicted the occulted LNM [127].

Our results confirm the prognostic value of TB in OTSCC, and the two-tier system with a cutoff of 5 buds/field is highly predictive of LNM and DSS, regardless the pathological Stage. This cutoff is the most reported in the literature, compared with 3 buds/field and to 10 buds/field [47]. Although the three-tier system further improve the risk stratification, our results do not show significant differences between high and intermediate-risk group. However, due to the uncertain prognostic value of these cutoff values, it is recommended to report the total bud count for each case, to avoid the loss of information. The integration of TB into a predictive model does not improve the patient's stratification. However, BD model resulted a prognostic factor of LNM, local recurrences, and OS, and the RG system showed a significant worsened DSS and DFS in RG3 OTSCC respect to G3 cases [36]. Since the poor prognostic value of the WHO grading and the inclusion of DOI as a staging parameter of pTNM, the BD model and the RG system do not improve the stratification of risk group compared with the only TB evaluation. Moreover, Boxberg et al. criticized the inclusion of DOI into the BD model,

because it is already a staging parameter [93]. Therefore, they proposed a model based on bud activity and intratumoral cell nest size (CNS), showing its prognostic value in predicting LNM in OSCC. The iBD model, based on Glasgow Microenvironment Score and BD score, significantly predicted the DFS and OS of OTSCC patients, suggesting the critical role of local inflammation and stroma reaction in the spreading of TB. Tumor cell dedifferentiation and dissemination at invasive front could be related to a decreased local anti-tumor activity, and the increased tumor–stroma ratio (TSR) might provide cell buds energy substrates. Contrary, Domingueti et al. did not confirm the prognostic value of inflammatory response of iBD model; indeed, they demonstrated the higher prognostic value of BD model compared with iBD model in predicting DSS, especially in early OSCC [128]. It has been suggested the prognostic value of TB does not differ between immunohistochemical (IHC) and HE evaluation. Therefore, the ITBCC group recommended its evaluation on HE sections. However, TB could be obscured by the peritumoral infiltrate, reactive stromal cells, and glandular fragmentation. Moreover, its assessment could be difficult in poorly differentiate OSCC, because of bud cells are surrounded by many lymphocytes, cancer-associated fibroblasts and other stromal cells . Furthermore, single bud cells could be confused with the adjacent tumoral stroma. So, a cytokeratin immunostaining would allow a better visualization, showing the limits of neoplastic epithelial cells; although, the IHC may also stain apoptotic bodies and cellular debris, which should not be counted [33]. Finally, the IHC showed a better reproducibility compared to the HE, resulting more easier, regardless the examiners experience. However, the ITBCC recommendations have been validated as a reliable and simple scoring method in early and/or advanced OTSCC[47, 124]. To ensure the field standardization, they recommended the evaluation by area (0.785 mm2) and by the "hotspot" method, scanning 10 separate fields (×10 objective) along with the infiltrative

front and counting TB in the “hotspot” area (×20 objective) [32]. A quantitative and semi-automatic digital image analysis algorithm was proposed by Pedersen et al. This method showed a better accuracy and reproducibility compared to the conventional ones, overcoming some limitations of TB detection, such as the different scoring system and the inter- and intra-observer variability [129]. Only few studies evaluated the TB on incisional biopsy [34, 35]. The small sample size and fragmentation, the possible lack of infiltrative front, and the presence of artifacts or extensive necrosis could prevent its accurate assessment. However, it has been demonstrated a good correlation between pre- and postoperative TB score, and it has been confirmed the value of preoperative TB as a good predictor of DFS and LNM in OSCC [35, 126]. Therefore, it has been recommended to perform a biopsy or several biopsies from different tumor sites, including its deepest infiltrative part. Recently, Seki-Soda et al. [130] suggested to perform a biopsy (8 mm × 5 mm) including the clinically health tissue. Alternatively, the intratumoral TB of fresh frozen sections could be evaluated. However, only one study demonstrated the prognostic role of CNS in OSCC patients [93]. TB seems to reflect the biological aggressiveness of neoplastic epithelial cells, representing a phenotype undergoing to partial EMT and promoting the tumoral invasion and metastasis. Indeed, bud cells are involved in the degradation of the peritumoral connective tissue and in the invasion of lymphatic and blood vessels leading to lymph node and distant metastasis [33-35, 125, 126]. The overexpression of EMT-transcriptional factors (EMT-TFs) and the downregulation of MET-TFs [33], the lower expression of EMT-TFs of epithelial cells of the infiltrative front rather than to the adjacent stroma, the keratins expression, and the up-regulation of N-cadherin, suggest a partial EMT [125]. Despite the advancements in improving prognostic stratification and accuracy, the AJCC staging system fails to identify OTSCC characterized by poor prognosis. In early Stage OTSCC, an elective neck dissection

(END) is strongly recommended for tumor with DOI ≥ 4 mm, whereas, if DOI < 4 mm, it is performed based on clinical judgment, potentially resulting in over- or under-treatment [119]. Therefore, the integration of TB could be relevant to select patients undergoing to END and/or adjuvant radiotherapy. During surgical treatment of early OTSCC, it has been recommend performing a cytokeratin staining on frozen sections to carry out a definitive surgical treatment without interrupting the anesthesia [35], while other authors suggested to assess TB and POI to select patients undergoing to closer follow-up or radical surgical treatment [126]. These data suggest TB should be included in daily practice to improve the pathological staging and better predict the patient's outcomes. Therefore, a standardized score system should be validate based on tumor site and Stage, and further studies and accuracy analysis should be conducted. Finally, TB could be a prognostic marker in oral cavity subsites in which the DOI is not suitable to predict the tumoral behavior.

The last complementary histopathological biomarker evaluated was tumour-associated tissue eosinophilia (TATE). Indeed, OSCC consists of a complex ecosystem where the interplay between cancer cells and tumour microenvironment takes place [43]. Therefore, several studies suggested that the investigation of morphological features of tumour tissue could be a valuable source of prognostic information [35, 42]. Among the morphological features of oral cancer, some have gained growing interest, such as the presence of TATE. However, the role of eosinophils in cancer pathophysiology is still controversial and both negative and positive prognostic outcomes in oral cancer have been associated with TATE. In the present study, we investigated the association between TATE and other clinicopathological parameters and the prognostic role of TATE in OTSCC patients. Because of the wide range of criteria used to classify TATE in oral cancer, we compared the most common methods and cutoff values reported in literature aiming to provide the

best approach of TATE as a prognostic marker in OTSCC. Univariate and multivariate survival analysis showed that, almost regardless of the method of eosinophil quantification used, OTSCC patients with high TATE had higher likelihood of survival compared to subjects with low TATE count. It should be noted that, although almost every tumor contains at least a small number of eosinophils, a certain number of OTSCC cases had a negligible level of TATE. Our results agree with several studies which indicated TATE as a favorable prognostic marker in oral cancer [49, 131]. Although many others failed to demonstrate a prognostic significance of this parameter, a recent study conducted in a large cohort of OTSCC patients even reported an association between high levels of TATE and worse overall survival [37]. Controversial results found in literature describe an uncertain relationship between the role of eosinophils and oral cancer progression. This may be due to several methodological inconsistencies related to TATE measurement. One of the most critical aspects is the method for eosinophils count, and two different approaches are used, namely the classical method and the density method, making comparison of results difficult [132, 133]. Indeed, some authors demonstrated that the density method was better than the classical method, although a good correlation between the two approaches could be achieved by modifying the cutoffs values [39]. A recent study compared the density method with a modified version of the classical method in evaluating TATE in oral cancer, showing an excellent interobserver agreement by the classical method [134]. Our results obtained from a large cohort of OTSCC, only partially support the hypothesis of a significant difference in methods of eosinophil counting. Indeed, both methods of eosinophil quantification demonstrated an association between high TATE and better DSS. However, the prognostic performance and model fit analyses showed that the density method, called TATE-1 method, had a better predictive performance. It should be emphasized that so far, only two studies, conducted on small

cohorts of oral cancer patients, compared the methods for eosinophils count, and therefore, the evidence is fair and conflicting [39, 134]. Another critical point is the cutoff categorization used to classify the degree of TATE. The cutoff values for TATE vary considerably in literature and many of them are based only on the cohorts under study (eg, by using the median value of TATE), with the risk of overfitting [37, 133]. The only way a prognostic model can be assessed accurately is by conducting an external validation. Therefore, we considered the most used cutoff values reported in literature with the aim to conduct a comparative evaluation. Our results showed that almost all cutoff categorization demonstrated an association between high TATE and better DSS. A single cutoff of 67 eosinophils/mm^2 (TATE-1a) or 100 eosinophils/mm^2 (TATE-1b) and a double cutoff of 50 and 120 eosinophils/mm^2 (TATE-1d) showed the better predictive performance. However, it must be noted that none of the cutoff used was significantly better than the others in predicting DSS. This was also indirectly confirmed by the good interobserver agreement between pathologists in scoring TATE, suggesting that the results obtained were little influenced by the cutoffs used. Indeed, although we found a striking variation in eosinophil infiltration, a certain clustering of TATE scores toward very high or very low values emerged. These findings agree with those reported by other studies [37, 133, 135]. It must be noted that this is a clinical study aimed to investigate the prognostic role of TATE evaluation in oral tongue cancer and to compare the different methods of eosinophil quantification reported in literature. Therefore, the cutoff values used had only a practical utility and did not suggest any biological plausibility of these values. The use of a rigorous definition of TATE, as suggested by Leighton et al., may have influenced the good interobserver agreement reported [136]. Indeed, the exclusion of blood vessels, extensive areas of necrosis and ulceration, as well as the evaluation of both tumoral stroma and neoplastic eosinophil infiltration at the invasive front, could

reduce the risk of overestimating or underestimating TATE [133]. Several other aspects could influence the accuracy and the reproducibility of TATE evaluation, such as the magnification used and the number of HPF analyzed for each patient. Data from literature show as the number of microscopic fields analyzed for each patient could range from 1 to 75.13, 15, 22-24 This aspect could hinder any comparison among the results obtained from different studies; furthermore, although a greater number of HPF evaluated can increase accuracy, this reduces its feasibility in daily practice. In particular, as for TATE-2 method, the random selection of 10 HPF for each case implies a certain degree of inaccuracy, mainly related to the irregular distribution of eosinophils in the tissue. Therefore, the choice to consider 10 HPF derives from the search for a balance between the accuracy and the feasibility. However, the good interobserver agreement obtained also with TATE-2 method allows us to hypothesize that the heterogeneity of the eosinophil distribution in the tissue is not such as to compromise the results.

Several mechanisms by which eosinophils could exert their role against cancer progression have been hypothesized and reported in literature. These cells have the capacity to release a broad range of proteins and peptides, such as the eosinophil cationic protein, the major basic protein, the eosinophil derived neurotoxin, and the eosinophil peroxidase, known to have cytotoxic properties [137, 138]. Furthermore, eosinophils can release a number of pro-inflammatory cytokines and chemokines such as IL-1, IL-3, TNF-α, and IFN-γ.22, 28 Therefore, the association of high TATE with favorable oral cancer prognosis could be related to the ability of eosinophils to induce and sustain a tumor immune response, mainly dependent on tumor-infiltrating lymphocytes. Regarding the tendency of eosinophils to accumulate along the tumor front, Lee et al. proposed the "LIAR hypothesis" (Local Immunity And/or Remodeling/Repair), suggesting that eosinophils could be involved in the remodeling of host connective tissue in response to

destruction caused by cancer cells at the invasive front [139]. The strength points of the present study are the use of a specific subtype of oral cancer, namely OTSCC, eliminating the presence of any "anatomical bias"; a rigorous definition of the histological evaluation methods for TATE; the comparison of different methods of eosinophil quantification and cut-off values; the relatively long follow-up period; and the evaluation of OTSCC-related death through the DSS. The main limitations of the study are its retrospective nature and the relatively low sample size of OTSCC patients, even if it is one of the largest studies ever done on this subject. In conclusion, evaluation of TATE is simple, cost-effective, and easy to implement in daily practice with the aim of improving risk stratification of OTSCC patients. However, further OTSCC cohorts should be analyzed to confirm such preliminary findings. In this regard, results of prognostic performance analysis suggest using density (TATE-1) method as the standard approach to evaluate TATE in future studies, enhancing replicability. Furthermore, since none of the cutoff reported in literature was significantly better than the others, we suggest reporting the main ones in future studies, in order to ensure the comparability of the results.

This project ended by developing a new classification system of the most mutated gene in HNSCC, TP53. Many efforts have been made to classify mutations according to their influence on structural changes, and to investigate if they could serve as prognostic factors, but limits have been identified due to the wideness of the mutational landscape of TP53. In this study, we propose a new classification method that identifies patients with mutations at high risk of death in squamous cell cancers and, in particular, in tumours from the head and neck district. Of the 14 million new cancers diagnosed worldwide every year, 50–60% is characterised by at least one somatic variant of p53 [59]. In the HNSCC cohort from TCGA included in this study, 69.9% of patients expressed a mutation in

TP53. A web platform has been created to collect and organise the increasing number of researches published about TP53 in cancer (http://www.p53.fr/) [61]. Due to the increase in detection of single mutations in TP53 gene, several studies have attempted to elucidate the correlation between mutational status and patients' clinicopathological characteristics, with discordant results. Most published studies have employed different classifications and mutation profiles for their analyses. This is a reasonable approach, since a broad range of mutations can affect the TP53 gene and its encoded protein; for example, the 286 HNSCC patients included in our study exhibited 129 different kinds of mutation, of which R273 was the most frequent but occurred in only 13 patients.

One of the simplest and most used approach to translate TP53 mutational profile into clinically useful information is to compare wild-type and mutated patients, with the latter subgroup predicting death in different types of cancers. An extensive analysis of 33 TCGA studies showed that the effects of TP53 mutations on patients' prognosis were statistically significant in nine malignancies (lung adenocarcinoma, hepatocellular carcinoma, HNSCC, acute myeloid leukaemia, clear-cell renal cell carcinoma (RCC), papillary RCC, chromophobe RCC, uterine endometrial carcinoma and thymoma) [66]. Although this method can be considered "quick and useful", this approach does not take into account some biochemical and functional characteristics of single TP53 mutations. A previous comprehensive genomic study on the same TCGA cohort provided fundamental insights into the correlation between mutational profile of TP53 and HNSCC; however it did not take into consideration the anatomical sublocalisation of tumours in the HNSCC area, in which HPV-positive oropharynx subgroup frequently exhibits wild-type TP53 and favourable prognosis [75]. After integrating the survival analysis according to the subsite of HNSCC onset, mutated TP53 resulted to be an independent prognostic factor for overall and disease-free survival only in OP. These

results have salient clinical implications, because, cells with wild-type or higher TP53 expression are more susceptible to radiation therapy, and HPV+ tumours usually display higher radiosensitivity [140]. Therefore, our data suggest that mutations in TP53 gene have a prognostic role in HNSCC, above all, in HPV+ OP tumours where mutational status of this gene should be investigated before considering treatment options [141]. These findings could let us speculate that mutations affecting TP53 in HPV+ tumours make them more similar to HPV− HNSCCs. Although this hypothesis should be analysed in future studies, the results of network analysis showed that MUT OP shared common alterations with other subgroups, in particular homozygous deletions and mutations affecting CDKN2A (78.9% of patients in MUT OP against 13.6% mRNA upregulation in WT OP). Because of the interaction between HPV E7 protein and host cells, CDKN2A mRNA upregulation was also observed in HPV+ tumours arising in the oropharynx. As it is known, HPV E7 protein ubiquitinates the protein of retinoblastoma (pRb) by binding to the cullin 2 ubiquitin ligase complex. Loss of pRb leads to the release of E2F with the transcription of S-phase genes. Hence, HPV+ tumours show an upregulation of CDKN2A as a consequence of negative feedback loop to control cell cycle, from pRb loss [142]. In addition, CX3CL1 and MYB shared common alteration (mRNA upregulation) both in WT OP and HPV+ OP, leading to a positive regulation of transforming growth factor beta production. They could be involved in a cell-response mechanism due to the effect of E7 proteins. It is reported that E7 is able to prevent both Smad transcriptional activity and the ability of TGF-β to inhibit DNA synthesis [143]. MYB has been shown to be related to HPV infection, above all in cervical cancer, but its role, together with CX3CL1, has never been elucidated in OP [144]. It is worth noting that BRCA1 was also upregulated in WT OP patients and HPV+ tumours (29.5% and 29.6%, respectively). From our network analysis, BRCA1 was present in both subgroups in complex with the

proliferating cell nuclear antigen (PCNA). PCNA is a protein produced in S phase of the cell cycle, and it acts in replication and repair machinery, favouring the cell-cycle progression [145]. PCNA seems to be an important factor for progression to malignancy in HPV+ tumours, by activation of S phase of the cell cycle. BRCA1 is involved in genome-integrity machinery and cell-cycle checkpoint control. BRCA1 plays a critical role in homologous recombination repair, and cells with deficiency in BRCA1 are more sensible to drugs causing DNA breaks or to ionising radiation [146]. Tian et al. showed that BRCA1 leads to mono- and polyubiquitination of PCNA by recruiting some effector proteins. It is reported that PCNA monoubiquitylation is necessary for efficient translesion synthesis. Through this mechanism, BRCA1 promotes translesion DNA synthesis and progression of the cell cycle [147, 148]. Taken together, these findings suggest that BRCA1 mRNA upregulation with PCNA could have an important role in HPV + tumours of oropharynx and in chemo-radioresistance of these patients, by promoting translesion DNA synthesis and cell-cycle progression, changing its classical function as tumour suppressor to an oncogene, as already reported in cancer stem cell models of different kinds of tumours [148]. Similar to what was performed in the previously cited genomic analysis [66], Poeta et al. [76] applied their algorithm only for the whole HNSCC cohort without investigating the results for each subgroup. The reported algorithm was able to prognostically stratify HNSCC patients; in particular, using the wild-type group as reference, only tumours with disruptive mutations showed a worse overall survival, whereas patients with conservative or nondisruptive mutations did not. Similar results were obtained in this study by applying the PA on the TCGA HNSCC cohort. In addition, conservative mutations were also linked to a worse overall survival, although without differences between disruptive and nondisruptive mutations. Starting from the findings of Poeta et al, we developed our own algorithm reclassifying mutations

in high risk of death according to their homozygous alteration, their zinc ligand and H+-forming bond alteration. Martin et al. and Baker et al. [73, 74] already stressed the important role of hydrogen bonding in protein residues. Hence, for example, the mutation Y220C is considered nondisruptive in the PA, since in its tertiary structure, this residue is located far from the functional part. This mutation was reclassified as high risk since tyrosine (Y) is able to create a hydrogen bonding, conversely to what happens when substituted by a cysteine (C). The same can be stated for the residues involved in the zinc ligand, since it is important for the stabilisation of the p53/DNA complex [74]. At last, mutations affecting residues in "unknown" predicted secondary structure were considered as high risk. Comparing the predictive capability of the two algorithms on the TCGA database, our model outperformed the PA. In particular, our classifier was able to better stratify a cohort of patients with higher risk of death, comparing it with both wild-type and nondisruptive mutation groups, while the PA was not able to find a significant difference between nondisruptive and disruptive mutations. Subsequently, we investigated the predictive performance of both algorithms in each subgroup. Of interest, PA failed to find any significant prognostic class in OSCC, where the new model found a class of mutations with a better overall survival (wild-type vs high-risk, multivariate analysis: HR = 0.714; 95% CI: 0.458–1.113; P = 0.137); (low-risk vs high-risk, multivariate analysis: HR = 0.499; 95% CI: 0.283–0.878; P = 0.016). However, both algorithms failed to find any significant prognostic factor in larynx, with contradictory results in lung and oesophageal cancer. A meta-analysis, published in 2015 [149], reported the same conflicting results in non-small-cell lung carcinoma, since TP53 mutations emerged to be associated with a worse overall survival compared with wild type. Although the meta-analysis included all patients with non-small-cell lung carcinoma, when performing subgroup analysis, only patients with early stages and

affected by adenocarcinoma, took advantage of the wild-type status. The same results were reported in other studies [150]. Molina-Vila et al. [151] were the only to apply Poeta et al. classification in a cohort of advanced-stage non-small-cell lung cancer; only nondisruptive mutations were associated with a shorter survival. Our results cannot be compared, since we included only patients with squamous cell carcinoma, and our cohort consisted of only 80/438 patients with advanced stage (III–IV); because of these promising results, we included all patients in a whole cohort, including patients with head and neck-, oesophageal- and lung squamous cell carcinoma. Patients included in the survival analysis were 914 with complete data about survival status, follow-up time, mutational status, staging, age and gender (grading was removed because it was only available for head and neck patients). Of these, 249 were from oral cavity, 62 from oropharynx, 89 from larynx, 9 from hypopharynx, 72 oesophagheal cancers and 433 lung squamous cell cancers. In the multivariate Cox regression model, the dichotomous mutational status (WT/MUT) did not correlate with overall survival (multivariate analysis: HR = 1.174; 95% CI: 0.912–1.511; P = 0.214); we therefore applied both classification systems on the new cohort. PA failed to find any significant association between disruptive and conservative mutations with the overall survival (wild-type vs disruptive mutations, multivariate analysis: HR = 1.125; 95% CI: 0.856–1.478; P = 0.397) (wild-type vs nondisruptive mutations, multivariate analysis: HR = 1.239; 95% CI: 0.937–1.639; P = 0.133). Nondisruptive mutations showed even a worse overall survival compared with disruptive mutations (nondisruptive vs disruptive mutations, multivariate analysis: HR = 1.101; 95% CI: 0.880–1.378; P = 0.399). Conversely, the new proposed algorithm showed a better predictive performance; in particular, patients in the high-risk group showed a worse prognosis, while the low-risk group showed even a better overall survival compared with wild type (wild-type vs high-risk mutations, multivariate

analysis: HR = 1.283; 95% CI: 0.991–1.663; P = 0.059); (wild-type vs low-risk mutations, multivariate analysis: HR = 0.881; 95% CI: 0.629–1.236; P = 0.464); (low- vs high-risk mutations, multivariate analysis: HR = 0.687; 95% CI: 0.518–0.911; P = 0.009).

For the first time, our study elucidated the mutational profile of TP53 gene in HNSCC subgroups. To the best of our knowledge, this was the first study to link different molecular aspects of TP53 alterations (mutational profile of TP53, coding gene structure, secondary structure and well-known hotspot mutations) to the clinical variables of HNSCC patients. Although most tumours arising from the mucosa of the head and neck district are studied together, the results from this study clearly show differences between the OC, OP and L subsites in terms of mutational profile and signalling pathways of TP53. Furthermore, this study suggests that there is a broad range of TP53 residues that could be mutated in HNSCC, which may determine differential effects in terms of mRNA and protein expression, secondary structure, apoptosis activity and DNA-binding affinity. This finding makes it difficult to develop drugs that target selective mutations of TP53 as these would have little implications in the clinical management of HNSCC patients. Finally, whilst this study indicates a prognostic role of TP53 mutations in HNSCC, the influence of TP53 status in cancer prognosis more broadly is still controversial and large, and well-standardised studies are needed.

5. CONCLUSIONS

This project led to a deeper, accurate and updated investigation of classic clinic-pathologic features, highlighting their role as prognostic biomarkers to be included in future staging systems in everyday practice. Standardization and classification issues were raised and compared, improving quality of current evidence. H&E assessment of these biomarkers might become a reliable and useful tool in everyday clinical practice, thanks to spread application, cheap and relatively easy evaluation. These histological

biomarkers might be combined to genomic ones, like mutations of the gene TP53, improving stratification. The search for prognostic and therapeutic factors for oral cancer remains a challenge.

REFERENCES

1. Sung, H., et al., *Global Cancer Statistics 2020: GLOBOCAN Estimates of Incidence and Mortality Worldwide for 36 Cancers in 185 Countries.* CA Cancer J Clin, 2021. **71**(3): p. 209-249.
2. Boldrup, L., et al., *Differences in p63 expression in SCCHN tumours of different sub-sites within the oral cavity.* Oral Oncol, 2011. **47**(9): p. 861-5.
3. Choi, Y.S., et al., *Analysis of prognostic factors through survival rate analysis of oral squamous cell carcinoma patients treated at the National Cancer Center: 20 years of experience.* J Korean Assoc Oral Maxillofac Surg, 2022. **48**(5): p. 284-291.
4. Puram, S.V., et al., *Single-Cell Transcriptomic Analysis of Primary and Metastatic Tumor Ecosystems in Head and Neck Cancer.* Cell, 2017. **171**(7): p. 1611-1624 e24.
5. Kurten, C.H.L., et al., *Investigating immune and non-immune cell interactions in head and neck tumors by single-cell RNA sequencing.* Nat Commun, 2021. **12**(1): p. 7338.
6. Li, H., et al., *Current trends of targeted therapy for oral squamous cell carcinoma.* J Cancer Res Clin Oncol, 2022. **148**(9): p. 2169-2186.
7. Brook, I., *Late side effects of radiation treatment for head and neck cancer.* Radiat Oncol J, 2020. **38**(2): p. 84-92.
8. Elaldi, R., et al., *Correlations between long-term quality of life and patient needs and concerns following head and neck cancer treatment and the impact of psychological distress. A multicentric cross-sectional study.* Eur Arch Otorhinolaryngol, 2021. **278**(7): p. 2437-2445.
9. Cavicchi, O., et al., *[Multicenter survey through a questionnaire on the prognostic value of surgical resection margin in head and neck tumors].* Acta Otorhinolaryngol Ital, 2000. **20**(6): p. 413-7.
10. Patel, S.G. and W.M. Lydiatt, *Staging of head and neck cancers: is it time to change the balance between the ideal and the practical?* J Surg Oncol, 2008. **97**(8): p. 653-7.
11. Mascitti, M., et al., *American Joint Committee on Cancer staging system 7th edition versus 8th edition: any improvement for patients with squamous cell carcinoma of the tongue?* Oral Surg Oral Med Oral Pathol Oral Radiol, 2018. **126**(5): p. 415-423.
12. Kano, S., et al., *Validation of the 8th edition of the AJCC/UICC TNM staging system for tongue squamous cell carcinoma.* Int J Clin Oncol, 2018. **23**(5): p. 844-850.
13. Fang, J., et al., *Prognostic significance of tumor infiltrating immune cells in oral squamous cell carcinoma.* BMC Cancer, 2017. **17**(1): p. 375.
14. Troiano, G., et al., *Prognostic significance of CD68(+) and CD163(+) tumor associated macrophages in head and neck squamous cell carcinoma: A systematic review and meta-analysis.* Oral Oncol, 2019. **93**: p. 66-75.
15. Wang, Z., M.A. Jensen, and J.C. Zenklusen, *A Practical Guide to The Cancer Genome Atlas (TCGA).* Methods Mol Biol, 2016. **1418**: p. 111-41.
16. Rahman, N., et al., *Reframing Histological Risk Assessment of Oral Squamous Cell Carcinoma in the Era of UICC 8th Edition TNM Staging.* Head Neck Pathol, 2021. **15**(1): p. 202-211.
17. Moeckelmann, N., et al., *Prognostic implications of the 8th edition American Joint Committee on Cancer (AJCC) staging system in oral cavity squamous cell carcinoma.* Oral Oncol, 2018. **85**: p. 82-86.
18. Russo, D., et al., *Development and Validation of Prognostic Models for Oral Squamous*

Cell Carcinoma: A Systematic Review and Appraisal of the Literature. Cancers (Basel), 2021. **13**(22).
19. Amin, M.B., et al., *The Eighth Edition AJCC Cancer Staging Manual: Continuing to build a bridge from a population-based to a more "personalized" approach to cancer staging.* CA Cancer J Clin, 2017. **67**(2): p. 93-99.
20. General Assembly of the World Medical, A., *World Medical Association Declaration of Helsinki: ethical principles for medical research involving human subjects.* J Am Coll Dent, 2014. **81**(3): p. 14-8.
21. Sauerbrei, W., et al., *Reporting Recommendations for Tumor Marker Prognostic Studies (REMARK): An Abridged Explanation and Elaboration.* J Natl Cancer Inst, 2018. **110**(8): p. 803-811.
22. Heerema, M.G., et al., *Reproducibility and prognostic value of pattern of invasion scoring in low-stage oral squamous cell carcinoma.* Histopathology, 2016. **68**(3): p. 388-97.
23. van Pelt, G.W., et al., *Scoring the tumor-stroma ratio in colon cancer: procedure and recommendations.* Virchows Arch, 2018. **473**(4): p. 405-412.
24. Salgado, R., et al., *The evaluation of tumor-infiltrating lymphocytes (TILs) in breast cancer: recommendations by an International TILs Working Group 2014.* Ann Oncol, 2015. **26**(2): p. 259-71.
25. Liebig, C., et al., *Perineural invasion in cancer: a review of the literature.* Cancer, 2009. **115**(15): p. 3379-91.
26. Hasmat, S., et al., *Multifocal perineural invasion is a better prognosticator than depth of invasion in oral squamous cell carcinoma.* Head Neck, 2019. **41**(11): p. 3992-3999.
27. Aivazian, K., et al., *Perineural invasion in oral squamous cell carcinoma: quantitative subcategorisation of perineural invasion and prognostication.* J Surg Oncol, 2015. **111**(3): p. 352-8.
28. Cracchiolo, J.R., et al., *Patterns of recurrence in oral tongue cancer with perineural invasion.* Head Neck, 2018. **40**(6): p. 1287-1295.
29. Wei, P.Y., W.Y. Li, and S.K. Tai, *Discrete Perineural Invasion Focus Number in Quantification for T1-T2 Oral Squamous Cell Carcinoma.* Otolaryngol Head Neck Surg, 2019. **160**(4): p. 635-641.
30. Chinn, S.B., et al., *Impact of perineural invasion in the pathologically N0 neck in oral cavity squamous cell carcinoma.* Otolaryngol Head Neck Surg, 2013. **149**(6): p. 893-9.
31. Subramaniam, N., et al., *Adverse pathologic features in T1/2 oral squamous cell carcinoma classified by the American Joint Committee on Cancer eighth edition and implications for treatment.* Head Neck, 2018. **40**(10): p. 2123-2128.
32. Lugli, A., et al., *Recommendations for reporting tumor budding in colorectal cancer based on the International Tumor Budding Consensus Conference (ITBCC) 2016.* Mod Pathol, 2017. **30**(9): p. 1299-1311.
33. Wang, C., et al., *Tumor budding correlates with poor prognosis and epithelial-mesenchymal transition in tongue squamous cell carcinoma.* J Oral Pathol Med, 2011. **40**(7): p. 545-51.
34. Seki, M., et al., *Tumour budding evaluated in biopsy specimens is a useful predictor of prognosis in patients with cN0 early stage oral squamous cell carcinoma.* Histopathology, 2017. **70**(6): p. 869-879.
35. Almangush, A., et al., *A simple novel prognostic model for early stage oral tongue cancer.* Int J Oral Maxillofac Surg, 2015. **44**(2): p. 143-50.
36. Elseragy, A., et al., *A Proposal to Revise the Histopathologic Grading System of Early Oral Tongue Cancer Incorporating Tumor Budding.* Am J Surg Pathol, 2019. **43**(5): p. 703-709.
37. De Paz, D., et al., *Clinical Implications of Tumor-Associated Tissue Eosinophilia in Tongue Squamous Cell Carcinoma.* Laryngoscope, 2019. **129**(5): p. 1123-1129.
38. Oliveira, D.T., et al., *Eosinophils may predict occult lymph node metastasis in early oral cancer.* Clin Oral Investig, 2012. **16**(6): p. 1523-8.
39. Alkhabuli, J.O. and A.S. High, *Significance of eosinophil counting in tumor associated*

tissue eosinophilia (TATE). Oral Oncol, 2006. **42**(8): p. 849-50.
40. Heinze, G. and D. Dunkler, *Five myths about variable selection.* Transpl Int, 2017. **30**(1): p. 6-10.
41. Sahoo, A., et al., *Perinerural, lymphovascular and depths of invasion in extrapolating nodal metastasis in oral cancer.* Clin Oral Investig, 2020. **24**(2): p. 747-755.
42. Mascitti, M., et al., *Addition of the tumour-stroma ratio to the 8th edition American Joint Committee on Cancer staging system improves survival prediction for patients with oral tongue squamous cell carcinoma.* Histopathology, 2020. **77**(5): p. 810-822.
43. Troiano, G., et al., *The immune phenotype of tongue squamous cell carcinoma predicts early relapse and poor prognosis.* Cancer Med, 2020. **9**(22): p. 8333-8344.
44. Caponio, V.C.A., et al., *Pattern and localization of perineural invasion predict poor survival in oral tongue carcinoma.* Oral Dis, 2021.
45. Raftery, A.E., et al., *Bayesian probabilistic projections of life expectancy for all countries.* Demography, 2013. **50**(3): p. 777-801.
46. Maes, H.H., et al., *Using Multimodel Inference/Model Averaging to Model Causes of Covariation Between Variables in Twins.* Behav Genet, 2021. **51**(1): p. 82-96.
47. Mascitti, M., et al., *Prognostic significance of tumor budding thresholds in oral tongue squamous cell carcinoma.* Oral Dis, 2022.
48. Zlobec, I. and A. Lugli, *Epithelial mesenchymal transition and tumor budding in aggressive colorectal cancer: tumor budding as oncotarget.* Oncotarget, 2010. **1**(7): p. 651-61.
49. Caponio, V.C.A., et al., *Prognostic assessment of different methods for eosinophils detection in oral tongue cancer.* J Oral Pathol Med, 2022. **51**(3): p. 240-248.
50. Siegel, R.L., K.D. Miller, and A. Jemal, *Cancer statistics, 2016.* CA Cancer J Clin, 2016. **66**(1): p. 7-30.
51. Ferlay, J., et al., *Cancer incidence and mortality worldwide: sources, methods and major patterns in GLOBOCAN 2012.* Int J Cancer, 2015. **136**(5): p. E359-86.
52. Hecht, S.S., *Tobacco carcinogens, their biomarkers and tobacco-induced cancer.* Nat Rev Cancer, 2003. **3**(10): p. 733-44.
53. Menzies, G.E., et al., *Base damage, local sequence context and TP53 mutation hotspots: a molecular dynamics study of benzo[a]pyrene induced DNA distortion and mutability.* Nucleic Acids Res, 2015. **43**(19): p. 9133-46.
54. Tuna, M., C.I. Amos, and G.B. Mills, *Genome-Wide Analysis of Head and Neck Squamous Cell Carcinomas Reveals HPV, TP53, Smoking and Alcohol-Related Allele-Based Acquired Uniparental Disomy Genomic Alterations.* Neoplasia, 2019. **21**(2): p. 197-205.
55. Li, X.C., et al., *A mutational signature associated with alcohol consumption and prognostically significantly mutated driver genes in esophageal squamous cell carcinoma.* Ann Oncol, 2018. **29**(4): p. 938-944.
56. Mirghani, H., et al., *Does smoking alter the mutation profile of human papillomavirus-driven head and neck cancers?* Eur J Cancer, 2018. **94**: p. 61-69.
57. Holloway, E., *From genotype to phenotype: linking bioinformatics and medical informatics ontologies.* Comp Funct Genomics, 2002. **3**(5): p. 447-50.
58. Kamada, R., et al., *Tetramer formation of tumor suppressor protein p53: Structure, function, and applications.* Biopolymers, 2016. **106**(4): p. 598-612.
59. Kandoth, C., et al., *Mutational landscape and significance across 12 major cancer types.* Nature, 2013. **502**(7471): p. 333-339.
60. Petitjean, A., et al., *Impact of mutant p53 functional properties on TP53 mutation patterns and tumor phenotype: lessons from recent developments in the IARC TP53 database.* Hum Mutat, 2007. **28**(6): p. 622-9.
61. Olivier, M., et al., *The IARC TP53 database: new online mutation analysis and recommendations to users.* Hum Mutat, 2002. **19**(6): p. 607-14.
62. Bernard, X., et al., *Proteasomal degradation of p53 by human papillomavirus E6 oncoprotein relies on the structural integrity of p53 core domain.* PLoS One, 2011. **6**(10): p. e25981.

63. Chen, Y., R. Dey, and L. Chen, *Crystal structure of the p53 core domain bound to a full consensus site as a self-assembled tetramer.* Structure, 2010. **18**(2): p. 246-56.
64. Zenz, T., et al., *TP53 mutation and survival in aggressive B cell lymphoma.* Int J Cancer, 2017. **141**(7): p. 1381-1388.
65. Christopoulos, P., et al., *Detection of TP53 Mutations in Tissue or Liquid Rebiopsies at Progression Identifies ALK+ Lung Cancer Patients with Poor Survival.* Cancers (Basel), 2019. **11**(1).
66. Li, V.D., K.H. Li, and J.T. Li, *TP53 mutations as potential prognostic markers for specific cancers: analysis of data from The Cancer Genome Atlas and the International Agency for Research on Cancer TP53 Database.* J Cancer Res Clin Oncol, 2019. **145**(3): p. 625-636.
67. Leroy, B., et al., *Recommended Guidelines for Validation, Quality Control, and Reporting of TP53 Variants in Clinical Practice.* Cancer Res, 2017. **77**(6): p. 1250-1260.
68. Gao, J., et al., *Integrative analysis of complex cancer genomics and clinical profiles using the cBioPortal.* Sci Signal, 2013. **6**(269): p. pl1.
69. Caponio, V.C.A., et al., *Computational analysis of TP53 mutational landscape unveils key prognostic signatures and distinct pathobiological pathways in head and neck squamous cell cancer.* Br J Cancer, 2020. **123**(8): p. 1302-1314.
70. Strom, S.P., *Current practices and guidelines for clinical next-generation sequencing oncology testing.* Cancer Biol Med, 2016. **13**(1): p. 3-11.
71. Moon, S., et al., *Systematic Inspection of the Clinical Relevance of TP53 Missense Mutations in Gastric Cancer.* IEEE/ACM Trans Comput Biol Bioinform, 2019. **16**(5): p. 1693-1701.
72. Tahara, T., et al., *Mutation spectrum of TP53 gene predicts clinicopathological features and survival of gastric cancer.* Oncotarget, 2016. **7**(27): p. 42252-60.
73. Martin, A.C., et al., *Integrating mutation data and structural analysis of the TP53 tumor-suppressor protein.* Hum Mutat, 2002. **19**(2): p. 149-64.
74. Baker, E.N. and R.E. Hubbard, *Hydrogen bonding in globular proteins.* Prog Biophys Mol Biol, 1984. **44**(2): p. 97-179.
75. Cancer Genome Atlas, N., *Comprehensive genomic characterization of head and neck squamous cell carcinomas.* Nature, 2015. **517**(7536): p. 576-82.
76. Poeta, M.L., et al., *TP53 mutations and survival in squamous-cell carcinoma of the head and neck.* N Engl J Med, 2007. **357**(25): p. 2552-61.
77. Ho, Y.Y., et al., *The significance of tumor budding in oral cancer survival and its relevance to the eighth edition of the American Joint Committee on Cancer staging system.* Head Neck, 2019. **41**(9): p. 2991-3001.
78. Wu, J., et al., *Association between tumor-stroma ratio and prognosis in solid tumor patients: a systematic review and meta-analysis.* Oncotarget, 2016. **7**(42): p. 68954-68965.
79. Zengin, M., *Tumour Budding and Tumour Stroma Ratio are Reliable Predictors for Death and Recurrence in Elderly Stage I Colon Cancer Patients.* Pathol Res Pract, 2019. **215**(11): p. 152635.
80. Zhang, X., et al., *Research on correlation between tumor-stroma ratio and prognosis in non-small cell lung cancer.* Minerva Med, 2019. **110**(6): p. 590-592.
81. Zou, M.X., et al., *The Relationship Between Tumor-Stroma Ratio, the Immune Microenvironment, and Survival in Patients With Spinal Chordoma.* Neurosurgery, 2019. **85**(6): p. E1095-E1110.
82. Vangangelt, K.M.H., et al., *The prognostic value of tumor-stroma ratio in tumor-positive axillary lymph nodes of breast cancer patients.* Int J Cancer, 2018. **143**(12): p. 3194-3200.
83. Mesker, W.E., et al., *The carcinoma-stromal ratio of colon carcinoma is an independent factor for survival compared to lymph node status and tumor stage.* Cell Oncol, 2007. **29**(5): p. 387-98.
84. Zhang, X.L., et al., *The tumor-stroma ratio is an independent predictor for survival in*

nasopharyngeal cancer. Oncol Res Treat, 2014. **37**(9): p. 480-4.
85. Karpathiou, G., et al., *Prognostic significance of tumor budding, tumor-stroma ratio, cell nests size, and stroma type in laryngeal and pharyngeal squamous cell carcinomas.* Head Neck, 2019. **41**(6): p. 1918-1927.
86. Almangush, A., et al., *Prognostic impact of tumour-stroma ratio in early-stage oral tongue cancers.* Histopathology, 2018. **72**(7): p. 1128-1135.
87. Choi, J.W., et al., *Intratumoural heterogeneity measured using FDG PET and MRI is associated with tumour-stroma ratio and clinical outcome in head and neck squamous cell carcinoma.* Clin Radiol, 2017. **72**(6): p. 482-489.
88. Huang, Z., et al., *The prognostic role of tumour-infiltrating lymphocytes in oral squamous cell carcinoma: A meta-analysis.* J Oral Pathol Med, 2019. **48**(9): p. 788-798.
89. Zhou, C., et al., *Density and location of CD3(+) and CD8(+) tumor-infiltrating lymphocytes correlate with prognosis of oral squamous cell carcinoma.* J Oral Pathol Med, 2018. **47**(4): p. 359-367.
90. Troiano, G., et al., *High PD-L1 expression in the tumour cells did not correlate with poor prognosis of patients suffering for oral squamous cells carcinoma: A meta-analysis of the literature.* Cell Prolif, 2019. **52**(2): p. e12537.
91. Hendry, S., et al., *Assessing Tumor-Infiltrating Lymphocytes in Solid Tumors: A Practical Review for Pathologists and Proposal for a Standardized Method from the International Immuno-Oncology Biomarkers Working Group: Part 2: TILs in Melanoma, Gastrointestinal Tract Carcinomas, Non-Small Cell Lung Carcinoma and Mesothelioma, Endometrial and Ovarian Carcinomas, Squamous Cell Carcinoma of the Head and Neck, Genitourinary Carcinomas, and Primary Brain Tumors.* Adv Anat Pathol, 2017. **24**(6): p. 311-335.
92. Pages, F., et al., *International validation of the consensus Immunoscore for the classification of colon cancer: a prognostic and accuracy study.* Lancet, 2018. **391**(10135): p. 2128-2139.
93. Boxberg, M., et al., *Composition and Clinical Impact of the Immunologic Tumor Microenvironment in Oral Squamous Cell Carcinoma.* J Immunol, 2019. **202**(1): p. 278-291.
94. Quan, H., et al., *The repertoire of tumor-infiltrating lymphocytes within the microenvironment of oral squamous cell carcinoma reveals immune dysfunction.* Cancer Immunol Immunother, 2020. **69**(3): p. 465-476.
95. Hadler-Olsen, E. and A.M. Wirsing, *Tissue-infiltrating immune cells as prognostic markers in oral squamous cell carcinoma: a systematic review and meta-analysis.* Br J Cancer, 2019. **120**(7): p. 714-727.
96. Shaban, M., et al., *A Novel Digital Score for Abundance of Tumour Infiltrating Lymphocytes Predicts Disease Free Survival in Oral Squamous Cell Carcinoma.* Sci Rep, 2019. **9**(1): p. 13341.
97. Chen, D.S. and I. Mellman, *Elements of cancer immunity and the cancer-immune set point.* Nature, 2017. **541**(7637): p. 321-330.
98. Kather, J.N., et al., *Topography of cancer-associated immune cells in human solid tumors.* Elife, 2018. **7**.
99. Diao, P., et al., *Immune landscape and subtypes in primary resectable oral squamous cell carcinoma: prognostic significance and predictive of therapeutic response.* J Immunother Cancer, 2021. **9**(6).
100. Li, B., et al., *The Immune Subtypes and Landscape of Squamous Cell Carcinoma.* Clin Cancer Res, 2019. **25**(12): p. 3528-3537.
101. Hegde, P.S., V. Karanikas, and S. Evers, *The Where, the When, and the How of Immune Monitoring for Cancer Immunotherapies in the Era of Checkpoint Inhibition.* Clin Cancer Res, 2016. **22**(8): p. 1865-74.
102. Cogdill, A.P., M.C. Andrews, and J.A. Wargo, *Hallmarks of response to immune checkpoint blockade.* Br J Cancer, 2017. **117**(1): p. 1-7.
103. Heikkinen, I., et al., *Assessment of Tumor-infiltrating Lymphocytes Predicts the Behavior of Early-stage Oral Tongue Cancer.* Am J Surg Pathol, 2019. **43**(10): p. 1392-

1396.
104. Watanabe, Y., et al., *Tumor-infiltrating lymphocytes, particularly the balance between CD8(+) T cells and CCR4(+) regulatory T cells, affect the survival of patients with oral squamous cell carcinoma.* Oral Surg Oral Med Oral Pathol Oral Radiol Endod, 2010. **109**(5): p. 744-52.
105. Katou, F., et al., *Differing phenotypes between intraepithelial and stromal lymphocytes in early-stage tongue cancer.* Cancer Res, 2007. **67**(23): p. 11195-201.
106. Miller, M.E., et al., *A novel classification system for perineural invasion in noncutaneous head and neck squamous cell carcinoma: histologic subcategories and patient outcomes.* Am J Otolaryngol, 2012. **33**(2): p. 212-5.
107. Tarsitano, A., M.L. Tardio, and C. Marchetti, *Impact of perineural invasion as independent prognostic factor for local and regional failure in oral squamous cell carcinoma.* Oral Surg Oral Med Oral Pathol Oral Radiol, 2015. **119**(2): p. 221-8.
108. Binmadi, N.O. and J.R. Basile, *Perineural invasion in oral squamous cell carcinoma: a discussion of significance and review of the literature.* Oral Oncol, 2011. **47**(11): p. 1005-10.
109. Brandwein-Gensler, M., et al., *Oral squamous cell carcinoma: histologic risk assessment, but not margin status, is strongly predictive of local disease-free and overall survival.* Am J Surg Pathol, 2005. **29**(2): p. 167-78.
110. da Silva, S.D. and L.P. Kowalski, *Perineural invasion in oral cancer: challenges, controversies and clinical impact.* Chin Clin Oncol, 2019. **8**(S1): p. S5.
111. Fagan, J.J., et al., *Perineural invasion in squamous cell carcinoma of the head and neck.* Arch Otolaryngol Head Neck Surg, 1998. **124**(6): p. 637-40.
112. Chatzistefanou, I., et al., *The role of perineural invasion in treatment decisions for oral cancer patients: A review of the literature.* J Craniomaxillofac Surg, 2017. **45**(6): p. 821-825.
113. Schmitd, L.B., C.S. Scanlon, and N.J. D'Silva, *Perineural Invasion in Head and Neck Cancer.* J Dent Res, 2018. **97**(7): p. 742-750.
114. Jardim, J.F., et al., *Prognostic impact of perineural invasion and lymphovascular invasion in advanced stage oral squamous cell carcinoma.* Int J Oral Maxillofac Surg, 2015. **44**(1): p. 23-8.
115. Ross, G.L., et al., *Improved staging of cervical metastases in clinically node-negative patients with head and neck squamous cell carcinoma.* Ann Surg Oncol, 2004. **11**(2): p. 213-8.
116. Sparano, A., et al., *Multivariate predictors of occult neck metastasis in early oral tongue cancer.* Otolaryngol Head Neck Surg, 2004. **131**(4): p. 472-6.
117. Chang, W.C., et al., *A histopathological evaluation and potential prognostic implications of oral squamous cell carcinoma with adverse features.* Oral Oncol, 2019. **95**: p. 65-73.
118. Shen, W.R., et al., *Perineural invasion and expression of nerve growth factor can predict the progression and prognosis of oral tongue squamous cell carcinoma.* J Oral Pathol Med, 2014. **43**(4): p. 258-64.
119. D'Cruz, A.K., et al., *Elective neck dissection for the management of the N0 neck in early cancer of the oral tongue: need for a randomized controlled trial.* Head Neck, 2009. **31**(5): p. 618-24.
120. D'Cruz, A.K., et al., *Elective versus Therapeutic Neck Dissection in Node-Negative Oral Cancer.* N Engl J Med, 2015. **373**(6): p. 521-9.
121. Lee, L.Y., et al., *Prognostic impact of extratumoral perineural invasion in patients with oral cavity squamous cell carcinoma.* Cancer Med, 2019. **8**(14): p. 6185-6194.
122. Ling, W., A. Mijiti, and A. Moming, *Survival pattern and prognostic factors of patients with squamous cell carcinoma of the tongue: a retrospective analysis of 210 cases.* J Oral Maxillofac Surg, 2013. **71**(4): p. 775-85.
123. Tai, S.K., et al., *Risks and clinical implications of perineural invasion in T1-2 oral tongue squamous cell carcinoma.* Head Neck, 2012. **34**(7): p. 994-1001.
124. Togni, L., et al., *The Emerging Impact of Tumor Budding in Oral Squamous Cell*

Carcinoma: Main Issues and Clinical Relevance of a New Prognostic Marker. Cancers (Basel), 2022. **14**(15).
125. Attramadal, C.G., et al., *Tumor Budding, EMT and Cancer Stem Cells in T1-2/N0 Oral Squamous Cell Carcinomas.* Anticancer Res, 2015. **35**(11): p. 6111-20.
126. Shimizu, S., et al., *Tumor budding is an independent prognostic marker in early stage oral squamous cell carcinoma: With special reference to the mode of invasion and worst pattern of invasion.* PLoS One, 2018. **13**(4): p. e0195451.
127. Hori, Y., et al., *Association between pathological invasion patterns and late lymph node metastases in patients with surgically treated clinical No early oral tongue carcinoma.* Head Neck, 2020. **42**(2): p. 238-243.
128. Domingueti, C.B., et al., *Prognostication for oral carcinomas based on two histological scoring systems (BD and iBD models).* Oral Dis, 2021. **27**(4): p. 894-899.
129. Pedersen, N.J., et al., *Construction of a pathological risk model of occult lymph node metastases for prognostication by semi-automated image analysis of tumor budding in early-stage oral squamous cell carcinoma.* Oncotarget, 2017. **8**(11): p. 18227-18237.
130. Seki-Soda, M., et al., *Histopathological changes in tumor budding between biopsy and resected specimens from patients treated with preoperative S-1 chemotherapy for oral cancer.* J Oral Pathol Med, 2019. **48**(10): p. 880-887.
131. Saxena, S., et al., *Evaluating the Role of Immunological Cells (Tissue Eosinophils and Mast Cells) in Progression of Oral Squamous Cell Carcinoma.* Mymensingh Med J, 2018. **27**(2): p. 382-388.
132. Mascitti, M., et al., *Tumour-associated tissue eosinophilia (TATE) in oral squamous cell carcinoma: a comprehensive review.* Histol Histopathol, 2021. **36**(2): p. 113-122.
133. Dorta, R.G., et al., *Tumour-associated tissue eosinophilia as a prognostic factor in oral squamous cell carcinomas.* Histopathology, 2002. **41**(2): p. 152-7.
134. Peurala, E., et al., *Eosinophilia is a favorable prognostic marker for oral cavity and lip squamous cell carcinoma.* APMIS, 2018. **126**(3): p. 201-207.
135. Lorena, S.C., et al., *Morphometric analysis of the tumor associated tissue eosinophilia in the oral squamous cell carcinoma using different staining techniques.* Histol Histopathol, 2003. **18**(3): p. 709-13.
136. Leighton, S.E., et al., *Prevalence and prognostic significance of tumor-associated tissue eosinophilia in nasopharyngeal carcinoma.* Cancer, 1996. **77**(3): p. 436-40.
137. PO, D.E.L., et al., *Effect of eosinophil cationic protein on human oral squamous carcinoma cell viability.* Mol Clin Oncol, 2015. **3**(2): p. 353-356.
138. Sakkal, S., et al., *Eosinophils in Cancer: Favourable or Unfavourable?* Curr Med Chem, 2016. **23**(7): p. 650-66.
139. Lee, J.J., et al., *Eosinophils in health and disease: the LIAR hypothesis.* Clin Exp Allergy, 2010. **40**(4): p. 563-75.
140. Eriksson, D. and T. Stigbrand, *Radiation-induced cell death mechanisms.* Tumour Biol, 2010. **31**(4): p. 363-72.
141. Smith, E.M., et al., *Association between p53 and human papillomavirus in head and neck cancer survival.* Cancer Epidemiol Biomarkers Prev, 2008. **17**(2): p. 421-7.
142. Chung, C.H. and M.L. Gillison, *Human papillomavirus in head and neck cancer: its role in pathogenesis and clinical implications.* Clin Cancer Res, 2009. **15**(22): p. 6758-62.
143. Lee, D.K., et al., *The human papilloma virus E7 oncoprotein inhibits transforming growth factor-beta signaling by blocking binding of the Smad complex to its target sequence.* J Biol Chem, 2002. **277**(41): p. 38557-64.
144. Tian, Y., et al., *CIP2A facilitates the G1/S cell cycle transition via B-Myb in human papillomavirus 16 oncoprotein E6-expressing cells.* J Cell Mol Med, 2018. **22**(9): p. 4150-4160.
145. Park, J.S., et al., *Presence of oncogenic HPV DNAs in cervical carcinoma tissues and pelvic lymph nodes associating with proliferating cell nuclear antigen expression.* Gynecol Oncol, 1996. **60**(3): p. 418-23.
146. Moynahan, M.E., et al., *Brca1 controls homology-directed DNA repair.* Mol Cell, 1999.

4(4): p. 511-8.
147. Tian, F., et al., *BRCA1 promotes the ubiquitination of PCNA and recruitment of translesion polymerases in response to replication blockade.* Proc Natl Acad Sci U S A, 2013. **110**(33): p. 13558-63.
148. Gorodetska, I., I. Kozeretska, and A. Dubrovska, *BRCA Genes: The Role in Genome Stability, Cancer Stemness and Therapy Resistance.* J Cancer, 2019. **10**(9): p. 2109-2127.
149. Gu, J., et al., *TP53 mutation is associated with a poor clinical outcome for non-small cell lung cancer: Evidence from a meta-analysis.* Mol Clin Oncol, 2016. **5**(6): p. 705-713.
150. Fukuyama, Y., et al., *K-ras and p53 mutations are an independent unfavourable prognostic indicator in patients with non-small-cell lung cancer.* Br J Cancer, 1997. **75**(8): p. 1125-30.
151. Molina-Vila, M.A., et al., *Nondisruptive p53 mutations are associated with shorter survival in patients with advanced non-small cell lung cancer.* Clin Cancer Res, 2014. **20**(17): p. 4647-59.

Appendix 1: Journal publications

1. Alejandro I. Lorenzo-Pouso, Alba Pérez-Jardón, **Vito Carlo Alberto Caponio***, Francesca Spirito, Cintia M. Chamorro-Petronacci, Óscar Álvarez-Calderón-Iglesias, Pilar Gándara-Vila, Lorenzo Lo Muzio and Mario Pérez-Sayáns

Oral Chronic Hyperplastic Candidiasis and Its Potential Risk of Malignant Transformation: A Systematic Review and Prevalence Meta-Analysis

(2022) Journal of Fungi, 8 (10), 1093 *Corresponding author

2. Donato Antonacci, **Vito Carlo Alberto Caponio**, Giuseppe Troiano, Mario Giulio Pompeo, Francesco Gianfreda, Luigi Canullo

Facial scanning technologies in the era of digital workflow: A systematic review and network meta-analysis

(2022) Journal of Prosthodontic Research

3. Francesca Spirito, Alessandra Amato, Giuseppe Scelza, Massimo Pisano, **Vito Carlo Alberto Caponio**, Stefano Martina

Education during the COVID-19 pandemic: the perception of Italian dental and medical students

(2022) Minerva Dent Oral Sci. 71(5), 277-286

4. Paolo Pesce, Eitan Mijiritsky, Luigi Canullo, Maria Menini, **Vito Carlo Alberto Caponio**, Andrea Grassi, Luca Gobbato, Domenico Baldi

An Analysis of Different Techniques Used to Seal Post-Extractive Sites-A Preliminary Report

(2022) Dentistry Journal, 10(10), 189

5. Khrystyna Zhurakivska, Lucio Lo Russo, Lorenzo Lo Muzio, **Vito Carlo Alberto Caponio**, Luigi Laino, Claudia Arena, Nicola Cirillo and Giuseppe Troiano

Antibiotic prophylaxis at the time of dental implant placement: a cost-effectiveness analysis

(2022) BMC Health Services Research, 22, 1073

6. Fábio França Vieira e Silva, María Elena Padín-Iruegas, **Vito Carlo Alberto Caponio**, Alejandro I. Lorenzo-Pouso, Paula Saavedra-Nieves, Cintia Micaela Chamorro-Petronacci, José Suaréz-Peñaranda and Mario Pérez-Sayáns

Caspase 3 and Cleaved Caspase 3 Expression in Tumorogenesis and Its Correlations with Prognosis in Head and Neck Cancer: A Systematic Review and Meta-Analysis

(2022) International Journal of Molecular Sciences, 23(19) 11937

7. Vittoria Perrotti, **Vito Carlo Alberto Caponio**, Lorenzo Lo Muzio, Eun Ha Choi, Maria Carmela Di Marcantonio, Mariangela Mazzone, Nagendra Kumar Kaushik and Gabriella Mincione

Open Questions in Cold Atmospheric Plasma Treatment in Head and Neck Cancer: A Systematic Review

(2022) International Journal of Molecular Sciences, 23(18) 10238

8. Lucrezia Togni, **Vito Carlo Alberto Caponio**, Nicoletta Zerman, Giuseppe Troiano, Khrystyna Zhurakivska, Lorenzo Lo Muzio, Andrea Balercia, Marco Mascitti and Andrea Santarelli

The Emerging Impact of Tumor Budding in Oral Squamous Cell Carcinoma: Main Issues and Clinical Relevance of a New Prognostic Marker

(2022) Cancers, 14(15) 3571

9. María Fernández-Agra, José González-Serrano, Miguel de Pedro, Leire Virto, **Vito Carlo Alberto Caponio,** Elena Ibáñez-Prieto, Gonzalo Hernández, Rosa María López-Pintor

Salivary biomarkers in burning mouth syndrome: A systematic review and meta-analysis

(2022) Oral Diseases, 00, 1-14

10. Nishith Bhargava, Vittoria Perrotti, **Vito Carlo Alberto Caponio**, Victor Haruo Matsubara, Diana Patalwala and Alessandro Quaranta

Comparison of heat production and bone architecture changes in the implant site preparation with compressive osteotomes, osseodensification technique, piezoelectric devices, and standard drills: an ex vivo study on porcine ribs

(2022) Odontology

11. Alessandra Campobasso, Eleonora Lo Muzio, Giovanni Battista, **Vito Carlo Alberto Caponio**, Domenico Ciavarella and Lorenzo Lo Muzio

The effect of orthodontic appliances on the Oral Candida colonisation: a systematic review

(2022) Australasian Orthodontic Journal, volume 38, issue 1

12. Mir Faeq Ali Quadri; Tenny John; Damanpreet Kaur; Maryam Nayeem; Mohammed Khaleel Ahmed; Ahmed M Kamel; Santosh Kumar Tadakamadla; **Vito Carlo Alberto Caponio**; Lorenzo Lo Muzio

Poor implementation of tobacco control measures and lack of education influences the intention to quit tobacco: a structural equation modelling approach

(2022) BMC Public Health

13. Maria Eleonora Bizzoca, Stefania Leuci, Michele Davide Mignogna, Eleonora Lo Muzio, **Vito Carlo Alberto Caponio**, Lorenzo Lo Muzio

Natural compounds may contribute in preventing SARS-CoV-2 infection: a narrative review.

(2022) Food Science and Human Wellness, volume 11, 5, 1134-1142

14. Roberto Pistilli, Luigi Canullo, Paolo Pesce, Valeria Pistilli, **Vito Carlo Alberto Caponio**, Luca Sbricoli

Guided implant surgery and sinus lift in severely resorbed maxillae: A retrospective clinical study with up to 10 years of follow-up

(2022) Journal of Dentistry, volume 121, 104137

15. Claudia Arena, **Vito Carlo Alberto Caponio**, Khrystyna Zhurakivska, Lucio Lo Russo, Lorenzo Lo Muzio, Giuseppe Troiano

Added effect of 1% topical alendronate in intra-bony and inter-radicular defects as part of step II periodontal therapy: a systematic review with meta-analysis and trial sequential analysis

(2022) BMC Oral Health, volume 22, I, 15.

16. **Vito Carlo Alberto Caponio**, Lucrezia Togni, Khrystyna Zhurakivska, Andrea Santarelli, Claudia Arena, Corrado Rubini, Lorenzo Lo Muzio, Giuseppe Troiano, Marco Mascitti

Prognostic assessment of different methods for eosinophils detection in oral tongue cancer

(2022) Journal of Oral Pathology and Medicine; 51: 240– 248

17. Mascitti, Marco; Togni, Lucrezia; **Caponio, Vito Carlo Alberto**; Zhurakivska, Khrystyna; Lo Muzio, Lorenzo; Rubini, Corrado; Santarelli, Andrea; Troiano, Giuseppe

Prognostic significance of tumor budding thresholds in oral tongue squamous cell carcinoma

(2022) Oral Diseases, 00:1-12

18. Ravidà, Andrea; Arena, Claudia; Tattan, Mustafac**; Caponio, Vito Carlo Alberto**; Saleh, Muhammad H. A.; Wang, Hom-Lay; Troiano, Giuseppe.

The role of keratinized mucosa width as a risk factor for peri-implant disease: A systematic review, meta-analysis, and trial sequential analysis

(2022) Clinical Implant Dentistry and Related Research 1-14

19. **Caponio, V.C.A**., Lipsi, M.R., Fortunato, F., Arena, F., Lo Muzio, L.
Symptomatic SARS-CoV-2 Infection with Ageusia after Two mRNA Vaccine Doses

(2022) International Journal of Environmental Research and Public Health, volume 19, 2, 886

20. Pierluigi Mariani, Diana Russo, Marco Maisto, Giuseppe Troiano, **Vito Carlo Alberto Caponio**, Marco Annunziata, Luigi Laino
Pre-treatment neutrophil-to-lymphocyte ratio is an independent prognostic factor in head and neck squamous cell carcinoma: Meta-analysis and trial sequential analysis.

(2022) Journal of Oral Pathology and Medicine, volume 51, 1, 39-51

21. Mascitti M.; Togni L.; **Caponio V.C.A**.; Zhurakivska K.; Bizzoca M.E.; Contaldo M.; Serpico R.; Lo Muzio L.; Santarelli A.
Lymphovascular invasion as a prognostic tool for oral squamous cell carcinoma: a comprehensive review

(2022) International Journal of Oral and Maxillofacial Surgery, volume 51, 1, 1 – 9

22. Dioguardi, Mario; Arena, Claudia; Sovereto, Diego; Aiuto, Riccardo; Laino, Luigi; Illuzzi, Gaetano; Laneve, Enrica; Raddato, Bruna;
Caponio, Vito Carlo Alberto; Dioguardi, Antonio; Zhurakivska, Khrystyna; Troiano, Giuseppe.

Influence of sterilization procedures on the physical and mechanical properties of rotating endodontic instruments: a systematic review and network meta-analysis.

(2021) Frontiers in Bioscience – Landmark, volume 26, 12, 1697 - 1713

23. Dioguardi, Mario; Alovisi, Mario; Troiano, Giuseppe; **Caponio, Carlo Vito Alberto**; Baldi, Andrea; Rocca, Giovanni Tommaso; Comba, Allegra; Lo Muzio, Lorenzo; Scotti, Nicola
Clinical outcome of bonded partial indirect posterior restorations on vital and non-vital teeth: a systematic review and meta-analysis

(2021) Clinical Oral Investigations, Volume 25, Issue 12, Pages 6597 - 6621

24. Pannone, G., **Caponio, V.C.A**., De Stefano, I.S., Ramunno, M.A., Meccariello, M., Agostinone, A., Pedicillo, M.C., Troiano, G., Zhurakivska, K., Cassano, T., Bizzoca, M.E., Papagerakis, S., Buonaguro, F.M., Advani, S., Muzio, L.L.
Lung histopathological findings in COVID-19 disease – a systematic review

(2021) Infectious Agents and Cancer, 16 (1), art. no. 34, .

25. Cantile, T., Coppola, N., **Caponio, V.C.A**., Russo, D., Bucci, P., Spagnuolo, G., Mignogna, M.D., Leuci, S.
Oral mucosa and nails in genodermatoses: A diagnostic challenge

(2021) Journal of Clinical Medicine, 10 (22), art. no. 5404, .

26. Russo, D., Mariani, P., **Caponio, V.C.A**., Lo Russo, L., Fiorillo, L., Zhurakivska, K., Lo Muzio, L., Laino, L., Troiano, G.
Development and validation of prognostic models for oral squamous cell carcinoma: A systematic review and appraisal of the literature

(2021) Cancers, 13 (22), art. no. 5755.

27. Canullo, L., Masucci, L., Quaranta, G., Patini, R., **Caponio, V.C.A.**, Pesce, P., Ravidà, A., Penarrocha-Oltra, D., Penarrocha-Diago, M.
Culturomic and quantitative real-time-polymerase chain reaction analyses for early contamination of abutments with different surfaces: A randomized clinical trial

(2021) Clinical Implant Dentistry and Related Research, 23 (4), pp. 568-578.

28. Arena, C., Bizzoca, M.E., **Caponio, V.C.A**., Troiano, G., Zhurakivska, K., Leuci, S., Lo Muzio, L.
Everolimus therapy and side-effects: A systematic review and meta-analysis

(2021) International Journal of Oncology, 59 (1), art. no. 5234, .

29. Perrotti, V., **Caponio, V.C.A.,** Mascitti, M., Lo Muzio, L., Piattelli, A., Rubini, C., Capone, E., Sala, G.
Therapeutic potential of antibody-drug conjugate-based therapy in head and neck cancer: A systematic review

(2021) Cancers, 13 (13), art. no. 3126.

30. **Caponio, V.C.A.,** Troiano, G., Togni, L., Zhurakivska, K., Santarelli, A., Laino, L., Rubini, C., Lo Muzio, L., Mascitti, M.
Pattern and localization of perineural invasion predict poor survival in oral tongue carcinoma

(2021) Oral Diseases

31. Khrystyna Zhurakivska, Nagaia Ciacci, Giuseppe Troiano, **Vito Carlo Alberto Caponio**, Roberto Scrascia, Lucia Pallecchi, Lorenzo Lo Muzio and Fabio Arena
Nitride-Coated and Anodic-Oxidized Titanium Promote a Higher Fibroblast and Reduced Streptococcus gordonii Proliferation Compared to the Uncoated Titanium

(2020) Prosthesis, 2, 333-339

32. Troiano, G., Rubini, C., Togni, L., **Caponio, V.C.A.,** Zhurakivska, K., Santarelli, A., Cirillo, N., Lo Muzio, L., Mascitti, M.
The immune phenotype of tongue squamous cell carcinoma predicts early relapse and poor prognosis

(2020) Cancer Medicine, 9 (22), pp. 8333-8344.

33. Mascitti, M., Zhurakivska, K., Togni, L., **Caponio, V.C.A**., Almangush, A., Balercia, P., Balercia, A., Rubini, C., Lo Muzio, L., Santarelli, A., Troiano, G.
Addition of the tumour–stroma ratio to the 8th edition American Joint Committee on Cancer staging system improves survival prediction for patients with oral tongue squamous cell carcinoma

(2020) Histopathology, 77 (5), pp. 810-822.

34. **Caponio, V.C.A**., Troiano, G., Adipietro, I., Zhurakivska, K., Arena, C., Mangieri, D., Mascitti, M., Cirillo, N., Lo Muzio, L.
Computational analysis of TP53 mutational landscape unveils key prognostic signatures and distinct pathobiological pathways in head and neck squamous cell cancer

(2020) British Journal of Cancer, 123 (8), pp. 1302-1314.

35. Di Stasio, D., Romano, A., Russo, D., Fiori, F., Laino, L., **Caponio, V.C.A**., Troiano, G., Muzio, L.L., Serpico, R., Lucchese, A.
Photodynamic therapy using topical toluidine blue for the treatment of oral leukoplakia: A prospective case series

(2020) Photodiagnosis and Photodynamic Therapy, 31, art. no. 101888.

36. Zhurakivska, K., Troiano, G., Pannone, G., **Caponio, V.C.A**., Lo Muzio, L.
An Overview of the Temporal Shedding of SARS-CoV-2 RNA in Clinical Specimens

(2020) Frontiers in Public Health, 8, art. no. 487.

37. Mascitti, M., Togni, L., Troiano, G., **Caponio, V.C.A**., Sabatucci, A., Balercia, A., Rubini, C., Lo Muzio, L., Santarelli, A.
Odontogenic tumours: a 25-year epidemiological study in the Marche region of Italy

(2020) European Archives of Oto-Rhino-Laryngology, 277 (2), pp. 527-538.

38. Dioguardi, M., Sovereto, D., Illuzzi, G., Laneve, E., Raddato, B., Arena, C., Alberto **Caponio, V.C**., Caloro, G.A., Zhurakivska, K., Troiano, G., Lo Muzio, L.
Management of Instrument Sterilization Workflow in Endodontics: A Systematic Review and Meta-Analysis

(2020) International Journal of Dentistry, 2020, art. no. 5824369.

39. Troiano, G., **Caponio, V.C.A**., Botti, G., Aquino, G., Losito, N.S., Pedicillo, M.C., Zhurakivska, K., Arena, C., Ciavarella, D., Mastrangelo, F., Russo, L.L., Muzio, L.L., Pannone, G.
Immunohistochemical analysis revealed a correlation between musashi-2 and cyclin-d1 expression in patients with oral squamous cells carcinoma

(2020) International Journal of Molecular Sciences, 21 (1), art. no. 121.

Appendix 2: Abstracts and Conference Proceedings

- XXVII Congresso Nazionale – Collegio dei Docenti Universitari di discipline Odontostomatologiche – 2020 Honorable mention for Best Paper award Simposio SIPMO: Computational analysis of TP53 mutational landscape unveils key prognostic signatures and distinct pathobiological pathways in head and neck squamous cell cancer; Vito Carlo Alberto Caponio.
- XXVII Congresso Nazionale - Collegio dei Docenti Universitari di discipline Odontostomatologiche - 2020 Winning poster presentation for "Pazienti con carcinoma a cellule squamose della regione testa-collo con TP53 mutato: nuovo algoritmo prognostico" Bizzoca M.E.; Zhurakivska K.; Mascitti M.; Santarelli A.; Mauceri R.; Di Fede O.; Caponio V. C. A.; Lo Muzio L.
- XXVII Congresso Nazionale – Collegio dei Docenti Universitari di discipline Odontostomatologiche – 2020 Honorable mention for Poster Presentation in "Microbioma orale e terapia ortodontica: cambi nella terapia ortodontica fissa" Lo Muzio E., Caponio V. C. A.; Arena F.; Laurenziello M.; Suriano C.; Barbato E.
- XXVII Congresso Nazionale – Collegio dei Docenti Universitari di discipline Odontostomatologiche – 2020 Honorable mention for Poster Presentation in "Eosinofili associati al tumore nel carcinoma squamocelullare della lingua" Lo Muzio E., Caponio V. C. A.; Mascitti M.; Togni L.; Mauceri R.; Campisi G.; Dedola A.; Lo Muzio L.
- XXVIII Congresso Nazionale – Collegio dei Docenti Universitari di discipline Odontostomatologiche Milano – 20-24 Aprile 2021 Honorable mention for Poster presentation: Analisi costo-efficacia dell'utilizzo degli antibiotici nelle procedure implantari K. Zhurakivska, M. Dioguardi, V. C. A. Caponio, C. Arena, G. Campisi, M. Mascitti, E. Lo Muzio, R. Mauceri, G.Troiano
- Wiley TOP CITED ARTICLE 2020-2021 The immune phenotype of tongue squamous cell carcinoma predicts early relapse and poor prognosis, DOI: 10.1002/cam4.3440
- XXIX Congresso Nazionale - Collegio dei Docenti Universitari di discipline Odontostomatologiche Bologna – 7-9 Aprile 2022 Winning poster presentation for "Use of radiomic features to define a predictive model of MBL around implants"; Fanelli F., Troiano G., Zotti M., Rapani A., Caponio V. C. A., Mastrangelo F., Stacchi C.
- XXIX Congresso Nazionale - Collegio dei Docenti Universitari di discipline Odontostomatologiche Bologna – 7-9 Aprile 2022 Winning poster presentation for "Role of TP53 as therapy predictive biomarker in patients with head and neck carcinoma"; F. Spirito, K. Zhurakivska, G. Troiano, M. Dioguardi, V. Panzarella, L. Lo Muzio, V. Perrotti, V.C.A. Caponio.
- XXIX Congresso Nazionale – Collegio dei Docenti Universitari di discipline Odontostomatologiche Bologna – 7-9 Aprile 2022 Honorable mention for Poster presentation "Surgical treatment of peri-implantitis. A systematic review"; Zhurakivska K., Di Cosola M., […], Mastrangelo F., Caponio V.C.A.
- XXIX Congresso Nazionale – Collegio dei Docenti Universitari di discipline Odontostomatologiche Bologna – 7-9 Aprile 2022 Honorable mention for Poster presentation "Evaluation of LGALS3BP as a potential target for OSCC immunotherapy"; Cela I., Lo Muzio E., Caponio V.C.A., Togni L., Capone E., Lattanzio R., Rubini C., Lo Muzio L., Sala G.and Perrotti V.

Appendix 3: Oral presentations

- Lecturer at XXVII Congresso Nazionale Collegio dei Docenti Universitari di discipline Odontostomatologiche – Session of Best Paper Award 2019 – SIPMO – Title: Prognostic significance of CD68+ and CD163+ tumor associated macrophages in head and neck squamous cell carcinoma: a systematic review and meta-analysis. Online Conference, 28/07/2020

- Lecturer at XXVIII Congresso Nazionale Collegio dei Docenti Universitari di discipline Odontostomatologiche – Session of Best Paper Award 2020 – SIPMO – Title: Computational analysis of TP53 mutational landscape unveils key prognostic signatures and distinct pathobiological pathways in head and neck squamous cell cancer. Online Conference 24/03/2021

- Lecturer at XXIX Congresso Nazionale Collegio dei Docenti Universitari di discipline Odontostomatologiche – Title: Marcatori prognostici nel carcinoma squamocellulare del testa-collo – Prognostic biomarker in the head and neck squamous cell carcinoma. Bologna, Italy 7-9/04/2022

- Poster presentation at "The VIII International Symposium Advances in oral Cancer" 25/09/2020 The prognostic role of tumor-associated tissue eosinophilia in oral tongue squamous cell carcinoma – online conference

- Poster presentation at "The XII European Congress on Cell Death (EWCD)" 26/06/2022-01/07/2022 Assessment of LGALS3BP in Adenoid Cystic Carcinoma of the salivary gland as a potential target for immunotherapy – Lattanzio R., Cela I., Lo Muzio E, **Caponio V.C.A.,** Togni L., Rubini C., Lo Muzio L., Capone E., Perrotti V and Sala G; Fiuggi (FR), Italy

- Poster presentation at "The IX International Symposium Advances in oral Cancer" 01/07/2022-02/07/2022 New developed TP53-mutations algorithm predicts poor treatment-response in patients with head and neck squamous cell carcinoma – online conference

- Lecturer at VI PhDay Faculdad de Odontologia – Escuela de Doctorado Universidad Complutense de Madrid – Title: Biomarcadores pronóstico en el carcinoma escamoso de cabeza y cuello– Prognostic biomarker in the head and neck squamous cell carcinoma. Madrid, Spain 13/10/2022

Appendix 4: Honors and awards

- XXVII Congresso Nazionale – Collegio dei Docenti Universitari di discipline Odontostomatologiche – 2020 Honorable mention for Best Paper award Simposio

SIPMO: Computational analysis of TP53 mutational landscape unveils key prognostic signatures and distinct pathobiological pathways in head and neck squamous cell cancer; Vito Carlo Alberto Caponio.

- XXVII Congresso Nazionale - Collegio dei Docenti Universitari di discipline Odontostomatologiche - 2020 Winning poster presentation for "Pazienti con carcinoma a cellule squamose della regione testa-collo con TP53 mutato: nuovo algoritmo prognostico" Bizzoca M.E.; Zhurakivska K.; Mascitti M.; Santarelli A.; Mauceri R.; Di Fede O.; Caponio V. C. A.; Lo Muzio L.
- XXVII Congresso Nazionale – Collegio dei Docenti Universitari di discipline Odontostomatologiche – 2020 Honorable mention for Poster Presentation in "Microbioma orale e terapia ortodontica: cambi nella terapia ortodontica fissa" Lo Muzio E., Caponio V. C. A.; Arena F.; Laurenziello M.; Suriano C.; Barbato E.
- XXVII Congresso Nazionale – Collegio dei Docenti Universitari di discipline Odontostomatologiche – 2020 Honorable mention for Poster Presentation in "Eosinofili associati al tumore nel carcinoma squamocelullare della lingua" Lo Muzio E., Caponio V. C. A.; Mascitti M.; Togni L.; Mauceri R.; Campisi G.; Dedola A.; Lo Muzio L.
- XXVIII Congresso Nazionale – Collegio dei Docenti Universitari di discipline Odontostomatologiche Milano – 20-24 Aprile 2021 Honorable mention for Poster presentation: Analisi costo-efficacia dell'utilizzo degli antibiotici nelle procedure implantari K. Zhurakivska, M. Dioguardi, V. C. A. Caponio, C. Arena, G. Campisi, M. Mascitti, E. Lo Muzio, R. Mauceri, G.Troiano
- Wiley TOP CITED ARTICLE 2020-2021 The immune phenotype of tongue squamous cell carcinoma predicts early relapse and poor prognosis, DOI: 10.1002/cam4.3440
- XXIX Congresso Nazionale - Collegio dei Docenti Universitari di discipline Odontostomatologiche Bologna – 7-9 Aprile 2022 Winning poster presentation for "Use of radiomic features to define a predictive model of MBL around implants"; Fanelli F., Troiano G., Zotti M., Rapani A., Caponio V. C. A., Mastrangelo F., Stacchi C.
- XXIX Congresso Nazionale - Collegio dei Docenti Universitari di discipline Odontostomatologiche Bologna – 7-9 Aprile 2022 Winning poster presentation for "Role of TP53 as therapy predictive biomarker in patients with head and neck carcinoma"; F. Spirito, K. Zhurakivska, G. Troiano, M. Dioguardi, V. Panzarella, L. Lo Muzio, V. Perrotti, V.C.A. Caponio.
- XXIX Congresso Nazionale – Collegio dei Docenti Universitari di discipline Odontostomatologiche Bologna – 7-9 Aprile 2022 Honorable mention for Poster presentation "Surgical treatment of peri-implantitis. A systematic review"; Zhurakivska K., Di Cosola M., […], Mastrangelo F., Caponio V.C.A.
- XXIX Congresso Nazionale – Collegio dei Docenti Universitari di discipline Odontostomatologiche Bologna – 7-9 Aprile 2022 Honorable mention for Poster presentation "Evaluation of LGALS3BP as a potential target for OSCC immunotherapy"; Cela I., Lo Muzio E., Caponio V.C.A., Togni L., Capone E., Lattanzio R., Rubini C., Lo Muzio L., Sala G.and Perrotti V.